



The
University
Of
Sheffield.

mRNA export and cancer

**Thesis submitted to obtain the degree of Doctor of Philosophy
Department of Molecular Biology and Biotechnology, the
University of Sheffield**

Marcus George Kwesi Cumberbatch

MRCS (Royal College of Surgeons of England, UK)

MBBS (University College London, UK)

MSc in Clinical Research (University of Sheffield, UK)

**BSc in Medical Sciences with The History of Medicine (University
College London, UK)**

March 2016

I hereby declare that no part of this thesis has previously been submitted for any degree or qualification at this, or any other university or institute of learning.

Acknowledgements

First and foremost, I would like to extend my greatest thanks to Professor Wilson for granting me the opportunity to complete this PhD in his laboratory. He has shown me every kindness and offered the very best guidance.

I would also like to thank Professor James Catto for reviewing my thesis, helping me to find a suitable project and overseeing the write up of my publications.

I am indebted to Dr Nicolas Viphakone for his everyday troubleshooting and overall bench training. I would like to thank Professor Nicola Brown for her help with my mouse experiments and Professor Angela Cox for her help during my meta-analyses. I am also grateful for the friendship of my lab mates Simon, Arthur, Catherine, Agata, Vicky, Janet, Steve, Lee and Karl.

Last but not least, I owe all of my successes to my parents Liz and Malcolm and to my wife Eleanor.

Index of Contents

INDEX OF CONTENTS	4
INDEX OF FIGURES	9
ABBREVIATIONS	14
ABSTRACT	17
PUBLICATIONS ARISING FROM THE WORK UNDERTAKEN IN THIS THESIS	19
PRESENTATIONS ARISING FROM THE WORK UNDERTAKEN IN THIS THESIS	20
PRIZES ARISING FROM THE WORK UNDERTAKEN IN THIS THESIS	21

CHAPTER 1: INTRODUCTION

1.1. THE UROLOGIST AND CANCER	22
1.2. BLADDER CANCER	25
1.3. NEED FOR A NEW BIOMARKER FOR BLADDER CANCER	27
1.4. CURRENT BEST ATTEMPTS AT FINDING A BIOMARKER FOR BLADDER CANCER	29
1.5. CURRENT TREATMENT FOR BLADDER CANCER	35
1.6. EXPORT OF NASCENT mRNA AND RNA PROCESSING EVENTS	36
1.7. TREX COMPLEX AND mRNA EXPORT ADAPTORS	42
1.8. mRNA EXPORT ADAPTORS AND LINKS TO CANCER	44
1.9. CANCER TESTIS ANTIGENS	46

1.10. DNA DAMAGE	46
1.11. POST TRANSLATIONAL MODIFICATIONS	50
1.12. “SEEING IS BELIEVING”: MODELS FOR MONITORING mRNA EXPORT PATTERNS	55
1.13. AIMS OF THIS PhD	58

CHAPTER 2: MATERIALS AND METHODS

2.1. MATERIALS	60
2.1.1. CELL LINES	60
2.1.2. BACTERIAL STRAINS	62
2.1. 3. GROWTH MEDIA	62
2.1.4. VECTORS	63
2.1.5. BUFFERS	64
2.1.6. MOLECULAR BIOLOGY KITS	66
2.2. METHODS	67
2.2.1. SYSTEMATIC REVIEWS AND META-ANALYSES	67
2.2.2. MOLECULAR BIOLOGY	67
2.2.3. BIOCHEMISTRY	80
2.2.4. CELL BIOLOGY	84

CHAPTER 3: UNDERSTANDING THE LITERATURE: THE ROLE OF TOBACCO SMOKE IN BLADDER CANCER

3.1. SYSTEMATIC REVIEW AND META-ANALYSIS OF RISK OF BLADDER CANCER IN SMOKERS	88
3.2. DATA ACQUISITION	89
3.3. CURRENT SMOKERS HAVE THE GREATEST BLADDER CANCER RISK INCIDENCE AND MORTALITY	91
3.4. SUMMARY	97

CHAPTER 4: UNDERSTANDING THE LITERATURE: OCCUPATIONAL CARCINOGEN EXPOSURE AND BLADDER CANCER

4.1. SYSTEMATIC REVIEW AND META-ANALYSIS OF RISK OF BLADDER CANCER BY OCCUPATIONAL CARCINOGEN EXPOSURE	98
4.2. DATA ACQUISITION	101
4.3. THE FACE OF OCCUPATIONAL BLADDER CANCER HAS CHANGED	104
4.4. SUMMARY	110

CHAPTER 5: LUZP4 FUNCTIONS AS AN ALTERNATIVE mRNA EXPORT ADAPTOR IN SOME CANCER CELLS

5.1 LUZP4 AND CANCER TESTIS ANTIGENS	112
5.2 PRESENCE OF LUZP4 IN BLADDER CANCER	116

5.3 EXPRESSION OF LUZP4 ACROSS CANCER TYPES	120
5.4 LUZP4 AS AN ONCOGENE	122
5.5 LUZP4 IMMUNOHISTOCHEMISTRY	127
5.6 EFFECTS OF DNA DAMAGE IN ALYREF RNAi CELL LINES	129
5.7 SUMMARY	131

CHAPTER 6: EFFECT OF DNA DAMAGE AND SUBSEQUENT POLY (ADP RIBOSYL)ATION ON TREX SUBUNIT INTERACTIONS

6.1. POLY (ADP-RIBOSYL)ATION	133
6.2. PARG RNAi	136
6.3. THERE IS A TOTAL mRNA EXPORT BLOCK UPON INDUCTION OF PARG RNAi IN CONDITIONS OF DNA DAMAGE	141
6.4. COIMMUNOPRECIPITATION PATTERNS OF ALYREF WITH UAP56 UNDER DNA DAMAGE STRESS	145
6.5. IDENTIFYING THE PAR BINDING SITE ON UAP56	148
6.6. IS LOCALISATION OF COMMON EXPORT FACTORS ALTERED UPON DNA DAMAGE?	160
6.7. LIVE mRNA IMAGING: CLONING OF SPINACH2 AND mCHERRY INTO pCINEO VECTOR	168
6.8. SUMMARY	170

CHAPTER 7: DISCUSSION

7.1. THE ROLE OF TOBACCO SMOKING AND OCCUPATIONAL CARCINOGEN EXPOSURE IN BLADDER CARCINOGENESIS: TWO META-ANALYSES	172
7.2. LUZP4	174
7.3. DNA DAMAGE	175
7.4. FUTURE DIRECTIONS	178

REFERENCES	181
-------------------	-----

COPIES OF PUBLICATIONS ARISING FROM THESIS	203
---	-----

Index of Figures

CHAPTER 1: INTRODUCTION

FIGURE 1.1. THE HALLMARKS OF CANCER	24
FIGURE 1.2a. PATHOLOGICAL STAGING OF BLADDER CANCER	34
FIGURE 1.2b. BLADDER CANCER STAGING EXPLAINED	34
FIGURE 1.3. mRNA PROCESSING EVENTS	41
FIGURE 1.4. DNA DAMAGE PATHWAYS	49
FIGURE 1.5. PROTEOME COMPLEXITY	53
FIGURE 1.6. POLY (ADP-RIBOSYL)ATION	54
FIGURE 1.7. SPINACH-2	57

CHAPTER 3: UNDERSTANDING THE LITERATURE: THE ROLE OF TOBACCO SMOKE IN BLADDER CANCER

FIGURE 3.1. SYSTEMATIC REVIEW SEARCH STRATEGY: TOBACCO	92
FIGURE 3.2. BLADDER CANCER INCIDENCE AND MORTALITY TABLE BY TOBACCO SMOKING STATUS	93
FIGURE 3.3. BLADDER CANCER INCIDENCE AND MORTALITY TABLE BY GENDER AND GEOGRAPHICAL REGION	94
FIGURE 3.4. FORREST PLOT OF BLADDER CANCER INCIDENCE IN CURRENT SMOKERS	95

FIGURE 3.5. BEGG PLOT OF BLADDER CANCER INCIDENCE IN CURRENT SMOKERS	96
--	----

CHAPTER 4: UNDERSTANDING THE LITERATURE: OCCUPATIONAL CARCINOGEN EXPOSURE AND BLADDER CANCER

FIGURE 4.1. SYSTEMATIC REVIEW SEARCH STRATEGY: OCCUPATION	103
FIGURE 4.2. BLADDER CANCER INCIDENCE BY GENDER BY DECADE	106
FIGURE 4.3. BLADDER CANCER MORTALITY BY GENDER BY DECADE	107
FIGURE 4.4. FORREST PLOT OF BLADDER CANCER INCIDENCE BY OCCUPATION	108
FIGURE 4.5. FORREST PLOT OF BLADDER CANCER MORTALITY BY OCCUPATION	109

CHAPTER 5: LUZP4 FUNCTIONS AS AN ALTERNATIVE mRNA EXPORT ADAPTOR IN SOME CANCER CELLS

FIGURE 5.1. SCHEMATIC OF THE UAP56 BINDING MOTIF BINDING SITE SHARED BY mRNA EXPORT ADAPTORS	115
--	-----

FIGURE 5.2. WESTERN BLOT OF LUZP4 PROTEIN EXPRESSION IN BLADDER CANCER	117
FIGURE 5.3. RT-qPCR OF LUZP4 RNA EXPRESSION IN BLADDER CANCER	118
FIGURE 5.4. CONCEPTUAL DIAGRAM OF ALTERNATIVE EXPORT PATHWAYS	119
FIGURE 5.5. RT-qPCR OF LUZP4 RNA EXPRESSION ACROSS 18 CANCER TISSUES	121
FIGURE 5.6. MOUSE TUMOURS	125
FIGURE 5.7. GROWTH CURVE OF MOUSE TUMOURS	126
FIGURE 5.8. IMMUNOHISTOCHEMISTRY OF BLADDER CANCER SECTIONS	128
FIGURE 5.9. COLONY FORMING ASSAYS IN DRUG TREATED ALYREF RNAi CELLS	130

CHAPTER 6: EFFECT OF DNA DAMAGE AND SUBSEQUENT POLY (ADP-RIBOSYL)ATION ON TREX SUBUNIT INTERACTIONS

FIGURE 6.1. SCHEMATIC OF TREX SUBUNIT PARYLATION TARGETS	135
FIGURE 6.2. TRANSIENT KNOCKDOWN OF PARG	138
FIGURE 6.3. KNOCKDOWN TEST OF STABLE FLP-IN CELL LINE FOR PARG RNAi	139

FIGURE 6.4. WESTERN BLOT SHOWING SPECIFICITY OF PARG RNAi FOR PARG	140
FIGURE 6.5. <i>CLICK IT</i> TECHNOLOGY EXPLAINED	143
FIGURE 6.6. mRNA EXPORT BLOCK SEEN BY <i>CLICK IT</i> UPON H ₂ O ₂ TREATMENT	144
FIGURE 6.7. CO-IMMUNOPRECIPITATION OF ALYREF AND UAP56 UNDER DNA DAMAGING CONDITIONS	147
FIGURE 6.8. PARYLATION SITES ON ALYREF AND CHTOP mRNA EXPORT ADAPTORS.	149
FIGURE 6.9. MODEL OF PUTATIVE PAR BINDING SITE ON UAP56 SECONDARY STRUCTURE	150
FIGURE 6.10. PULLDOWN OF UAP56 TRUNCATIONS BY BIOTINYLATED PAR	152
FIGURE 6.11. IDENTIFYING THE PUTATIVE PAR BINDING SITE ON UAP56	154
FIGURE 6.12. PULLDOWN OF PAR BINDING SITE MUTATIONS OF UAP56 BY WILD TYPE ALYREF N-TERMINAL UAP56-BINDING MOTIF	156
FIGURE 6.13. PULLDOWN OF WILD TYPE FULL LENGTH ALYREF AND PAR BINDING SITE MUTATIONS OF UAP56	157
FIGURE 6.14. PULLDOWN OF CIP29 BY WILD TYPE AND PAR BINDING SITE MUTATIONS OF UAP56	158
FIGURE 6.15-17. INTRA-CELLULAR LOCALISATION STUDIES OF TREX SUBUNITS AFTER H ₂ O ₂ TREATMENT	162-164

FIGURE 6.18-19. INTRA-CELLULAR LOCALISATION STUDIES OF
THE EXPORT RECEPTOR NXF1 AND COFACTOR NXT1 AFTER H₂O₂
TREATMENT 166-167

FIGURE 6.20. LIVE IMAGING OF mRNA USING SPINACH 2 169

CHAPTER 7: DISCUSSION

FIGURE 7.1. A MODEL OF THE PROPOSED INTERACTION
BETWEEN PAR AND TREX 179

FIGURE 7.2. A DIAGRAM EXPLAINING OUR COMPLEMENTATION
CELL LINE 180

Abbreviations

ADP	Adenosine di-phosphate
ATP	Adenosine tri-phosphate
APS	Ammonium persulfate
BC	Bladder Cancer
BLAST	Basic Local Alignment Search Tool
BSA	Bovine Serum Albumin
CI	Confidence interval (95 %)
dH2O	De-ionized distilled water
DMEM	Dulbecco's modified Eagle's medium
DMSO	Dimethyl sulfoxide
DNA	Deoxynucleic acid
DSM	Disease-specific mortality
DTT	Dithiotretol
ECL	Enhanced chemiluminescent substrate
E.Coli	Escherichia coli
EDTA	Ethylendiaminetetraacetic acid
FACT	Facilitates Active Chromatin Transcription
FCS	Fetal calf serum
F.I.S.H	Fluorescence in situ hybridization
g	Gram
GFP	Green fluorescent protein
GST	Gluthathione-S-Transferase
H ₂ O ₂	Hydrogen peroxide

HP	Hairpin
IHC	Immunohistochemistry
IP	Immuno-precipitation
IPTG	isopropyl- β -D-thiogalactopyranoside
L	Litre
Mg	Milligram
MIBC	Muscle-invasive bladder cancer
Min	Minute
miRNA	Micro RNA
ml	Milliliter
mM	Millimolar
mRNA	Messenger RNA
mRNP	Messenger ribonucleic particle
Ng	Nanogram
NCI	National Cancer Institute
NMIBC	Non muscle-invasive bladder cancer
NTF2	Nuclear transport factor 2
ORF	Open reading frame
PARP	Poly (ADP-ribose) polymerase
PARG	Poly (ADP-ribose) glycohydrolase
PCR	Polymerase chain reaction
PMSF	Phenylmethylsulfonylfluoride
PTM	Post translational modification
qRT-PCR	Quantitative real time polymerase chain reaction
RNA	Ribonucleic acid

RNAi	RNA interference
Rpm	Revolutions per minute
RR	Relative risk
RT	Room temperature
SCC	Squamous cell carcinoma
SCID	Severe combined immune-deficient
SDS-PAGE	Sodium dodecyl sulphate polyacrylamide gel electrophoresis
Sec	Second
SIR	Summary incidence ratio
siRNA	Small interference RNA
SMR	Summary mortality ratio
TB	Terrific broth
TCC	Transitional cell carcinoma
TEMED	N',N',N',N', -tetramethylethylenediamine
TREX	Transcription export complex
TRIS	Tris (hydroxymethyl) – aminomethane
U	Units (standard)
UCC	Urothelial Cell Carcinoma
UTR	Untranslated region
UV	Ultra-violet
WHO	World Health Organisation
µg	Microgram
µl	Microliter

Abstract

Bladder cancer (BC) is the fourth commonest male malignancy worldwide and one of the most expensive to manage. The two greatest risk factors are tobacco smoking and occupational carcinogen exposure. In chapters 3 and 4, I contemporize the landscape of two leading causes for BC via a systematic review and meta-analysis of the published literature. I find that current smokers (versus ex-smokers or non-smokers) and those in tobacco, dye and factory industries have the greatest BC incidence.

Carcinogenesis is the result of many molecular interactions and pathways that are not completely understood. Changes to RNA processing and transport are known to play a role in cancer biology. Transport of mRNA from the nucleus to the cytoplasm is essential for eukaryotic gene expression. ALYREF is central to the major mRNA export pathway involving the TREX complex; however, it is frequently down-regulated in high grade tumours. In chapter 5, we show that a previously uncharacterized cancer testis antigen LUZP4 defines a novel mRNA export pathway up-regulated in cancer.

Post-translational modifications provide another level of gene expression control. In chapter 6, we show that poly (ADP-ribosyl)ation results in a global mRNA export block and alters TREX assembly by modifying the interaction between ALYREF and the RNA helicase UAP56 upon DNA damage. We show for the first time that PAR can bind UAP56 and identify the specific binding site. By advancing our

knowledge of the LUZP4 mRNA export pathway and the effects of poly (ADP-ribosyl)ation on mRNA export we identify possible future targets for manipulation as biomarkers or therapeutic avenues.

Publications arising from the work **undertaken in this thesis**

Cumberbatch MG, Rota M, Catto JW, La Vecchia C. (2015) **The Role of Tobacco Smoke in Bladder and Kidney Carcinogenesis: A Comparison of Exposures and Meta-analysis of Incidence and Mortality Risks.** Eur Urol. Jul 3. pii: S0302-2838(15)00548-5

Cumberbatch MG, Cox A, Teare D, and Catto JWF. (2015) **Changing trends in occupational bladder cancer: A systematic review and meta-analysis.** JAMA Oncol. Dec 1;1(9):1282-90

Viphakone N, Cumberbatch MG, Livingstone MJ, Heath PR, Dickman MJ, Catto JW, Wilson SA. (2015) **Luzp4 defines a new mRNA export pathway in cancer cells.** Nucleic Acids Res. Feb 27;43(4):2353-66

Presentations arising from the work undertaken in this thesis

LUZP4 a novel mRNA export adaptor in cancer. The 30th Annual meeting of the **European Association of Urology (EAU)**, Madrid, Spain. Mar 2015 [oral].

mRNA and Cancer. Section of Academic Urology, **British Association of Urological Surgeons (BAUS)**, The Royal College of Surgeons of England, Dec 2014 [poster].

Contemporary occupational bladder cancer: a systematic review and meta-analysis of occupations currently at risk. Section of Academic Urology, **British Association of Urological Surgeons (BAUS)**, The Royal College of Surgeons of England, Dec 2014 [poster].

Contemporary occupational bladder cancer: a systematic review of occupations currently at risk. Section of Academic Urology, **British Association of Urological Surgeons (BAUS)**, The Royal College of Surgeons of England, Dec 2014 [poster].

mRNA and Cancer: a novel export pathway. **The RNA Society** Quebec City, Canada. June 2014 [contributions to poster].

Prizes arising from the work undertaken in this thesis

mRNA and Cancer. Section of Academic Urology, **British Association of Urological Surgeons (BAUS)**, The Royal College of Surgeons of England, Dec 2014 [**poster prize**].

Chapter 1: Introduction

In this chapter I will introduce the background work and concepts that informed my hypotheses. In particular, attention is given to the biology of cancer, the advents of novel cancer detection mechanisms and the details involved in mRNA export and its potential links to cancer.

1.1 THE UROLOGIST AND CANCER

Cancer is the creation of abnormal cells that grow beyond their usual boundaries (World Health Organisation (WHO), 2015). In the UK there are 331,487 incident cases of cancer and 161,823 deaths per year. The 10-year survival rate for all cancers combined was 50% as of 2011 (Cancer Research UK, 2014). Whilst we understand a lot about carcinogenesis there is still much room for improvement. It is clear that cancer has a molecular basis. In other words, all cancers result from molecular alterations in the cell's machinery, which occur as changes in genetic content or epigenetic expression of cellular proteins. These alterations create abnormal cells, which may then develop into malignant tissues that may metastasize leading to morbidity and death.

Hanahan and Weinberg (2000 and 2011) in a landmark review proposed 6 hallmarks of cancer in detail; 1) resisting cell death, 2) sustaining proliferative signaling, 3) evading growth suppressors, 4)

activating invasion and metastasis, 5) enabling replicative immortality and 6) inducing angiogenesis (Hanahan and Weinberg, 2000) (Figure 1,1). DNA repair was subsequently included (Hanahan and Weinberg, 2011). Whilst, these hallmarks are shared amongst all cancers, there are differences in how (and to what extent) each cancer implements these phenotypes and so clinical oncologists worldwide now accept the view that each cancer may be *personalized* at the genetic and molecular level. This is true for the aetiology, natural history and also for the potential molecular targets for diagnostics and treatment.

As an Urologist, my interests lie predominantly in bladder cancer (BC). BC mostly arises from the urothelial lining (see Figure 1.2a.) of the urinary tract. These tumours are termed urothelial cell carcinoma (UCC), although historically the term transitional cell carcinoma (1973 WHO definition) was used. Around 10% BC are not UCC, and include squamous cell carcinoma, adenocarcinoma and sarcoma.

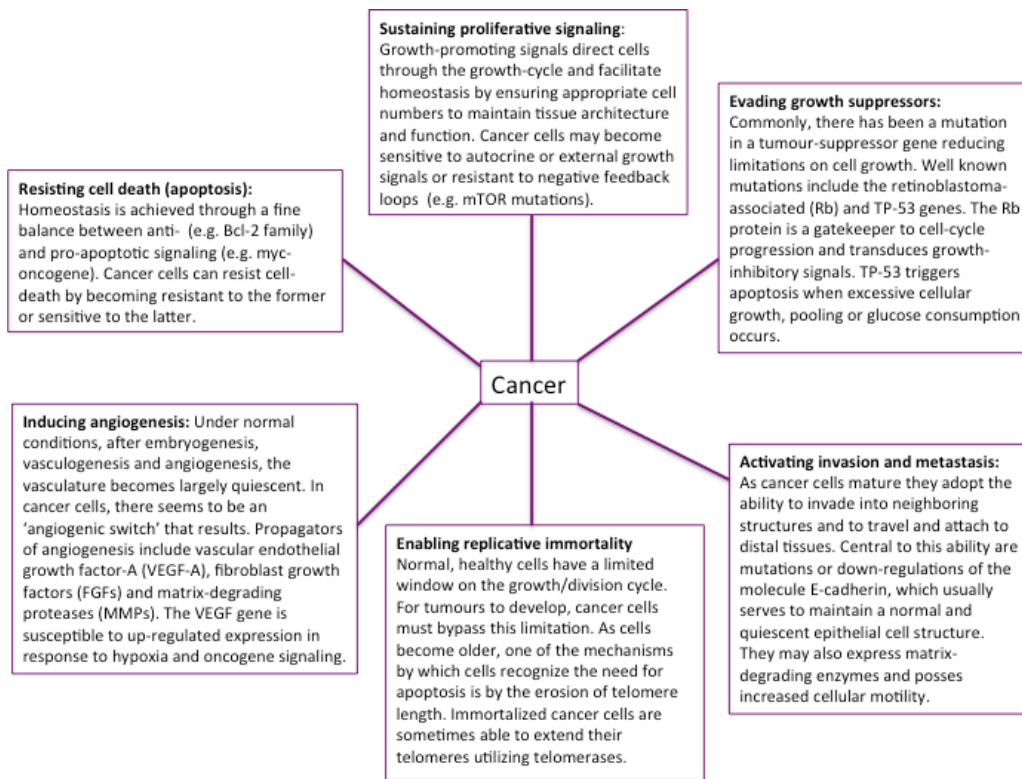


Figure 1.1. The hallmarks of cancer. Adapted from Hanahan D and Weinberg RA. (2000) *The hallmarks of cancer*. Cell. Jan 7;100(1):57-70.

1.2 BLADDER CANCER

BC is the 4th most common malignancy in males worldwide (Chavan et al., 2014; van Rhijn et al., 2009). In 2008 there were an estimated 382,700 new cases of BC worldwide, with 150,300 resultant deaths (Chavan et al., 2014). Tobacco smoking and exposure to occupational carcinogens are the two most common aetiological risk factors (Burger et al, 2013). Most tumors arise following exposure to exogenous carcinogens that enter the circulation through inhalation, ingestion or skin contact.

The urinary bladder is made of numerous layers, from a urothelial luminal surface layer through to muscle and peri-vesical fat tissue (see Figure 1.2a). BC is commonly stratified into non-muscle invasive (NMIBC) and muscle-invasive (MIBC). NMIBC depicts cancers which are confined to the lamina propria and do not invade beyond into the muscle layers of the urinary bladder. Prognostic profiles and treatment approaches vary between these two categories of disease, with MIBC having a far worse prognosis and requiring more aggressive clinical and surgical management, which confers a high morbidity burden. In the UK, the overall survival rate from BC is 50 % at 10 years. However, this ranges from 90 % to 10 % from disease stage 1 to 4 (see Figures 1.2a. and b.) (Cancer research UK, 2015).

BC is also an expensive disease. In the USA, BC represents >3 % of all cancer-related spending, with the average cost associated with a diagnosis of muscle-invasive bladder cancer set at approximately

\$150,000 per patient (Svatek et al., 2014). For early stage (NMIBC) cancers, the cost per capita was approximately \$8,000 as of 2002, but this was noted to be widely variable depending upon the management strategies of the host centre (e.g. intensity of cystoscopic surveillance – the gold standard). One review has suggested that BC has the greatest cost per cancer patient (van Rhijn et al., 2009).

BC has a latency period from carcinogenic insult to presentation of disease of approximately 20 years (Cohen et al., 2000). It is suggested that following a carcinogenic exposure the transcriptional programme of the urothelium undergoes a malignant transformation, with alterations in several genes (e.g. TP53) (Cheng et al., 2010). This effect may be dependent on somatic mutations or on epigenetic changes. Another way of describing this phenomenon is 'field cancerization', where there is a pre-neoplastic shift in fields of cells leading to cancerous phenotypes (Gabriel et al., 2012). Gravity is given to this hypothesis by the multifocality frequently displayed by BC. Catto et al (2006) showed that 90% of multifocal tumours arise from the same clone (Catto et al., 2006). Certainly it does seem that there is both reversible and permanent DNA damage that contributes to BC onset. This is supported by the observation that tobacco smokers that quit still have an increased incidence compared to never-smokers but a decreased risk compared to current-smokers (Cumberbatch et al., 2015a).

1.3. NEED FOR A NEW BIOMARKER FOR BLADDER CANCER

BC survival has not improved in more than 30 years (Lotan et al., 2014). Potential areas in which improved survival may occur are 1). novel therapies and 2). improved early detection mechanisms. There have been few therapeutic breakthroughs, with the recent exception of PDL-1 inhibitors (Powles et al., 2014), and so better diagnostic or prognostic biomarkers seem a more realistic opportunity. Biomarkers can be diagnostic (is there disease or not?) or prognostic (what is the likely outcome of this disease going to be?). There is no accepted serum marker for BC. The presence of haematuria (blood in the urine) is the current best marker of disease, but this can be caused by a number of pathologies including infection and kidney stones. The ideal biomarker should be detectable/interpretable at an early stage of disease prior to unsalvageable changes; it should be sensitive enough to correlate with disease severity; the mode of extraction should be non-invasive and acceptable to patients and the mechanism of action should be known (National Academies, 2008). The key principle is detecting BC before it becomes invasive (MIBC). The rate of cancer specific survival is more than 90% in patients with NMIBC, but this reduces to less than 50% in invasive disease (Lotan et al., 2014; Cancer research UK, 2015). At diagnosis, roughly one-quarter of BCs are invasive. Currently, there is no screening programme for BC in the UK (unlike breast and cervical cancers (Breast cancer screening, www.nhs.uk; cervical screening, www.gov.uk). The merits of a BC screening programme have been

extensively tested using haematuria as a surrogate marker of disease. Messing et al (2006) studied the use of home urine dipstick measuring of non-visible haematuria in a group of 258 patients in the US. They found that screening men aged 50+ resulted in detecting tumours earlier and reduced overall mortality. Britton et al (1989 and 1992) and Whelan et al (1993) found similar results. The criticisms/limitations of these studies are that all study patients were at least 50 years old, diagnosis of BC relies on further invasive testing and there are non-cancer causes of haematuria resulting in false-positives for BC. However, these studies showed that haematuria is a precursor to BC and early detection will confer benefit to patient outcomes.

In the UK, patients with haematuria are referred to clinic on a '2-week wait' emergency referral pathway due to the persistence of microscopic (non-visible (NVH), which is blood in the urine detected on a dip-stick test) or macroscopic (visible haematuria (VH)). 2-5% of patients with NVH, will have cancer (Lotan et al., 2014) and therefore many patients referred to clinic will be disease-negative (hence there are a lot of unnecessary investigations) but the risk of cancer increases to around 40% in patients with VH.

The current gold-standard investigation for the patient suspected of having BC is the flexible cystoscopy. This involves roughly a 30-minute hospital slot. During this appointment, the patient is first dressed appropriately into a gown by an attending nurse. The patient is then asked to provide a urine sample to rule out current infections. Next, the

surgeon will consent the patient for the procedure and following this explanation will perform it under a local anaesthetic. The patient is then given a description of the findings and discharged from clinic after re-dressing. If the findings at flexible cystoscopy are suspicious, then to clinch the diagnosis of BC, the patient will usually have a formal, *rigid cystoscopy* under a general anaesthetic. At which point the area of suspicion will be biopsied or more convincing tumours will be resected and the patient may or may not be given intra-vesical (intra-bladder) chemotherapy.

There is a consensus that cystoscopy is time-consuming, invasive and expensive and hence any breakthrough that can obviate the need for this procedure entirely or make selection of patients for cystoscopy more narrowed-down would be well received.

1.4. CURRENT BEST ATTEMPTS AT FINDING A BIOMARKER FOR BLADDER CANCER

NMP-22: The presence of this urinary nuclear matrix protein (NMP) in the urine of BC patients has been known since the 1990's (Soloway et al., 1996). During the life cycle of the bladder urothelial surface, the old, dead, luminal surface is shed into the passing urine. NMP is found in bladder urothelium, therefore when this layer is shed it is found in the excreted urine. The relevance to BC of NMP is that it reflects the mitotic activity of cells test (Lotan et al., 2014). The *NMP22 bladdercheck*® detection test is an FDA approved point-of-care test (Lotan et al., 2014)

based on an ELISA kit using an antibody to NMP22. The assay is performed by adding 4 drops of voided urine onto the device; this can be read approximately 40 minutes later (Lotan et al., 2014). The average kit can detect NMP22 at a sensitivity of up to 0.06ng/ml (Mybiosource.com, 2016). In a study by Stampfer et al (1998), NMP22 was compared with urinary cytology as a means of BC detection. The sensitivity and specificity of NMP22 was 68% and 80% respectively, compared to a sensitivity of urinary cytology of 31-40% (Stampfer et al., 1998). Other studies have also found NMP-22 to share favorable predictive rates when couple with urine cytology (Soloway et al., 1996). However, NMP22 has failed to provide more reliable diagnostic evidence than cystoscopy (Friedrich et al., 2003). Grossman et al (2006) found in a prospective cohort study of 103 US patients that NMP22 correctly identified 90% of BC (Grossman et al., 2006). The test was 99% accurate with concurrent cystoscopy. Grossman et al (2006) concluded that because neither cystoscopy nor NMP22 were 100% sensitive, that combination investigation was best practice. Subsequently, NMP22 is used more widely in the US but is not in the UK. Sensitivity rates have been a persistent rate-limiting step in the pursuit of a BC biomarker. One future approach may be to use such markers as adjuncts in clinic to help stratify patients as low- versus high-risk, so that cystoscopy can be more focused. Similar stumbling blocks have been found with UroVision, Immunocyst and the Bladder Tumour Antigen testing (BTA stat).

ImmunoCyt: An immunocytological test that uses fluorescence-labelled antibodies to 3 commonly exfoliated antigens in urothelial cancer cells (Greene et al., 2006). One antibody is directed against a high-molecular weight form of glycosylated carcinoembryonic antigen (CEA) and the other two are against mucins (Reinhert, 2012; Greene et al., 2006). Mucins are normally occurring high-molecular weight proteins found on epithelial layers. In malignant cells, the mucins are of lower glycosylation, which exposes their protein backbone making them more accessible to the antibodies (Greene et al., 2006) and as such are detected in greater number. The test is positive when at least one cell of either a green or red fluorescence is seen (Reinhert et al., 2012). The test is better at detecting MIBC than NMIBC (Reinhert et al., 2012). Limitations are that at least 500 cells without a fluorescent signal must be present for the sample to be called negative. Furthermore, there are issues with background signal (noise) that can cause inter-user error/bias (Greene et al., 2006).

UroVysion: This kit is designed to detect aneuploidy for chromosomes 3, 7, 17, and the loss of 9p21 locus (tumour suppressor). It uses FISH (fluorescence in situ hybridization) technology to detect these abnormalities in patient urine (Abbotmolecular.com, 2016). A DNA probe is used to identify the aneuploidy (Reinhert et al., 2012). A positive result is achieved if the correct ratio is seen between number of cells and abnormal chromosomes. Limitations of the system are: a reduced reading accuracy if there are excessive amounts of

granulocytes or bacteria in the sample and that it is also dependent on the user having normal colour vision to read the detection device. Lastly, tumours less than 5mm are not detectable (Abbotmolecular.com, 2016).

BTastat®: This test relies on an agglutination reaction for basement membrane complexes (Murphy et al., 1997). The technology was generated after analysis of BC patient urine (confirmed on biopsy) was conducted for common antigens (Kinders et al., 1998). The *BTastat®* test uses monoclonal antibodies directed towards human complement factor H related protein (hCFHrp) and human complement factor H (hCFH). These proteins serve to block the alternative complement cascade at sites of cancer cell growth, thus preventing the normal cell lysis of 'foreign' cells as detected by the host immune system. *BTastat®* uses a FISH based technique (*BTastat®*Test, *btastat.com*). The benefits of this test, alongside NMP-22 are that they are 'point of care tests', whereas others require trained technicians (Dey, 2004). Limitations include the unknown effects of some benign diseases on the test results.

Emerging fields: As we understand the molecular profile of cancer we have learned that each cancer uses different ways to achieve the necessary common hallmarks. As the unfolding of each cancer can happen in different ways, with genetic alterations being somewhat *personalized*. In more recent years, researches have focused more and

more on the aberrant expression of non-coding RNAs such as *micro RNAs*, epi-transcriptomic events such as *DNA methylation* and the ectopic expression of *cancer testis antigens (CTAs)*. For the purpose of this PhD, I focus predominantly on the role of CTAs and post-translational events that may cause alterations in mRNA export.

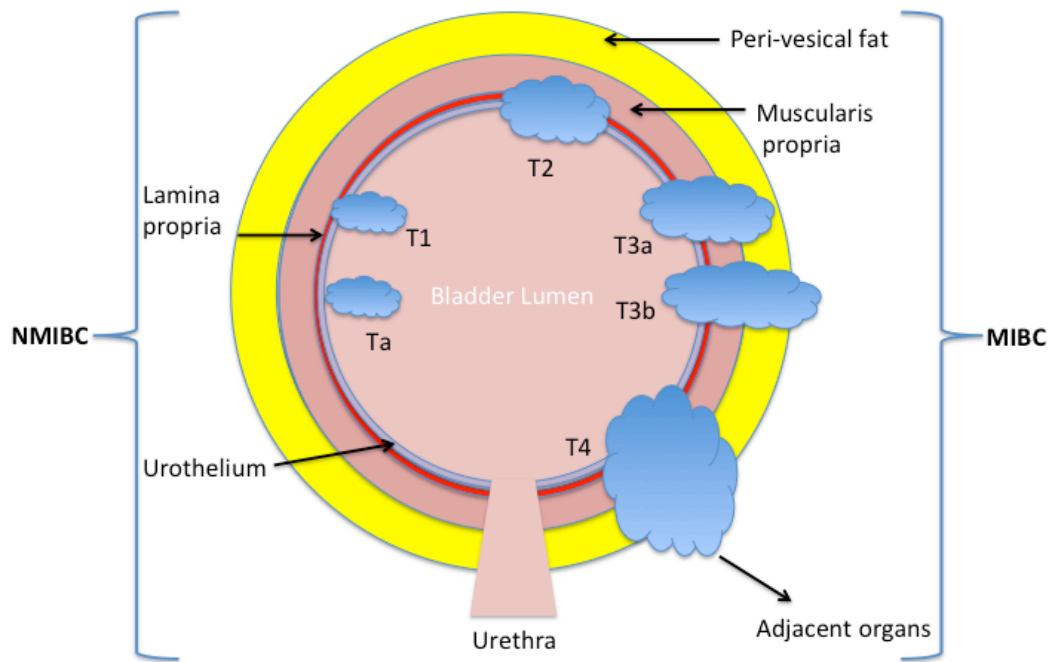


Figure 1.2a. A diagram depicting the different pathological stages of BC
(Based upon the TNM staging of bladder cancer)

T-stage	Description
Tx	Tumour unable to be assessed due to lack of information/tissue
T0	No tumour evidenced from histology
TiS	Carcinoma <i>in-situ</i> : A flat tumour
Ta	Non-invasive papillary carcinoma
T1	Tumour invades subepithelial connective tissue
T2a and T2b	T2a invades superficial muscle. T2b invades deep muscle
T3a and T3b	T3a microscopically invades perivesical tissue. T3b invades macroscopically
T4a and T4b	T4a invades prostate, uterus or vagina. T4b invades pelvic or abdominal wall

Figure 1.2b. Staging of urinary bladder cancer. Adapted from Babjuk M et al. (2015). Guidelines on non-muscle-invasive bladder cancer (Ta, T1 and CIS). European Association of Urology.

1.5. CURRENT TREATMENT OF BLADDER CANCER

NMIBC is typically treated with a transurethral resection of the tumour (TUR) with the stratified use of adjunctive intravesical chemotherapy. TURs are performed under a general anaesthetic and involve cystoscopic inspection and thermal coagulation or resection of tumours. Adjuvant chemotherapy usually comes in the form of Mitomycin C. This is an alkylating agent that ultimately results in DNA cross-linking and inhibition of cell growth. It is normally administered immediately following the TUR and must remain in the bladder for 1 hour. Alternative regimes include the use of *Bacille Calmette Guerin* (BCG), which is an attenuated form of mycobacterium bovis. This is normally administered as a 6-week course of intravesical instillations. MIBC requires radical treatment if cure is to be obtained. This may be with radical surgery (cystectomy) or radiotherapy (with/without radio sensitizers or systemic chemotherapy). Radical cystectomy in males includes the prostate and seminal vesicles, and in females usually includes removal of all the organs within the anterior pelvic compartment (pelvic exenteration). If the disease is metastatic or is non-organ confined then survival may be improved with chemotherapy. Regimes may include in Cisplatin, Carboplatin, Gemcitabine, monoclonal antibodies, or Docetaxel among others (Babjuk et al., 2015; Witjes et al., 2015). A randomized controlled trial by Sternberg et al (2015) involving 284 patients evaluated the difference in overall survival between those given immediate versus deferred chemotherapy. Four different combination chemotherapy regimes were used including gemcitabine,

cisplatin, methotrexate, vinblastine and doxorubicin. There were no statistically significant differences between administering chemotherapy within 90 days of cystectomy or at the first relapse (Sternberg et al., 2015). The concluding remarks suggested that further analysis is required to assess subgroup patient populations who may benefit from specific treatment regimes at more defined time-points

There is a drive in oncology to engineer *tailored* diagnostic and treatment avenues. To achieve this, we must understand the molecular basis of carcinogenesis.

1.6. EXPORT OF NASCENT mRNA AND RNA PROCESSING EVENTS

Central to molecular biology is the concept, in eukaryotic cells, that DNA must be transcribed into messenger RNA (mRNA) and then delivered through the nuclear pore to the cytoplasm where it can be translated into a protein. This is the pathway of gene expression. When a particular mRNA transcript is nascently synthesized, there is no guarantee that it will create a functional protein. To become an active protein, pre-mRNA must be processed and licensed into mRNA (Kelly and Corbett, 2009). mRNA export involves a process of co- and post-transcriptional quality control applied to these nascent RNA transcripts generated by RNA polymerase 2 from DNA (Moore and Proudfoot, 2009). These include splicing (removal of introns and eventual formation of exon-junction complexes at sites of exon fusion), 5' capping (with a 7-methylguanosine

cap that protects nascent transcripts from degradation) and polyadenylation (the placement of multiple adenosine residues at the 3' end of the transcript by poly(A) polymerase) followed by chaperoning these transcripts in the form of a messenger ribonucleic particle (mRNP) to the nuclear pore receptor NXF1 (Moore and Proudfoot, 2009; Hung et al., 2010; Viphakone et al., 2012). In eukaryotes, there is a nuclear pore that must be negotiated (Rabut et al., 2004). Macromolecular 'cargo' is exported via nuclear pore complexes made up from aqueous channels known as nucleoporins (Cronshaw et al., 2002; Rout et al., 2000). Such transcripts are eventually permitted into the cytoplasm for translation into proteins and eventually degraded by the RNA decay machinery (Moore and Proudfoot, 2009). Post-transcriptional regulation provides a further level of control, whether this is for homeostatic or quality assurance purposes. Levels of transcripts with quick turnovers and short half-lives can be more tightly regulated, and mRNAs within similar functional groups share similar decay characteristics (Yang et al., 2003). Decay can occur via deadenylation, decapping (both of which permit access of exonucleases to the mRNA). Alternatively, the exosome may be recruited to mRNAs via surveillance mechanisms including nonsense-mediated decay and non-stop decay (where premature stop-codons are erroneously incorporated during splicing (Mitchell and Tollervey, 2003; Wu and Brewer, 2012).

Transcription of pre-mRNA by Pol II: RNA polymerase II (Pol II) has a globular structure with an enlarged central active site wherein the double stranded DNA template to be transcribed is forced apart into two

strands (Moore and Proudfoot, 2009) (Figure 1.3). This site permits nucleotide access (to build the complementary RNA from the single stranded DNA template strand) and RNA exit (Moore and Proudfoot, 2009). Next to this exit channel lies the CTD (carboxyl terminal domain) of the large subunit of Pol II. Reversible phosphorylation occurring at different sites in this domain directs the elongation fate of the transcript (Moore and Proudfoot, 2009). Transcriptional termination requires a poly(A) signal (see later) and termination is triggered by the recognition of this signal and subsequent pre-mRNA cleavage. Cleavage of nascent transcripts at this stage is necessary to optimize mRNA processing downstream (West and Proudfoot, 2009).

5'Capping: This is the first RNA processing event. Pol II transcripts, such as mRNA are marked by an N7-methylated guanine (m^7G) cap that is co-transcriptionally tethered to the 5' end of the RNA. This serves as a signal for appropriate engagement of proteins required for downstream processing such as splicing (Gebhardt et al., 2015; Izauralde et al., 1994). The 'cap' is bound to the RNA by the nuclear cap-binding complex (CBC). This complex has a heterodimer arrangement formed by CBP20 and CBP80 (Izauralde et al., 1995). CBP20 directly associates with the cap and CBP80 (its adaptor) stabilises this interaction (Gebhardt et al., 2015). The ability of CBP80 to bind ALYREF, a component of the canonical Transcription Export Complex (TREX), provides evidence that this process is related to mRNA export. Finally, the cap protects the mRNA from 5'-3'

exonuclease activity (Shatkin and Manley, 2000).

Splicing: Splicing is the removal of non-coding introns from the nascent pre-mRNA. There is a consensus view that the majority of splicing occurs co-transcriptionally. The spliceosome is recruited to actively transcribing genes, and this assembly is coordinated by small nuclear RNA proteins (snRNPs) (Moore and Proudfoot, 2009). The U1 snRNP is the first to associate to the newly formed 5' splice site in the first intron of the transcript followed by U2 and U5 snRNPs when the remainder of the first intron is synthesized (Moore and Proudfoot, 2009). The spliceosome then forms. The exons are joined together to form the RNA coding sequence and an exon-junction complex is deposited at sites of exon-fusion (Le Hir et al., 2001). Splicing occurs more efficiently on transcripts transcribed by Pol II (Moore and Proudfoot, 2009).

Polyadenylation: The presence of a poly(A)⁺ tail on mRNA has been known since the 1970s. Proudfoot et al (1976) showed that pre-mRNA harbours a hexanucleotide sequence AAUAAA "cleavage signal" (Proudfoot and Brownlee, 1976). Once the pre-mRNA is ready for cleavage and polyadenylation, four subunits (WDR33, CPSF160, CPSF30 and hFip1) of CPSF (cleavage/polyadenylation specificity factor) are reconstituted and then polypeptide WDR33 binds to the AAUAAA-containing RNA. Cleavage of the pre-mRNA commences in a reaction stimulated by CstF (cleavage stimulation factor) (Schonemann

et al., 2014; Hirose et al., 1999). Poly(A) polymerase then adds adenosine repeats to the cleaved 3' end of the nascent mRNA.

To facilitate these processes, there are a large number of proteins that bind to mRNA as it matures and progresses towards export. A family of these proteins that bind RNA and facilitate its maturity and nuclear export are known as mRNA export adaptors (Walsh et al., 2010).

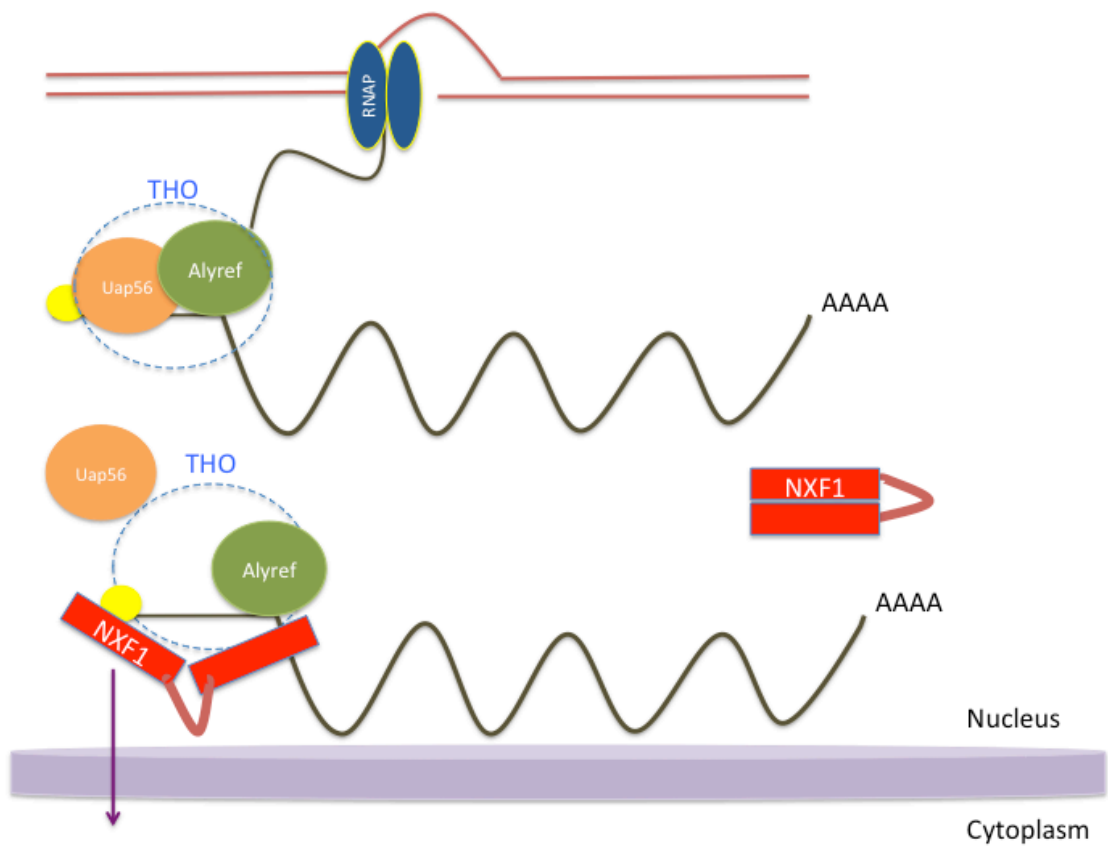


Figure 1.3. Schematic of mRNA processing events. Following transcription, the nascent pre-mRNA undergoes processing events facilitated and driven by the transcription export complex (TREX). Once licensed for export, the mRNP is delivered to the nuclear receptor NXF1, flipping open its resting closed state and driving handover of mRNA for export and translation (Viphakone et al., 2012).

1.7. TREX COMPLEX AND mRNA EXPORT ADAPTORS

Transcription of mRNA is tightly coupled to recruitment of mRNA processing and export factors to form export-competent mRNPs (Iglesias et al, 2008). The transcription export complex (TREX) in humans consists of subunits THOC1, THOC2, THOC5, THOC7, ALYREF, TEX1, UAP56, CIP29, ELG, ERH, POLDIP3, CHTOP and ZC3H11A (Dufu et al., 2010). In 2009, the Wilson laboratory showed that an alternative TREX complex exists in which ALYREF is replaced by UIF (UAP56-interacting protein) and both types of TREX complex may exist on a single mRNA (Hautbergue et al., 2009; Walsh et al., 2010).

The TREX assembly process is driven by the RNA helicase UAP56, and three TREX subunits, ALYREF, UIF and CHTOP harbor a short transient helical peptide, the UAP56-binding motif (UBM), which acts as a binding platform for UAP56 to the rest of TREX (Golovanov et al., 2006; Chang et al., 2013). Fully assembled TREX bound to mRNA provides a signal that nuclear processing is complete and the mRNA is licensed for export as an mRNP cargo (Kohler et al., 2007).

TREX, subsequently, acts as a binding platform for the mRNA export receptor NXF1, which itself forms a heterodimer with NXT1 (also known as P15). On recruitment of the NXF1:NXT1 heterodimer to TREX UAP56 is displaced. In the absence of TREX, NXF1 sequesters its own RNA binding domain through an intramolecular interaction [Viphakone et al., 2012) and this is important to prevent inappropriate binding and export of unspliced mRNA. Once bound to TREX, NXF1 undergoes a

conformational change such that the N-terminal RNA binding domain is exposed and docks onto the mRNA destined for export (Viphakone et al., 2012). This conformational change is dependent on two TREX components, ALYREF and THOC5, which directly bind distinct domains on NXF1. This increases the binding-affinity of NXF1 to RNA by 4-fold (Walsh et al., 2010). Once NXF1 is bound to the mRNA, it escorts the mRNP to the nuclear pore, thus the TREX:NXF1 partnership plays a central role in the mRNA export pathway.

The mRNA export adaptors provide an important quality assurance link between multiple nuclear mRNA processing events and the mRNA export receptor NXF1. They are recruited to mRNA through a cascade of interactions between each other (as described above). Not all is known about the precise interactions of the TREX unit with RNA nor the timings of each event; however, some details have been shown experimentally. The TREX complex is poorly recruited to transcripts that lack a 5' cap and those that have not been spliced. This signifies a prejudice for 'quality controlled' mRNA. Evidence of this is that UAP56 is involved in spliceosome assembly, and is recruited to intronless mRNA (Walsh et al., 2010). Furthermore, ALYREF is recruited to the polyadenylation complex at the 3' end by PCF11 and ALYREF assembles with UAP56 at the 5' end once capping has occurred. This frees up a shared binding site on PCF11 for CLP1, which is involved in 3' end cleavage (Walsh et al., 2010). Lastly, some evidence suggests that certain TREX subunits are required for export of specific mRNAs.

For example THOC5 is required for nuclear export of HSP70 (a heat shock protein), suggesting that TREX subunits may be pivotal for export of differing classes of mRNA (Katahira et al., 2009).

1.8. mRNA EXPORT ADAPTORS AND LINKS TO CANCER

Studies in the past several years highlight important features of the mRNA export process. Experiments on primary tumor specimens indicate that many common and specialized mRNA export factors are deregulated in cancer (Siddiqui et al., 2012). Interestingly, this includes eukaryotic translation initiation factor 4E (eIF4E), ALYREF, and the THO complex. This has positioned these pathways as interesting avenues for interrogation as potential therapeutic targets. For example, (at the time of referencing) specific targeting of the eIF4E-dependent mRNA export pathway in a phase II proof-of-principle trial with ribavirin (an anti-viral drug) led to impaired eIF4E-dependent mRNA export correlating with remissions in leukemia patients (Siddiqui et al., 2012).

It has been known for sometime that the TREX component ALYREF levels are down-regulated in some cancer cells (Dominquez-Sanchez et al., 2009). It is not clear why this is but this finding has led to the quest to find other proteins that may share mRNA binding characteristics with ALYREF that are brought out of redundancy when levels of ALYREF are no longer sufficient. A BLAST search by the Wilson laboratory seeking to identify proteins that shared the UAP56 binding site peptide (UBM) sequence revealed the two proteins, UIF and LUZP4 (Hautbergue et al., 2009). Efforts were focused first on UIF, and data quickly showed that

UIF could function as an mRNA export adaptor. UIF can bind mRNA, UAP56 and NXF1. One interesting difference between ALYREF and UIF was the identification that the histone chaperone FACT (facilitates chromatin transcription) was required to recruit UIF to mRNA through the subunit SSRP1 (but not ALYREF). This became functionally intriguing when work by Gasparian et al (2011) on a group of small molecule inhibitors known as Curaxins was published. They showed that upon inhibition of the FACT molecule by the Curaxins there is an up-regulation of p53 and down-regulation of NFkB, and these inhibitors can kill cancer cells with excellent selectivity (Gasparian et al., 2011). At the time of referencing, Curaxins were in phase 1 clinical trials (Gasparian et al., 2011). One hypothesis is that by trapping FACT onto DNA, UIF can no longer bind mRNA and support mRNA export in cells that may have low levels of ALYREF.

As well as UIF, our BLAST search for proteins that contained the same peptide sequence as ALYREF at the UBM domain [DMSLDDII] found a second candidate *LUZP4*. At the time of project conception, *LUZP4* (also known as CT-8/HOM-TES-85) was a novel, previously uncharacterized cancer testis antigen (CTA). Cancer testis antigens are proteins that are normally only expressed in human testes but are aberrantly expressed in some cancers (Tureci et al., 2002). The first paper to discuss *LUZP4* was by Tureci et al (2002). In this paper, Tureci et al (2002) describe qRT-PCR results performed on cDNA extracted from tumour specimens, that reveal *LUZP4* levels are increased in ovarian, lung, glioma and melanoma cancer cells. Tureci et al (2002)

postulated that LUZP4 might be “involved in cancer associated alterations of transcription or co-transcriptional processes”. Given these conclusions that LUZP4 expression is up-regulated in a range of cancers, and given that LUZP4 showed homology with the canonical mRNA export adaptor ALYREF, we were excited to explore the potential for functional overlap with ALYREF within TREX. We generated the hypothesis that, like UIF, LUZP4 may continue to export mRNAs in some cancer cells that have lost ALYREF.

1.9. CANCER TESTIS ANTIGENS

At the time when this project was devised, there were 70 known families of CTA. As mentioned above, cancer testis antigens are proteins that are normally only expressed in human testes but are aberrantly expressed in some cancers. They reside on the X-chromosome and a key element in their induction is promoter demethylation (Simpson et al., 2005). That they display tumour-restricted expression characteristics, together with a strong immunogenicity, have made CTAs an attractive target for a possible diagnostic and/or prognostic biomarker, or as a chemotherapeutic access point (Fratta et al., 2011).

1.10. DNA DAMAGE

Eukaryotic cell DNA is constantly under attack from exogenous and endogenous DNA damage (Houtgraaf et al., 2006). “Genomic instability is one of the most pervasive characteristics of tumour cells” (Lord and

Ashworth, 2012) and leads to the hallmarks of cancer outlined by Hanahan and Weinberg (2011). Genomic instability occurs through the combined effect of DNA damage (e.g. UV radiation), tumour-specific DNA repair defects (e.g. BRCA1&2 mutations), and a failure to stop/stall the cell cycle before damaged DNA is passed on to progenitor cells (e.g. p53 mutations) (Lord and Ashworth, 2012). Cells have to develop a repertoire of mechanisms to deal with these insults (Pearl et al., 2015; Houtgraaf et al., 2006). Whilst DNA damage and the subsequent genomic instability that ensues, drives disease processes such as cancer, they also provide windows for therapeutic opportunities (Lord and Ashworth, 2012).

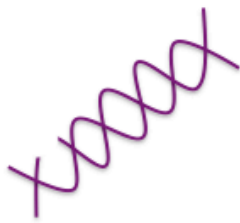
There are numerous types of DNA damage, these include single- and double-strand breaks (breaks across DNA), bulky adduct formation (covalent bonds between DNA and a chemical), base mismatches (non-Watson-Crick base-pairing), insertions and deletions, and base alkylation (transfer of an alkyl group to a DNA base) (see Figure 1.4) (Houtgraaf et al., 2006). Each type of DNA damage is accompanied by a unique type of DNA repair mechanism, which may fail or be subject to modification. The umbrella term for all DNA repair pathways is the 'DNA damage response' (DDR). The DDR can largely be subdivided into three categories: 1) detection of damage 2) recruitment of DDR factors to sites of damage 3) physical repair of damage.

Some of the more familiar DDR pathways include: 1) Base excision repair (BER), in which damaged sections of the DNA helix are removed

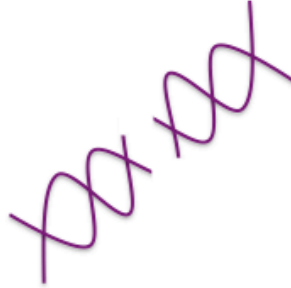
and replaced with 'healthy' new DNA. Poly (ADP-ribose) polymerase 1 and 2 (PARP) are important in this pathway as sensors and signalers of damage (Lord and Ashworth, 2012). PARP will be discussed in detail below. 2) Nucleotide excision repair (NER) is a similar process to BER but is utilised when there are larger breaks in the DNA helix (Lord and Ashworth, 2012; Houtgraaf et al., 2006). Typically in these situations the actual structure of the helix is distorted. Both of these processes are employed in situations of single strand breaks (SSB). When tackling double-stranded DNA breaks (DSBs) the main pathways of repair involve: 1) non-homologous end joining (NHEJ) and 2) homologous recombination (HR). HR involves the use of a complementary sister chromatid to provide the template for new DNA synthesis to match that which has been damaged and resected, again PARP activity is key in this process under certain conditions (e.g. BRCA2 deficient tumours) (Bryant et al., 2004). NHEJ involves the direct repair of the broken ends by sticking them back together. NHEJ is an ongoing process throughout the cell cycle; however, HR is restricted to S and G2 phases (Lord and Ashworth, 2012). Mismatch repair deals with insertion and deletion loops that form during DNA replication. These cause mismatches between bases.

Furthering our understanding of the sequence of DNA damage, and learning how we might predict DNA damage behaviour and rescue such defects are all part of the process of utilizing these pathways to benefit cancer detection and treatments.

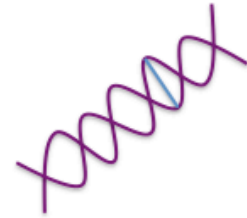
Single strand break



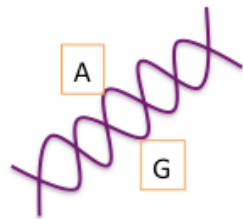
Double strand break



Bulky adduct formation



Base mismatch



Base alkylation

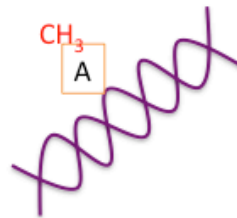


Figure 1.4. Diagram summarizing the DNA damage pathways. Adapted from Lord CJ, Ashworth A. The DNA damage response and cancer therapy. *Nature*. 2012 Jan 18;481(7381):287-94

1.11. POST TRANSLATIONAL MODIFICATIONS

In recent decades the scientific community has discovered that the human proteome contains vastly more proteins than are accounted for by genes in the genome (International Human Genome Sequencing Consortium, 2004). Genomic recombination and alternative splicing are examples of how the resultant proteins coded for by a single gene can be numerous and varied (Ayubi and Van De Ven, 1996) (Figure 1.5). Post-translational modifications (PTMs) are responsible for some of these variances. These changes affect protein activity, localization and function. PTMs are often initiated by an external stimulus such as heat shock or DNA damage. These stimuli may then engage enzymes such as kinases, phosphatases, ligases and transferases to add or remove functional groups and subunits from proteins (ThermoScientific, 2015).

The PTM family consists of phosphorylation, acetylation, ubiquitination, methylation, glycosylation and ribosylation amongst others. This work focuses on poly (ADP-ribosyl)ation (also known as PARylation) as a method of gene regulation. Poly (ADP-ribosyl)ation is one of many post-translational modifications (PTMs) that can alter protein function. To achieve this change in function, the enzyme poly(ADP-ribose) polymerase (PARP) adds one or many ribose moieties (can be in the order of 100's) onto target proteins (Fahrer et al., 2007). This entails the rapid synthesis of long (sometimes 200-300 copies), branched PAR chains (poly (ADP-ribose)) from nicotinamide adenine dinucleotide (NAD^+) (Sato and Lindahl, 1992; Jungmichel et al., 2013). The

glycosidic bonds of the ribose chains may then be cleaved by poly (ADP-ribose) glycohydrolase (PARG). Poly (ADP-ribosyl)ation is a transient and cyclical process, with a half-life of between 1 minute and 8 hours (Alvarez-Gonzalez and Althaus, 1989). Downstream effects are similar to those seen by PTMs such as methylation and ubiquitination (e.g. altered cellular location, altered protein-protein interactions or degradation). Poly(ADP-ribose) (PAR) is rapidly produced at DNA breaks by PARP. This triggers local chromatin relaxation and recruitment of repair factors. Many repair factors have a strong affinity for PAR. The quantity of PAR produced at these sites is reflective of the severity of the insult, and contributes to the cellular decision of whether to initiate survival or cell death programmes (Mortusewicz et al., 2011). In particular, PARP has been shown to be involved in repairing stalled replication forks (Bryant H et al., 2009), which has been recognized as an important mechanism for preventing carcinogenesis (Bartkova et al., 2006).

Mass spectrometry based proteome wide studies of poly (ADP-ribose) targets by Jungmichel et al (2013) and Zhang et al (2013). Identified numerous new targets for this post-translational modification including a large number of RNA binding proteins and proteins involved in RNA processing.

In one study (Zhang et al., 2013) PARylated peptides arising from TREX subunits account for 20% of all identified sites indicating that mRNA export factors are a major intracellular target for poly (ADP-ribose)ation. PARylation sites were identified for the TREX subunits ALYREF,

CHTOP, POLDIP3, ERH, UIF and within NXF1 and NXT1.

Poly (ADP-ribosyl)ation has been shown to occur as part of the DNA damage response mechanism (Fathers et al., 2012) and deregulation of this process may render cells more sensitive to noxious stimuli. We hypothesized that mRNA export factors may be subject to functional changes upon DNA damage and that this would affect global mRNA export.

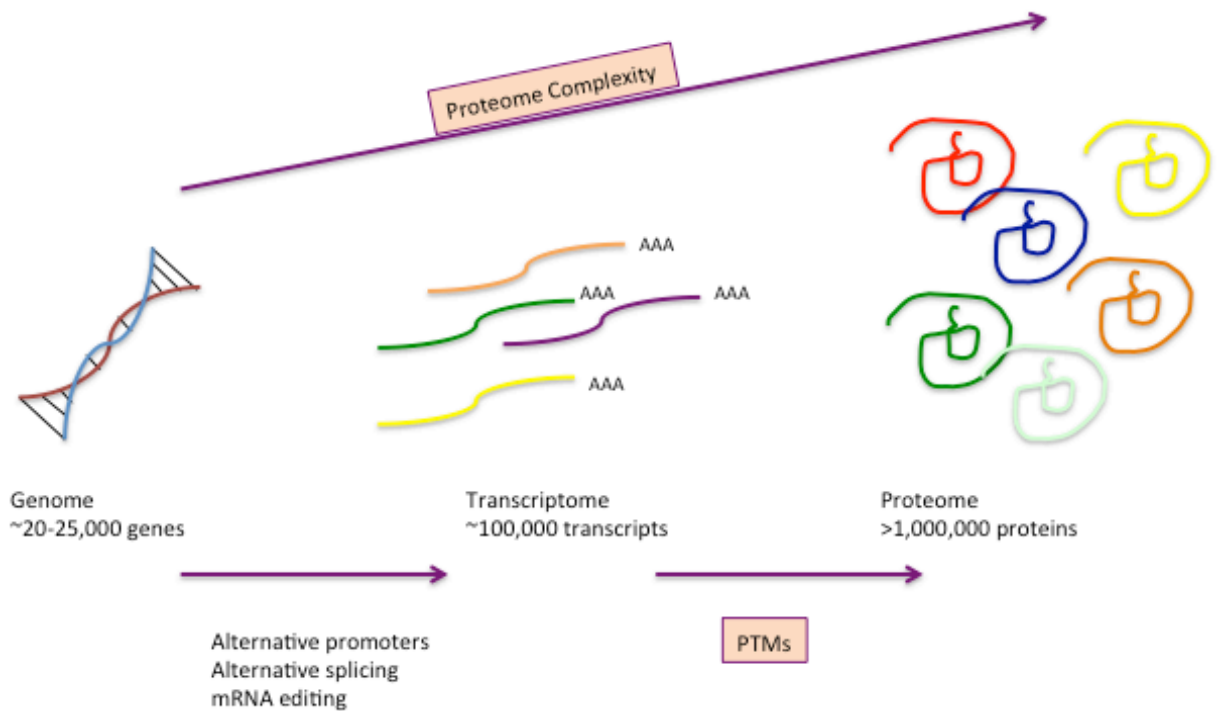


Figure 1.5. Picture illustrating the evolving complexities of the proteome. Adapted from: Overview of Post Translational Modifications, ThermoScientific. [Cited Sept 2015]. Available at URL <https://www.lifetechnologies.com/uk/en/home/life-science/protein-biology/protein-biology-learning-center/protein-biology-resource-library/pierce-protein-methods/overview-post-translational-modification.html>

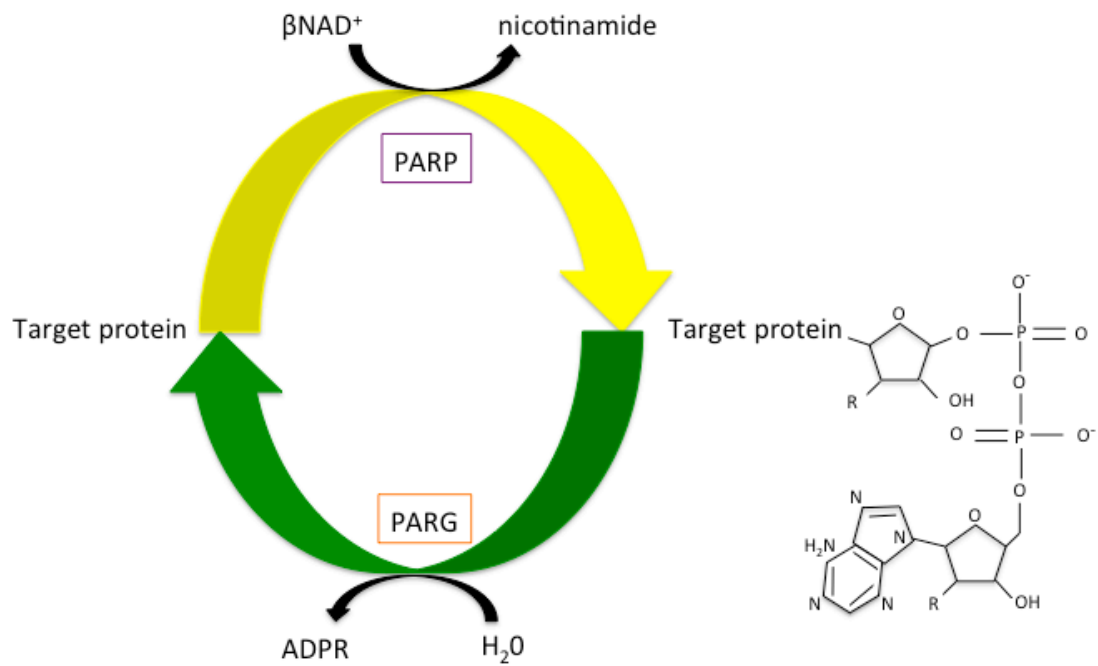


Figure 1.6. Model showing the transfer of ribose moieties on to target proteins by PARP, and their removal by PARG. Image adapted from Mueller-Dieckmann C, Kernstock S, Lisurek M et al. The structure of human ADP-ribosylhydrolase 3 (ARH3) provides insights into the reversibility of protein ADP-ribosylation. *Proc Natl Acad Sci U S A.* 2006 Oct 10;103(41):15026-31

1.12. “SEEING IS BELIEVING”: MODELS FOR MONITORING mRNA EXPORT PATTERNS

RNA localization is the process by which a cell transports and anchors specific RNA transcripts and it is dynamically regulated in cells (Blower, 2013; Strack et al., 2013). Appropriate localization can make cells more efficient (e.g. localizing mRNAs near sites of active translation) and prevent harmful effects (e.g. toxic accumulation at one site) (Blower, 2013). Understanding the cellular localization of RNA can deepen our knowledge of the fate of particular RNAs. In cancer and other diseases, RNA transcripts can be found in the ‘wrong’ place (Baker, 2012) and where the RNA is localized, and under what conditions, may help inform us about cellular events. For example, observing mRNA nuclear/cytoplasmic export blocks during RNAi studies.

RNA localization can be studied using fluorescence in situ hybridisation (FISH) (which uses RNA transcript specific probes that consist of complementary oligonucleotides tagged to a fluorophore (Baker, 2012). FISH has typically relied on cells being fixed on a microscope slide (i.e. there is no ‘live’ image capture). Other assays include MS2 or GFP. MS2 studies involve the co-expression of an MS2-RNA binding protein with a tagged fluorophore and RNA with MS2 binding motifs. Upon binding one another a fluorescence signal is released denoting the location of the RNA (Broude, 2011). GFP (green-fluorescent protein) is a protein composed of approximately 230 amino acids and exhibits a green fluorescence when exposed to/excited by blue light (Tsuji, 2010). The protein was originally extracted from jellyfish (mCherry, a red

fluorophore, is a derivative of this protein). With the GFP tag, expression vectors for GFP fusion proteins can be transfected into living cells and then monitored for localization in different cells and under different conditions (Chudakov et al. 2010).

In recent years, the Jaffrey lab at Cornell University developed a novel RNA monitoring system known as *Spinach*. Spinach is a 98-nucleotide RNA aptamer that binds 3,5-difluoro-4-hydroxybenzylidene imidazolinone (DFHBI), a small GFP-like molecule that is non-fluorescent on its own, but in complexing Spinach forms a bright signal (Strack et al., 2013). It can be genetically encoded into RNA's in order to image RNA in *living cells*. Spinach2 is a second-generation construct that has been modified with more folding complexity to provide a greater level of thermal stability and can fluoresce more brightly (Strack et al., 2013).

The Spinach system may allow the monitoring of RNA export in living cells but little work has been done to map mRNA export using the Spinach2 system. Our final aim in this project was to try and record mRNA export blocks in conditions of DNA damage or in TREX component RNAi cell lines.

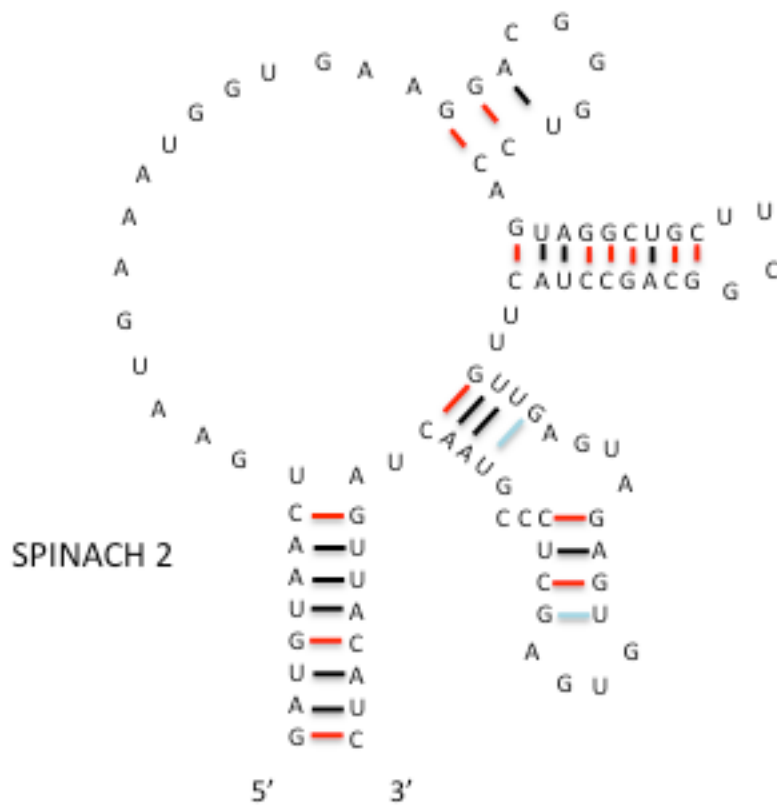


Figure 1.7. Folding of Spinach. Adapted from Strack RL et al, Nat Methods, 2013)

1.13. THE AIMS OF THIS PhD

The clinical need of a reliable biomarker for BC and for new treatment modalities for cancer in general provide a great research opportunity.

At the commencement of this project, there has been much work interrogating possible non-invasive biomarker for BC that might replace the gold standard of cystoscopy. In addition, BC treatment is expensive (NMIBC) and morbid (MIBC) and current chemotherapy regimes for metastatic MIBC achieve unsatisfactory results.

We believed that LUZP4 might provide a potential target that may provide an answer to both of these needs. Furthermore, research into the links between types of DNA damage and the onset of cancer is an ever evolving and exciting field, and this project aims to push forward the frontiers of this branch of molecular biology. In particular, we believe that mRNA export plays a crucial role in this relationship.

Therefore, my project aims are:

- 1) To evaluate the expression pattern of the mRNA export adaptor LUZP4 in a range of cancer cell lines and tissue types
- 2) To investigate the potential of LUZP4 as a biomarker experiments on human urine and bladder tissue
- 3) To examine the extent to which cancer tissues lose expression of ALYREF as an mRNA exporter
- 4) To interrogate the impact of DNA damage on TREX assembly and function

- 5) To determine whether the post-translational modification, poly (ADP-ribosyl)ation, is responsible for observed changes in mRNA export upon DNA damage.
- 6) To develop a model in the Wilson laboratory for monitoring real-time mRNA export using the Spinach-2 system as a means of investigating mRNA export patterns under differing conditions of stress.

However, epidemiological data suggest that the phenotype of BC is changing. As such, I wanted to place these findings into a contemporary picture of BC. Thus, I also undertook systemic reviews of the current epidemiology of BC.

Chapter 2: Materials and Methods

2.1 MATERIALS

2.1.1. CELL LINES

Bladder Cancer cell lines:

Cell line	Body part	Metastatic when harvested	Cell type
RT112-CP3	Bladder	Unknown	Epithelial (TCC)
5637	Bladder	Unknown	Epithelial (TCC)
SW780	Bladder	Lung	Epithelial (TCC)
HT1376	Bladder	Unknown	Epithelial (TCC)
SCaBER	Bladder	Metastatic	Epithelial (SCC)
HT1197	Bladder	Unknown	Epithelial (TCC)
TCC-SUP	Bladder	Bone and Brain	Epithelial (TCC)

NCI-60 cell lines:

Cell line	Body part	Metastatic at harvest	Cell type
MDA-MB-435	Skin	Lungs	Fibroblast (melanoma)
RT112	Bladder	No	Epithelial
RT4	Bladder	Lungs	Epithelial
EJ	Bladder	Lungs	Epithelial
DU 145	Prostate	Bone	Epithelial

PC-3	Prostate	Bone	Epithelial
SK-0V3	Ovary	Lymph node	Epithelial
T47D	Breast	Yes, unknown site	Epithelial
HS578T	Breast	Yes, unknown site	Epithelial
HCT116	Colon	Liver	Epithelial
HT29	Colon	Liver	Epithelial
SW620	Colon	Lymph node	Epithelial
COLO205	Colon	Yes, unknown site	Epithelial
A549	Lung	No	Epithelial
NCIH460	Lung	Lymph node	Epithelial (large cell)
U937	Blood	Unknown	Histiocytic/myeloid
K562	Blood	No	Lymphoblast
HL-60	Blood	Yes, unknown site	Lymphoblast
THP-1	Blood	Unknown	Monocyte
U87-MG	Brain	No	Epithelial

Routine cell lines used in the Wilson Lab:

Cell line	Origin	Use
293T	Kidney	Negative Control for LUZP4 experiments

MeWo	Skin	Positive Control for LUZP4 experiments
HeLa	Cervical	Fluorescence in Situ Hybridization
Cos-7	Monkey	Spinach 2 experiments

2.1.2. BACTERIAL STRAINS

Stain	Genotype	Use
DH5alpha	E.coli supE44	Molecular cloning
BL21 (RP)	E.coli	Recombinant protein production

Antibiotic	Final Concentration
Ampicillin	100 µg/ml
Kanamycin	50 µg/ml (30 µg/ml in LB agar)
Spectinomycin	50 µg/ml
Chloramphenicol	34 µg/ml

2.1.3. GROWTH MEDIA

All media was sterilized by autoclaving.

Luria Bertani (LB): 10 % Tryptone, 10 % NaCl, 5 % yeast extract.

LB Agar: As above, with addition of 2 % Agar w/v.

Terrific Broth (TB): 12 g/L Tryptone, 24 g/L, 24 g/L Yeast Extract, 4 ml/L Glycerol, 2.31 g/L KH_2PO_4 , 12.54 g/L K_2HPO_4 .

2.1.4. VECTORS

PLASMID	FEATURES
PET-24b	Prokaryotic expression vector, T7 promoter, kanamycin resistance, 3' 6 x His-tag. Used for expression of His-tagged recombinant proteins in E.Coli, induced by IPTG
pGEX-6P1	Prokaryotic expression vector, ampicillin resistance, 5'GST-tag. Used for expression of GST-tagged recombinant proteins in E.coli, induced by IPTG.
pcDNA-FRT-TO	Mammalian expression vector containing an FRT site for Flp recombinase-dependent stable integration into the Flp-In 293 genome. CMV promoter, 2 tetracycline operator sequences, ampicillin resistance for plasmid

	selection. Hygromycin resistance for stable integration selection
pCI-neo	Mammalian expression vector, CMV promoter, neomycin resistance

2.1.5. BUFFERS

All buffers requiring sterilization were autoclaved. Those requiring filtration we passed through a 0.2 µm filter.

DNA and RNA protocol buffers

- **6 x DNA loading buffer:** 0.25 % (w/v) Xylene Cyanol; 0.25 % (w/v) Bromophenol Blue; 30 % (v/v) Glycerol.
- **1 x TBE:** 90 mM Tris; 90 mM boric acid; 2.5 mM EDTA, pH 8.0.

SDS-PAGE/western buffers

- **4 x SDS-PAGE Loading Buffer:** 200 mM Tris-HCl, pH 6.8; 1 % (w/v) Bromophenol Blue; 50 % (v/v) glycerol; 10 % (w/v) SDS.
- **4 x SDS-PAGE Stacking Gel Buffer:** 0.5 M Tris-HCl, pH 6.8; 0.15% (w/v) SDS.
- **4 x SDS-PAGE Resolving Gel Buffer:** 1.5 M Tris-HCl, pH 8.8; 0.15% (w/v) SDS.
- **SDS PAGE Running Buffer:** 25 mM Tris; 250 mM glycine; 0.1 % (w/v) sodium dodecyl sulphate (SDS).

- **Coomassie Brilliant Blue Stain:** 0.1 % (w/v) Coomassie Brilliant Blue R-250, 40 % Methanol, 10 % Acetic Acid.
- **Destain solution:** 40 % (v/v) Methanol, 10 % (v/v) Acetic Acid
- **Transfer Buffer:** 39 mM Glycine, 48 mM Tris, 0.037 % (w/v) SDS, 20 % Methanol.

Miscellaneous Buffers

- **1 x PBS (phosphate buffered saline):** 137 mM NaCl; 2.7 mM KCl, 4.3 mM Na₂P₀₄; and 1.47 mM KH₂P₀₄. pH to 7.4 using HCl. 0.1% (v/v) Tween-20 added to make 1 x PBS-Tween (PBST).
- **1 x TBS (Tris buffered saline):** 50 mM Tris-HCl, pH 7.5; 150 mM NaCl. 2 % Tween-20 added to make 1 x **TBST**.
- **3.7% Paraformaldehyde Fixing Solution:** 10 ml 1 x PBS, 33.4 ml 11.1% Paraformaldehyde (pH 7.4), 0.6 ml 30 % Triton X-100, 56 ml Millipore-filled H₂O.
- **ECL Solution #1:** 100 mM Tris-HCl pH 8.5, 2.5 mM luminol; 400 μM p-coumaric acid; **ECL Solution #2:** 100 mM Tris-HCl, pH 8.5; 5.3 mM hydrogen peroxide.
- **FISH fix solution:** A boiled mixture of 33.4 ml Millipore-filtered H₂O, 3.7 g Paraformaldehyde, 20 mls 5 x PBS is made above pH 9 (1 M NaOH is used to achieve this). Once dissolved 180 μL Tritonx100 is added along with 1 M HCl acid to achieve a final pH of 7.4. Final this is filtered using 0.2 μM filter and the volume is made up to 100 mls using Millipore-filtered H₂O.
- **FISH hybridization buffer:** for 100 mls; 20 mls formaldehyde, 10 mls of 20 x saline sodium citrate, 10 g dextran sulphate, 1 g bovine serum

albumin and made up to 100 mls with Millipore-filtered H₂O and stored at 4°C or 20°C. When ready for use the following was added; 1 ng/μL of dt-Cy3, 0.5 μg/ml ssDNA, 0.5 μg/μL tRNA.

- **Crystal Violet Colony Forming Assay Stain:** 0.5 g Crystal Violet (0.05% w/v) 27 ml 37 % Formaldehyde (1%), 10 ml 10 x PBS (1x), 10 ml Methanol (1 %), up to 1 L with Millipore-filtered H₂O.
- **TFB1 buffer:** 30 mM KOAc, 50 mM MnCl₂, 100 mM KCl, 10 mM CaCl₂, 15% glycerol, pH 7.0. **TFB2 buffer:** 10 mM MOPS, 75 mM CaCl₂, 10 mM KCl, 20 % glycerol, pH 7.0.
- **Cobalt buffers: Loading:** 50 mM Tris-HCl (pH 8.0), 1 M NaCl, 5 mM Imidazole, 0.5 % Triton X-100, 10% glycerol. **Wash:** 50 mM Tris-HCl (pH 8.0), 1 M NaCl, 10 mM Imidazole, 0.5 % Triton X-100, 10% glycerol. **Elution:** 50 mM Tris-HCl, 0.5 M NaCl, 200 mM Imidazole, 0.5 % Triton X-100, 10% glycerol.

2.1.6. MOLECULAR BIOLOGY KITS

- **Small scale plasmid DNA purification:** QIAGEN Mini spin preparation kit
- **Midi scale plasmid DNA purification:** QIAGEN Midi spin preparation kit
- **DNA extraction from agarose:** QIAGEN Gel Extraction Kit
- **In vitro transcription/translation:** T7 Quick Coupled Transcription/Translation system (Promega)
- **CLICK-iT:** Life technologies nascent RNA capture kit.

2.2 METHODS

2.2.1 SYSTEMATIC REVIEW AND META-ANALYSIS

Both systematic reviews and meta-analyses were conducted according to accepted protocols (PRISMA) to search recognized databases (PubMed, Embase, Medline). Meta-analysis was performed using the STATA statistical suite (Version 12.0) to generate risk ratios for the outcome of interest.

2.2.2 MOLECULAR BIOLOGY

Polymerase chain reactions (PCR)

50 µl reactions were used containing 10-100 ng DNA template, 1 x reaction buffer, 200 µM dNTP, 0.5 µM each for forward and reverse primers, and 1 unit of DNA polymerase (Biotaq, Bionline). We then used a mastercycler (Eppendorf) to cycle the reactions using the protocol below:

Step	Cycles	Temperature (°C)	Time (minutes)
1	1	96-98 (Initial Denaturation)	0.5-1
2	25-30	96-98 (Denaturation)	0.5
		56-60 (Annealing)	0.5
		72 (Extension)	0.5/Kb product length
3	1	72 (Final Extension)	10

DNA agarose gels

Gels were made using TBE agarose at concentrations of 0.4 to 4% concentrations with the addition of 20µg/ml of Ethidium Bromide. Gel mixtures were typically heated until boiling in a microwave oven before being poured into a gel-cassette and allowed to cool solid.

Cloning

This is the process of introducing a DNA fragment (insert) into a plasmid (vector). PCR is most often used to produce the insert but they can also be liberated from a stock vector in order to transfer it to a new host vector with different genetic properties.

The host plasmids were linearized by digestion with the pre-designed restriction enzymes. 5 µg of plasmid was digested for 2 hours at 37°C with 50 units (U) of each enzyme, followed by 30 minutes incubation with calf intestinal alkaline (CIAP) (1µl at 37°C). The CIAP prevents the plasmid from re-ligating with itself (removes the 5' phosphate). Following this, the plasmid DNA is purified by phenol-chloroform extraction and ethanol precipitation.

In conditions where the required insert was excised from an existing plasmid, to isolate the desired DNA fragment, the digestion products were separated by agarose gel electrophoresis. The desired DNA fragment was cut from the agarose gel with a sterile blade, and then purified using QIAGEN's gel extraction kit. The resultant DNA was ethanol precipitated and re-suspended in Millipore-filtered H₂O.

Where insert fragments were generated by PCR, the primers required were designed with the required restriction sites juxtaposed by 6 additional 5' bases. These were incorporated to provide a 'landing platform' for the restriction enzymes. After amplification using the above protocol, the reaction mix was gel extracted and digested overnight at 37°C with 100 U of the chosen restriction enzymes. Digestion reactions were phenol-chloroform extracted and ethanol precipitated before re-suspension with Millipore-filtered H₂O.

Spinach 2 concatemers were made using the following PCR primers:

```
5'GGCGCTCGAGGCCCGGATAGCTCAGTCGGTAGAGCAGCGGCCG
GATGT
3'CCGCCGTCGACTGGCGCCCGAACAGGGACTTGAACCCTGGACC
CGCGGCCCGG
```

DNA ligation

To determine relative DNA concentrations, and to ensure that linearization was complete, samples were run on an agarose gel. After this, 100 ng of linear vector was added to the insert DNA, along with 10 U of T4 ligase (Roche) in 1x T4 ligase buffer (Roche). These ligation reactions were standardly incubated at 16°C overnight. Half of the ligation mix (typically 5-10 µl) was transformed into competent E.coli.

Phenol chloroform-isoamyl alcohol DNA purification

One volume of phenol chloro-isomyl alcohol (25:24:1, pH 6.6/8) was added to DNA solution. Mixture was vortexed for 1 minute and then centrifuged for 5 minutes at 13,000 rpm. The upper phase was transferred to a fresh tube and 2.5-3 volumes of 100% ethanol were added. 3 M Sodium acetate (pH 5.3) was also added to a final volume of 10 %. This mixture was incubated on ice or -20°C for 20 minutes and then centrifuged for 20 minutes 13,000 rpm. The supernatant was removed and discarded before 1 ml of 70% ethanol was added. The sample was then centrifuged again for 20 minutes at 13,000 rpm. The supernatant was discarded and the pellet was air-dried. Dried pellets were then re-suspended in the required volume of Millipore-filtered H₂O.

Isolation of plasmid DNA from E.Coli

For spin-prep/mini-preps, 3 mls of LB medium containing the correct selection antibiotic was inoculated with a single E.coli colony. The culture was then placed in a rotating incubator at 37°C overnight. For midi-preps, 50 mls of LB medium was used. Before storage at -20°C, the DNA plasmid was purified using the appropriate QIAGEN kit.

DNA restriction digest

Restriction digests were performed using the optimal buffer/enzyme combination as per the manufacturer (Thermoscientific). The enzyme content never exceeded 10 %. This was to avoid an excess glycerol concentration. Digestions were carried out at 37°C for 1 hour unless

fast-digest enzymes were available, in which case restrictions lasted for 30-45 minutes.

Chemically competent E.Coli

Overnight cultures were prepared by inoculating the appropriate strain in 10 ml LB then incubated at 37°C. This culture was used to inoculate 500 ml LB to a final density of $OD_{600} = 0.05$ and incubated at 37°C until $OD_{600} = 0.48$. The cells were placed on ice for 10 minutes before being centrifuged at 600 x G at 4°C for 10 minutes in pre-sterilized centrifuge pots. The resulting pellets were re-suspended in 250 ml, ice cold, filter-sterilized TFB1 and then left on ice for 10 minutes before being centrifuged again. The resulting pellet was then gently re-suspended in 25 ml ice cold, filter-sterilized TFB2 and left on ice for 10 minutes. The suspension was then aliquoted into sterile, pre-cooled eppendorf tubes kept in a tray half submerged in liquid nitrogen. The tubes were then flash frozen in liquid nitrogen and stored at -80°C.

Transforming chemically competent E.Coli

DH5alpha or BL21 (RP) cells were defrosted on ice for 20 minutes alongside the defrosting aliquot of DNA to be transformed. After 20 minutes, the DNA was added to the cells, mixed gently and left to rest on ice for a further 20 minutes. The cells were then subjected to a heat-shock for 5 minutes at 37°C or 30 seconds at 42°C and recovered on ice for 10 minutes. Following this 900 µl of sterile LB media was added to the cells and they were placed in a 37°C incubator, rotating at 200 rpm

for 1 hour. The cells were then centrifuged at 7200 rpm for 1 minute. 900 µl of the supernatant was discarded and the cell pellet was then resuspended in the remaining supernatant and spread over pre-warmed and pre-dried LB agar plates made with the correct antibiotic selection.

***In vitro* site-directed mutagenesis**

This method uses standard PCR to introduce a single or multiple nucleotide changes into a wild-type sequence. Primers were designed to mutate the target nucleotides by positioning said target in the centre of flanking nucleotides from the WT sequence (between 18 and 24 depending on the number of nucleotides to be mutated) to ensure adequate annealing. Reactions contained: 100 ng DNA plasmid, 125 ng each primer, 200 µM dNTP, 2.5 Pfu Turbo polymerase and 1 x Pfu Turbo polymerase buffer in a final volume of 50 µl.

The PCR cycle for these reactions was carried out according to the parameters below:

Cycles	Temperature (°C)	Time (min)
1	95	0.5
25	95	0.5
	55	1.0
	68	1.0/Kb plasmid size

Following this, samples were Dpn1 treated for 1 hour at 37°C, with the aim of removing methylated DNA. These reactions were then ethanol precipitated and transformed into E.Coli (DH5alpha). Colonies were sent for sequencing.

Mutations were made using site directed mutagenesis with the following sequence primers:

Wild Type UAP56: KDFQRRIL:

5' AAAGATTTTCAACGACGAATTCTT

3' AAGAATTCGTCGTTGAAAATCTTT

UAP56 with mutation KDAQRRIL:

5' TATCAGCAGTTTAAAGATGCGCAACGACGAATTCTTGTG

3' CACAAGAATTCGTCGTTGCGCATCTTTAAACTGCTGATA

UAP56 with mutation KDAARRIL:

5'
TATCAGCAGTTTAAAGATGCGGCCGACGAATTCTTGTGGCTACC

3'
GGTAGCCACAAGAATTCGTCGGGCCGCATCTTTAAACTGCTGATA

Polyacrylamide gels

Throughout the experiments 6 %-15 % acrylamide gels were used.

These consisted of an upper and a lower gel component containing a variable mixture of deionized water, 30 % acrom/0.8 % biscocryl (acrylamide), tris-buffers, TEMED and 10 % APS.

Western blotting

40 µg of whole cell lysates were added to 4 x SDS page loading buffer and boiled at 90 degrees for 3 minutes to denature the proteins.

Samples were then loaded onto the polyacrylamide gel and run at 35 mAmps for approximately 1 hour or until the migration of the dye was deemed complete. The gel was then transferred onto a nitrocellulose membrane using 150 mAmps current for 1-2 hours. Membranes were then incubated in 5% milk (made in TBST) for 1 hour and then washed in TBST three times. Membranes were then incubated in milk containing a primary and relevant secondary each for 1 hour, followed by three more TBST washes each for 5 minutes. Finally, the membrane was washed in 1 ml of ECL 1 & and 1 ml of ECL 2 (mixed) for 1 minute and then the membrane was exposed on the Biorad gel-doc system to look for protein bands.

Total RNA extraction and quantitative real time polymerase chain reactions

Cells pellets were lysed using reporter lysis buffer (5x) and water. 230 µls of lysate per cell line was kept on ice in a micro-centrifuge (eppendorff) tube and mixed in trizol at a ratio of 1:3. Once homogenized, 200µl of chloroform was added to each cell line and homogenized by repeated shaking and inversions of the eppendorff tubes. Each was then left to stand for 5 minutes at room temperature before being centrifuged at 11200 rcf for 10 minutes. All supernatant was then transferred to new eppendorffs and added to isopropanol

(volume 1:1) and 0.5 µl of glycogen. This solution was again homogenized by several inversions before a further 10 minute incubation at room temperature and a centrifugation at 16100 rcf. The new supernatant was discarded and the cell pellet washed with 1 ml of 70 % ethanol. The pellets were then spun at 16100 rcf for 5 minutes. The supernatant was again discarded and the cell pellet was dried at room temp for 15 minutes.

The next step in RNA extraction and cDNA synthesis was DNase treatment of the pellets. Each pellet was re-suspended in a mix of 44 µl water and 5 µl 10x buffer that was homogenized by pipetting. 1µl DNA 1 Roche (RNase-free) was added and gently homogenized followed by a 30min incubation at 37c. Once incubated a further 50 µl of water and 100 µl of RNA phenol (pH4.7) was added and vortexed to form a white emulsion. The mix was then centrifuged at 16.1 x 1000 rcf for 5 minutes. 90 µl of supernatant was then transferred to new tubes for precipitation with 10 µl sodium acetate (pH 5.8), 400 µl of 100 % ethanol and 0.5 µl glycogen. This was centrifuged for 30 minutes at 16100 rcf. The pellet was then washed in 70 % ethanol and spun for a further 8 minutes at 16100 rcf and air dried for 15 minutes following removal of the supernatant.

RNA concentrations were then calculated using the Nanodrop (ThermoScientific). Pellets were re-suspended in 10 µl of water and 1 µl samples run through the Nanodrop. Once concentrations were known, cDNA synthesis was conducted by first adding polyDN to the RNA mix and denaturing at 70°C in the PCR machine, followed by the addition of

4 µl buffer 5x (Bioscript), 4 µl of 250 mM dNTPs and 0.5 µl reverse transcriptase (Bioscript) and a run of PCR. The PCR programme was set to incubate at 25°C for 10 minutes, perform cDNA synthesis for 1 hour by incubating at 42°C, followed by inactivation of reverse transcriptase by incubating for 10 minutes at 70°C.

Once the cDNA was produced, samples were diluted by the addition of 20 µl-80 µL of deionized water and homogenized. A qRT-PCR robot was then used to mix 4 primer stocks (1 µg/µl diluted to 20 x final), with Sybr green (sensimix 2 x, Bioline) and water. 10 µl final volume samples, in duplicates, of each cell line plus a no template control sample was loaded to each mix in the qRT-PCR tubes and a 'three steps with melt' qRT-PCR programme was cycled to provide our results.

LUZP4 RT-PCR primers were:

Forward: 5'-GGAGAGGCTACTCAAGATGCAGAAGC-3'

Reverse: 5'-GAGATCACTCTGAGTGTCCACAAGATCTCC-3'.

U1 RT-PCR primers were:

Forward: 5'-ACCTGGCAGGGGAGATACCA-3'

Reverse: 5'-GGGGAAAGCGCGAACGCAGT-3'

GST-Tagged Proteins

Cell pellets were resuspended in 1 x PBS + 0.1 % Tween (PBST) using at least 5 times the pellet volume. The suspension was supplemented with protease inhibitors before sonicating on ice at 15 microns to lyse the cells. The lysate was then centrifuged at 16000 rcf at 4°C to pellet

the cell debris and the supernatant was applied to glutathione sepharose beads. This mix was incubated at 4°C on a rotating wheel for 1 hour. The beads were then pelleted by centrifugation at 400 rcf and the supernatant discarded. Beads were then washed 3 times with ice cold PBST. Proteins were then eluted by the addition of GSH elution buffer at 2.5 times the bed volume of the beads and then incubated on ice for 15 minutes with regular agitation. After centrifugation at 400 rcf, the supernatant was transferred to a fresh tube, and then stored at 4°C or -80°C.

6 x Histidine-Tagged Proteins

Cell pellets were re-suspended in cobalt loading buffer and then supplemented with protease inhibitors before sonication and centrifugation (as per GST-Tagged Proteins). This time, the supernatant was applied to Cobalt sepharose beads and incubated on a rotating wheel for 1 hour at 4°C. The beads were then washed with a cobalt wash buffer. Proteins were eluted using a cobalt elution buffer and incubated for 30 minutes on ice with regular agitation. The supernatant was then stored at 4°C or -80°C.

Gibson Assembly

This facilitates the joining of overlapping DNA fragments in a single isothermal reaction. In the first step, an exonuclease creates single stranded 3' over-hangs to permit annealing of fragments that share complementarity at one end (overlap). Steps 2 and 3 involve a DNA

polymerase and ligase to fill fragment gaps and seal the nicks in the DNA [Gibson Assembly Mastermix guide Vsn 3.2].

RNA interference

RNAi hairpins were designed and constructed according to the Block-IT kit manual (Invitrogen). The designed pre-miRNA sequences were cloned into pcDNA 6.2GW miR vector. When transfected into cells, these vectors were used to “knockdown” the levels of the mRNA for which the pre-miRNA was specific. In order to create a stable RNAi cell line, successful hairpins were cloned into the pcDNA5-FRT-TO-His vector.

Transfections

Cell lines were transfected with the appropriate concentrations of DNA plasmid in accordance to manufacturer’s guidelines using Turbofect (gelifesciences) as a transfection agent diluted in Hyclone MEM-RS media (Thermoscientific). Cells were typically transfected one day following splitting and plating.

Stable cell lines

This involves the production of a stable mammalian cell line exhibiting tetracycline inducible expression of a gene of interest from a specific genomic location [LifeTechnologies]. To do this, an expression vector for the gene of interest is integrated into the genome via a Flp recombinase-mediated DNA recombination at the FRT site under the

control of a tetracycline-inducible promoter [O’Gorman et al, Science.1991]

On day zero the FlpIn-293 cells were split in DMEM+FCS-Tetracycline free media without any selection drugs, into a 6cm dish. One day following this, the cells were transfected with 4.6 µg of recombinase (pPGKFLPobpA) and 2.4 µg of FRT vector DNAs with 12 µL of Turbofect and 600 µL of Hyclone MEM-RS media. On day two, the media was renewed with DMEM+FCS-Tetracycline free without selection antibiotics. On the morning of day 3 the cells were split into 2 x 10cm dishes in DMEM+FCS-Tetracycline free media. On the same afternoon, the medium was changed to selection media (DMEM+FCS-Tetracycline free media + Hygromycin 0.1 mg/mL and Blastocidin 15ug/mL). Two days later, all dead cells were removed and the selection media was renewed. After 5 further days, the medium was again renewed. At this stage, the plates were inspected to ensure that all cells appeared dead. Over the next two weeks, the plates were observed for the formation of new patches of cells. Once these were confluent, the dishes were split into a T75 flask. If specific colonies were to be tested and used (as with the PARG RNAi cell line), then instead of splitting the cells into a T75 flask, cloning disks (Sigma) coated in trypsin were placed on a few identified colonies in the 10cm dishes. These disks were then placed in a 24 well plate with selection media. Following this, each colony was grown further and put into routine cell culture. Some of the cells were siphoned off, induced with tetracycline and tested for knockdown efficiency.

PARG cDNA sequences used for building PARG RNAi cell line:

5' GGGCCCGAATCATGAATGCGGGCCCCGGC

3' GGGCCCCTCGAGGGTCCCTGTCCTTTGCCCTG

DNA sequencing

The sequence of cloned inserts was checked by industrial DNA sequencing at Source biosciences' Nottingham laboratory. Various primers were used, including stock primers for T7/T3 promoters. Inserts were shipped at 100 µg/µL in 10 µL total volume. Fidelity of the sequence was checked using *SerialCloner*.

2.2.3. BIOCHEMISTRY

In vitro GST-pulldown assays

GST-tagged proteins were purified as above and used as a target for radiolabelled proteins produced in rabbit reticulocyte lysate using the T7 Quick Coupled Transcription/Translation system (Promega).

Reactions were conducted on ice using RNase free eppendorf tubes.

Reactions in 10 µl final volume contained: 1.5 µl plasmid DNA (usually 200 ng), 0.5 µl S³⁵ methionine and 8 µl of reticulocyte lysate from the Promega kit. The reaction mix was homogenized and then incubated at 30°C for 1 ½ hours at room temp. 1-2 µl of this reaction mix was kept as an input for the pulldown and mixed with RNase-free water and 4 x SDS page loading buffer to a final volume of 10 µl. The remaining lysate was

incubated on a rotating wheel at 4°C for 1 hour in a bead mixture with the purified GST-tagged proteins (10-20 µl bead volume) in 400 µl of PBST binding buffer. When investigating direct binding between proteins, 10 µg/ml of RNase A was added to ensure interactions were not bridged by RNA.

Following this incubation, the beads were washed x 3 with 1 ml of PBST. After the final wash the supernatant was discarded and the beads were dried using gel-loading tips to ensure no unspecific binders were included in the elution. Elutions were performed using 3 x bed volume of 1 x SDS page loading buffer and incubating the mixture at 95°C for 5 minutes. The mixture was then centrifuged at 400 rcf for 1 minute. Using a gel-loading tip to avoid inadvertently aspirating beads, 2 x bed volume of supernatant was extracted and placed in a new eppendorf ready for loading onto a polyacrylamide gel. Following gel electrophoresis the gel was incubated in Coomassie Brilliant Blue stain for 30 minutes, followed by de-staining (using a methanol/acetic acid solution) and gel drying. The dried gel was then exposed to a phosphor screen, typically for at least 16 hours. The screen was then scanned in a phosphorimager (Biorad) to produce the phosphor image.

***In vivo* Immunoprecipitations**

Protein glutathione sepharose beads were incubated with 10 µg of antibody at 4 °C over night the night before the IP. Two 15 cm dishes per condition of 293T cells were also plated the day before the experiment. Each plate was lysed in 5 mls of IP lysis buffer (2.5 mls 1 M

Hepes-NaOH pH 7.5, 1.67 ml 3M NaCl, 0.1 ml 0.5 M Edta pH 8.0, 0.25 ml triton x 100, 5 ml glycerol 100 %, 50 µl 1M DTT), and spun down at 16100 rcf for 3 minutes. The concentration of protein in the supernatant was ascertained by spectography and the maximum, equal, possible amount loaded across conditions and added to 50 µl of protein glutathione sepharose beads that were pre-washed three times in IP lysis buffer. Next was an incubation on protein glutathione sepharose beads for 1 hour at 4 degrees. IP wash buffer (IP lysis buffer at pH 8.0 with 5 mM imidazole) was applied three times. The protein was eluted off the beads using an acid shock of 90 µl of 0.5 M L-arginine HCL pH 3.5 applied for 2 minutes and then spun down for a further 1 minute at 400 rcf. Eluate was buffered by addition of 1.75 µl 1.5M TRIS-HCl pH8.8. 20 µl of protein eluate was then added to 4x SDS page loading buffer and a western blot was performed as above.

2.2.4. CELL BIOLOGY

Tissue culture

Tissue culture was performed on a twice-weekly basis. We used primarily human cells, which were stored in incubators at a constant temperature of 37°C with CO₂ levels also kept constant at 5%.

Depending upon the number of cells required for downstream use, cells were kept in T175, T75 or T25 sterile flasks in Dulbecco's Modified Eagle Media (DMEM media) (Life Technologies)) with 10% Fetal Calf Serum (FCS) and 1% (v/v) penicillin/streptomycin (Life Technologies), with or without selection antibiotics. When cells reached confluency they

were split at 1/4 or 1/5 ratios. During cell splitting, the media was removed and the cells were washed in 1 x PBS. Cells were then detached from the flask surface using trypsin EDTA (1ml for a T75). Once cells were detached, the trypsin solution was neutralized by the addition of DMEM media. Cell suspensions were then distributed into new flasks or plated for use. All the above was conducted under a sterile fume hood in a specified tissue culture room.

Cell pelleting and storage

A standard protocol was used in each experiment to minimize error.

The first step was to examine the flask/plate under a microscope to check for cell health and confluence. Once a clear layer of cells was apparent the cells were considered eligible for harvesting.

The next step was to remove the FCS from the cells and wash them with 5mls of 1 % PBS solution. For T75 flasks, once the PBS was removed, 1 ml of trypsin was added to each flask, which was then tapped until all cells became non-adherent. Finally, 5 mls of medium was added to the flask and the contents were siphoned into a 15 cm falcon tube (kept on ice) for centrifugation. Cells were centrifuged at 500 rcf for 5 minutes and the supernatant was discarded. The cell pellet was then re-suspended in 1 % PBS and centrifuged for at 500 rcf for a further 5 minutes. All supernatant was completely discarded at this stage and the cell pellets were frozen in liquid nitrogen and stored at -80°C.

Immunohistochemistry

Formalin fixed, paraffin embedded human bladder cancer tissue was sectioned and wax-mounted on slides for storage. These were dewaxed using xylene washes x 2 for 10 minutes. The samples were then rehydrated using sequential washes in 100 %, then 95 % ethanol for 2-3 minutes each. The slides were then incubated in an H₂O₂/Methanol (30 ml H₂O₂ + 270 ml methanol) mix at room temperature for 20 minutes. This was washed using running tap water for 5 minutes. For antigen retrieval the slides were incubated in a slide rack in 0.01 M citrate, which was boiled in a microwave for 4 minutes and then allowed to cool on the bench for 10 minutes. Following this the slides were rinsed using PBST for 10 minutes before blocking with Avidin/biotin for 30 minutes immediately followed by a second block with 10 % goat serum for another 30 minutes.

The primary antibody (diluted in 2% goat serum) and negative controls (1 x PBS with 2 % goat serum) were then added to the slides (1 ml per slide). This incubation was typically for 2 hours or overnight in the fridge (4-8°C). Following this the slides were washed in 1 x PBS for 2 x 5 minutes. A secondary antibody was then added (goat anti-mouse biotinylated) at the desired dilution in 2 % goat serum for 1 hour at room temperature. Next a couple of drops of a premixed Avidin Biotin Complex ((ABC) Vecta Shield) was added to each slides followed by 3 x 5 minute PBST washes. Following this a DAB mixture (Vecta Shield) with H₂O₂ and buffer was added to the slides for between 4 and 10 minutes (the slides were observed for a brown colour saturation

signifying when the incubation was long enough) followed by another wash with running tap water for 5 minutes. Gills haematoxylin dye was added for 1 minute followed by a second wash in tap water. Finally the slides were re-dehydrated using incrementally more pure ethanol (70 %, 90 %, 95 %, 100 %) to incubate the slides in for 3 minutes a time. The slides were then mounted after a brief submersion in Xylene with poly para-xylene (PPX).

Fluorescence in situ hybridization (FISH)

Typically 293T or HeLa cells were used in 24-well plates with coverslips. On the day of processing, the media was first aspirated and then the slides were washed with 1 x PBS three times. 150-200 μ L of FISH fix solution (see miscellaneous *buffers*) was added to each well and left to incubate for 20-30 minutes under the fume hood. This was followed by three washes with 500 μ L of 1 x PBS to remove the fix. The slides were then placed on 3 mm Whatmann filter paper and placed in a 60 mm Petri-dish. 100 μ L of FISH hybridization buffer (see miscellaneous *buffers*) was added to each slide and left to incubate at 37°C for 2 hours. This was followed by another three washes with 1 x PBS. The slides were then mounted using mounting glue (Vecta Shield) containing DAPI. This was sealed and left to dry overnight. Slides were stored at 4°C.

For immuno-staining, a similar process was followed, however, after the hybridization incubation the slides were incubated with 100 μ L of a primary antibody diluted in 1 x PBS with 1 % BSA for 1 hour at room

temperature in the dark. A secondary antibody was added following three 1 x PBS washes for 30 minutes in the dark, also diluted in 1 x PBS with 1% BSA.

Colony counting assays

Plated cells were subjected to different levels or types of DNA damage one day after plating into a 6 well plate. Each well was subjected to DNA damage for a period of 7 days. At 7 days, the media was removed and a staining solution (crystal violet) was added (enough to cover base of well (typically 1 ml). This was left for 20 minutes at room temperature and then carefully removed using slowly running tap water washes. The plates were left to air dry and then counted by eye using a hand held cell counter.

Nascent mRNA capture

Control RNAi and PARG RNAi cells were plated in an 'Ibidi' 8 well dish and induced every 48 hours for 72 hours. Following this the cells were labeled using 1 mM 5-ethynyl uridine (diluted in 250 μ l of DMEM + 10 % FCS media) incubation for 1 hour at 37°C. The media was then changed and the cells were subjected to 2 mM H₂O₂ and left to incubate for 0 to 8 hours (0 time point cells were collected immediately following H₂O₂ treatment). After the incubation with H₂O₂ the media was removed and cells were washed once in 1 x PBS and then fixed using the FISH fix solution for 15 minutes. The cells were then washed in 1 x PBS a further

time and permeabilised using an incubation of 250 μ L of 0.5 % Triton X 100 in 1 x PBS for 15 minutes at room temperature. Next 1 ml of *Click-iT* reaction mixture was added to the cells and incubated for 30 minutes as per protocol (see Life Technologies). The cells were given a last wash using *Click-iT* rinse buffer and then mounted on slides. The slides were then examined under the microscope.

Chapter 3: The role of tobacco

smoke in bladder cancer

Work in this chapter contributed to the publication of:

Cumberbatch MG, Rota M, Catto JW, La Vecchia C. (2015) **The Role of Tobacco Smoke in Bladder and Kidney Carcinogenesis: A Comparison of Exposures and Meta-analysis of Incidence and Mortality Risks.** Eur Urol. Jul 3. pii: S0302-2838(15)00548-5

Herein, I investigate part one of the contemporary landscape behind the epidemiology of bladder cancer (BC).

3.1. SYSTEMATIC REVIEW AND META-ANALYSIS OF RISK OF BLADDER CANCER IN SMOKERS

Tobacco smoke is the commonest cause of BC and includes a mix of carcinogens implicated in the aetiology of BC. In general, the WHO estimates that in 2013 there were more than 1 billion smokers worldwide (Islami et al., 2015) and around 6 million people die each year from tobacco related illnesses. The risks of tobacco related illnesses vary with the duration and intensity of smoking (Freedman et al., 2011; Samanic et al., 2006), together with the type of tobacco and mode of

administration (cigarettes versus pipe smoking or chewing), and an individual's ability to detoxify (Samanic et al., 2006). What is less clear is whether smoking cessation reduces the risk of BC to baseline.

Tobacco may be prepared through flue (blonde) and air curing (black). The latter contains a greater concentration of nitrosamines, biphenyls and arylamines and is hence thought to be more carcinogenic (Samanic et al., 2006; De Stefani et al., 1991; Momas et al., 1994). With regards to carcinogen detoxification, variations in the activity of NAT2 (N-acetyltransferase 2) and GSTM1 (Glutathione S-transferase Mu 1) due to polymorphism appear to affect cancer risk from smoking (Burger et al., 2013). It is also evident that tobacco smoke can induce changes in the DNA damage response (DDR) machinery which can additively/synergistically impair the host response to carcinogens (Borzym-Kluczyk et al., 2009; Rouissi et al., 2011). I look more closely at the DDR in Chapter 6.

I conducted a systematic review and meta-analysis of the literature to: better understand the contemporary relationship of tobacco smoking in the epidemiology of BC, to facilitate an understanding of the current most 'at risk' populations and to evaluate whether smoking cessation does reduce risk (and by what margin).

3.2. DATA ACQUISITION

I commenced this systematic review in August 2013 with myself as lead author and three other senior co-authors (full methods are explained in

Cumberbatch et al., 2015a). Briefly, the PubMed database was searched for all to-date original articles in English using the string terms 'tobacco', 'smoking' AND 'bladder cancer'. Articles were included in the meta-analysis if they met the following inclusion criteria: i) case-control, cohort or nested case-control studies published as original articles in English investigating the relationship between smoking and the risk of BC in humans ii) the outcome was incidence or disease-specific mortality (DSM) and iii) odds ratio (OR), hazard ratio (HR) or relative risk (RR) estimates with their 95% confidence intervals (CI), or enough information to calculate them, were reported. We excluded summary data (reviews) and reports not focusing on our research question or describing molecular effects in cell lines. We report our findings in accordance with the PRISMA guidelines (Moher et al, 2009). If multiple RRs or ORs were presented in the original articles, we extracted the estimates from the maximally adjusted model in order to reduce the risk of possible unmeasured confounding (Greenland, 1987).

Because cancer is a relatively rare outcome, we assumed that ORs, risk ratios and rate ratios were all comparable estimates of the RR. To conduct the meta-analysis, measures of association and the corresponding CIs were translated into $\log(\text{RR})$ s and their variances.

3.3. CURRENT SMOKERS HAVE THE GREATEST BC RISK INCIDENCE AND MORTALITY

We identified 2,683 papers, of which 83 studies investigating BC met the inclusion criteria. The pooled relative risk (PRR) of BC incidence in “all”-smokers was 2.53 (95% CI 2.37-2.80), in “current”-smokers was 3.47 (3.13-3.88), and in “ex”-smokers was 2.04 (1.85-2.25). The pooled RR of BC disease specific mortality risk (DSM) was 1.47 (1.20-1.84), 1.43 (1.24-1.75) and 1.44 (0.99-2.11) in “all”, “current” and “ex” smokers, respectively.

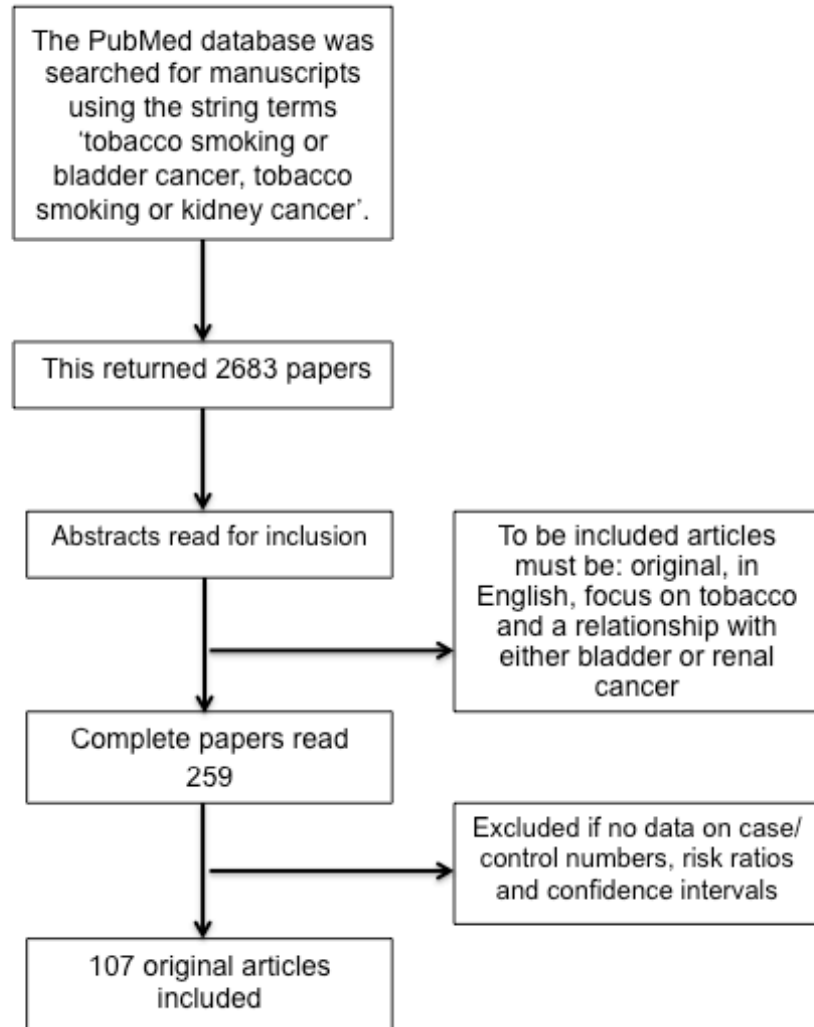


Figure 3.1. Consort flow diagram demonstrating the search strategy for the systematic review.

	Incidence			Mortality		
	No. of comparisons [†]	Pooled RR (95% CI)	I ² % (p for heterogeneity)	No. of comparisons [†]	Pooled RR (95% CI)	I ² % (p for heterogeneity)
All cigarette smokers						
Case-control studies	109	2.76 (2.50-3.05)	89.8 (<0.001)	--	--	--
Cohort studies	37	2.17 (1.89-2.48)	82.7 (<0.001)	12	1.47 (1.24-1.75)	30.9 (<0.001)
Overall	146	2.58 (2.37-2.80)	87.9 (<0.001)	12	1.47 (1.24-1.75)	30.9 (<0.001)
Ever cigarette smokers						
Case-control studies	47	2.46 (2.13-2.84)	89.1 (<0.001)	0	--	--
Cohort studies	6	1.80 (1.19-2.73)	78.0 (<0.001)	3	1.57 (1.16-2.12)	0.0 (0.5)
Overall	53	2.38 (2.08-2.72)	90.1 (<0.001)	3	1.57 (1.16-2.12)	0.0 (0.5)
Current cigarette smokers						
Case-control studies	33	3.84 (3.29-3.47)	80.2 (<0.001)	0	--	--
Cohort studies	13	2.53 (2.27-3.47)	84.5 (<0.001)	5	1.45 (1.12-2.09)	42.0 (0.1)
Overall	46	3.47 (3.07-3.91)	80.9 (<0.001)	5	1.45 (1.12-2.09)	42.0 (0.1)
Ex cigarette smokers						
Case-control studies	29	2.18 (1.87-2.54)	78.1 (<0.001)	0	--	--
Cohort studies	18	1.92 (1.72-2.15)	63.3 (<0.001)	4	1.44 (0.99-2.11)	53.1 (0.09)
Overall	47	2.04 (1.85-2.25)	78.6 (<0.001)	4	1.44 (0.99-2.11)	53.1 (0.09)

[†] Some studies may include separate estimates for males and females, and for smoking category.

Figure 3.2. Pooled relative risks (RRs) and 95% confidence intervals (CIs) for incidence and mortality from Bladder Cancer in relation to selected measures of cigarette smoking with respect to nonsmoking.

	Incidence			Mortality		
	No. of comparisons [†]	Pooled RR (95% CI)	I ² % (p for heterogeneity)	No. of comparisons [†]	Pooled RR (95% CI)	I ² % (p for heterogeneity)
Gender[†]						
Male	42	2.56 (2.17-3.01)	92.1 (<0.001)	6	1.87 (1.50-2.33)	0.0 (0.9)
Female	31	2.36 (1.95-2.86)	85.5 (<0.001)	3	1.59 (1.02-2.32)	0.0 (0.07)
Mixed	73	2.68 (2.40-2.99)	84.9 (<0.001)	3	1.11 (0.93-1.32)	0.0 (0.9)
Study area						
Europe	59	3.09 (2.71-3.53)	79.9 (<0.001)	4	1.92 (1.37-2.25)	0.0 (0.6)
Asia	16	2.16 (1.72-2.71)	82.3 (<0.001)	5	1.56 (1.24-1.97)	0.0 (0.9)
Americas	62	2.39 (2.12-2.70)	92.3 (<0.001)	3	1.11 (0.93-1.32)	0.0 (0.9)
Africa	8	1.99 (1.25-3.15)	88.4 (<0.001)	0	--	--

[†] Some studies may include separate estimates for males and females and/or for smoking category.

[‡] The sum does not add up to the total number of studies included in the meta-analysis since only studies reporting estimates separately for men and women were selected.

Figure 3.3. Pooled relative risks (RRs) and 95% confidence intervals (CIs) for incidence and mortality from bladder cancer in relation to ever cigarette smokers with respect to nonsmokers stratified by gender and geographical region.

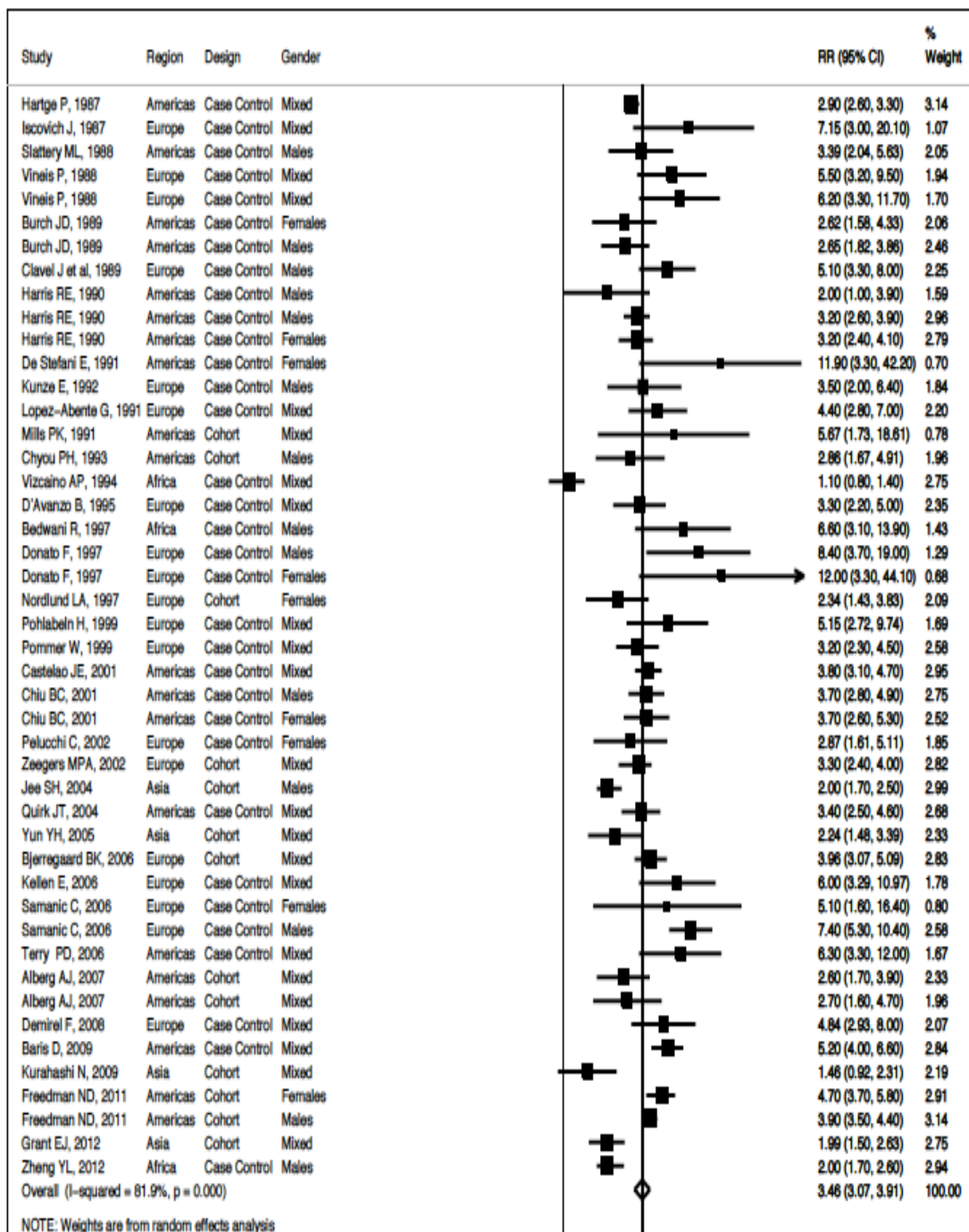


Figure 3.4. Forrest plot of BC incidence in Current smokers.

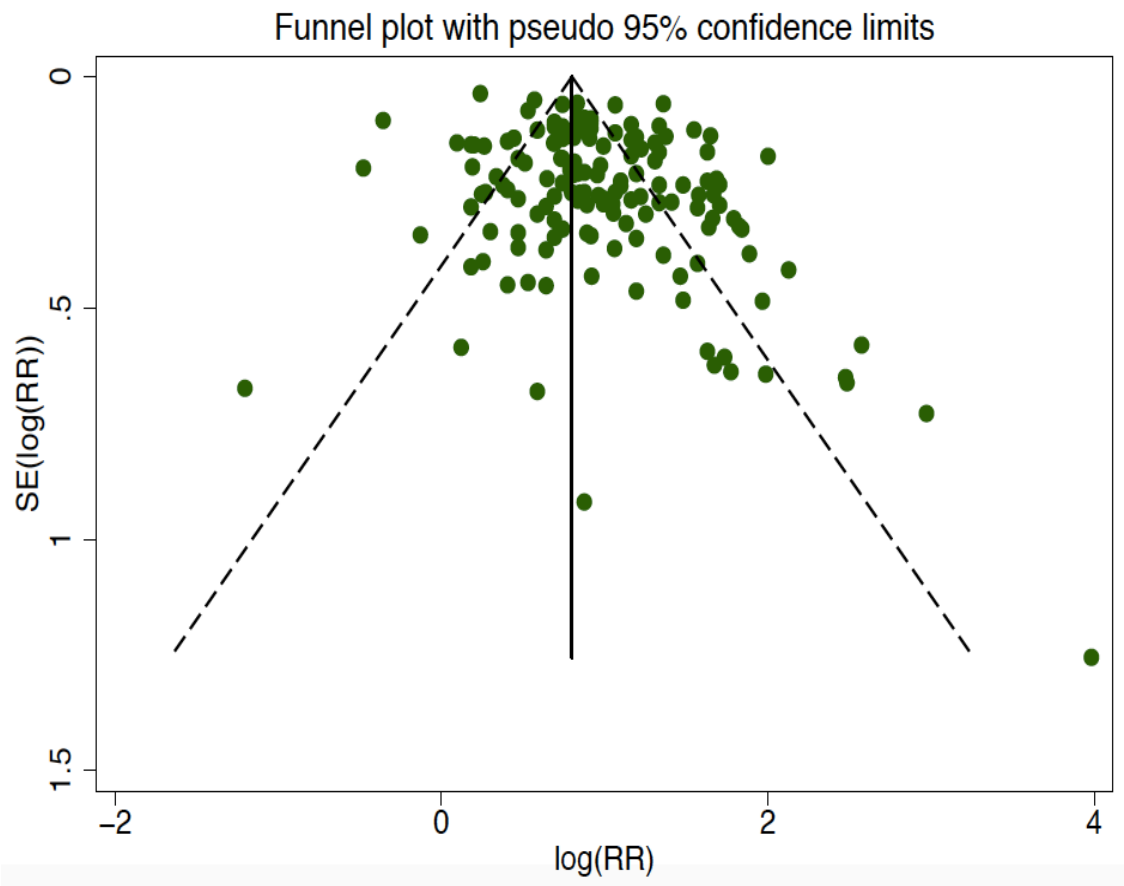


Figure 3.5. A Begg plot of BC incidence. Visual inspection of this plot shows that the spread of studies is symmetrical around the midline suggesting that there is an absence of publication bias (Begg and Mazumdar, 1994).

3.4 SUMMARY

This review has shown that tobacco smoking still significantly increases incidence risk of BC. I have quantified these risks using the most up to date published literature.

Incidence and DSM risk is greatest in current smokers and lowest in ex-smokers, indicating that quitting confers benefit. However, the risk does not return to the baseline levels of non-smokers suggesting both a reversible and non-reversible harm from tobacco. There may be a permanent cellular change that occurs in the lining of the bladder that is responsible for this and more work is needed to determine this.

Chapter 4: Occupational carcinogen exposure and bladder cancer

Work in this chapter contributed to the publication of:

Cumberbatch MG, Cox A, Teare D, and Catto JWF. (2015) **Changing trends in occupational bladder cancer: A systematic review and meta-analysis.** JAMA Oncol. Dec 1;1(9):1282-90

Herein, I investigate part two of the contemporary landscape behind the epidemiology of bladder cancer (BC).

4.1. SYSTEMATIC REVIEW AND META-ANALYSIS OF RISK OF BLADDER CANCER BY OCCUPATIONAL CARCINOGEN EXPOSURE: BACKGROUND

As discussed in Chapter 3, BC has two main aetiological risk factors. The second commonest exposure to carcinogens is through occupational tasks (Reulen et al., 2008). Such exposure can be direct (e.g. solvents from paint) or indirect (e.g. diesel exhaust in lorry drivers). Despite workplace hygiene reducing carcinogen exposure, many BCs still arise through occupational exposure. Most tumors arise following

exposure to exogenous carcinogens that enter the circulation through inhalation, ingestion or skin contact. This route has been known for many years and has been reduced through workplace health and safety regulations in most countries. Examples include European Union directives (e.g. 90/394/EEC and 98/24/EC) and the 2002 Control of Substances Hazardous to Health Regulations in the UK. More recently studies have focused on an interaction between tobacco products and genetic polymorphisms in detoxification enzymes (Pesch et al., 2013; Porru et al., 2014). This is a developing area with genome wide association studies (GWAS) becoming ever more important (Figueroa et al., 2016).

In 1981 Doll and Peto estimated that 10% of BCs arose from occupational exposure (Doll and Peto, 1981). Given the 20-30 year latency between exposure and cancer, we felt that a renewed appraisal of the attributable risk of occupational BC was required, as we expected that workplace legislation has now reduced this rate. Indeed at first glance of contemporary literature, workplace legislation has changed the incidence of BC arising from occupational exposure to 5.3% of all BC, and 7.1% in males (Rushton et al., 2010). However, these attributable fraction estimates are derived from exposure prevalence and relative risks for recognized carcinogens. They exclude tumors where carcinogen exposure is unrecognised (occult) (Noon et al., 2012), unregulated or the agent is unknown. Evidence of uncontrolled occupational exposures can be derived from demographic data where

BC incidence mirrors industrial rather than smoking patterns. For example, the incidence of BC in the UK varies considerably between regions in a pattern not reflected by smoking difference. In 2011 data showed that the number of total BC cases in England was 11.1/100,000, whereas in Northern Ireland it was 8.6/100,000 (UK avg. 10.9). However, smoking incidence in England was 18.4/100,000 (the lowest in UK) compared with Scotland, which was 21.1/100,000 for (UK avg. 18.7). Interestingly, regional industries differ considerably (<http://www.ons.gov.uk/ons/taxonomy/index.html?nscl=Businesses+by+Industry+Sector>) (Cumberbatch et al., 2015b).

So what agents are responsible? With regards carcinogenicity, chemical agents are classified according to the surety of cancer risk. To date, many definitive bladder carcinogens (International Agency for Research on Cancer (IARC) category 1) have been identified (Baan et al., 2009). The use of most high-risk bladder carcinogens is now controlled. Therefore contemporary occupational exposures are likely to be to lower risk chemicals with less clearly defined carcinogenic potential (IARC 2a (probable) or 2b (possible)) (Cumberbatch et al., 2015b). We hypothesized a change in occupational risk has occurred through social and workplace legislative changes, and that this has led to a change in profile of occupations and workforces at risk of BC. To examine this hypothesis, we undertook a systematic review and meta-analyses of contemporary reports of occupational exposure and bladder carcinogenesis. We compared these to similar historical reports.

4.2. DATA ACQUISITION

In May 2014 a final systematic search was performed using the PubMed, Medline, Embase and Web of Science databases. We included full-text articles published or in press, with no time or language limits applied. We used a variety of terms for occupation and either BC or urothelial/transitional cell carcinoma. Abstracts of all reports were read and full papers retrieved for those appearing to fulfill selection criteria. This was performed by two independent reviewers, myself and my supervisor, James Catto. Articles were eligible if they reported original data on occupational risk for BC in adults. Reports were case-control or cohort studies by design, and were required to focus on occupational exposures as the main analysis, they needed to have sufficient data to calculate confidence intervals with no missing data. We selected the most recent and maximally adjusted data from populations with multiple reports to ensure contemporaneity and to minimize bias (from confounders such as tobacco smoking or socio-economic factors). Risk estimates were annotated by occupational class using NYK and ISCO-1958 codes (Pukkala et al., 2009) and dates of exposure (taken as the mid-time point of documented exposure interval). For meta-analysis, we used manuscripts reporting risk estimates (e.g. odds ratio (OR), standardized incidence ratio (SIR), standardized mortality ratio (SMR) or relative risk (RR)) and 95% confidence intervals, or enough information to calculate these (Cumberbatch et al., 2015b).

Meta-analysis of risks was performed using a random effects model using STATA (Vsn 12.0, StataCorp LP, TX). This model was chosen as

we anticipated heterogeneity between studies given the nature of occupational BC reports (e.g. few with large populations, most have low disease incidences, all are non-randomised and most are retrospective in design). We assessed heterogeneity (I^2) between studies for each occupation. Incidence and disease specific mortality (DSM) risk were computed separately. Publication bias was evaluated by visual inspection of funnel plots, Egger's linear regression (Egger et al., 1997) and Begg's rank correlation tests (Begg and Mazumdar, 1994).

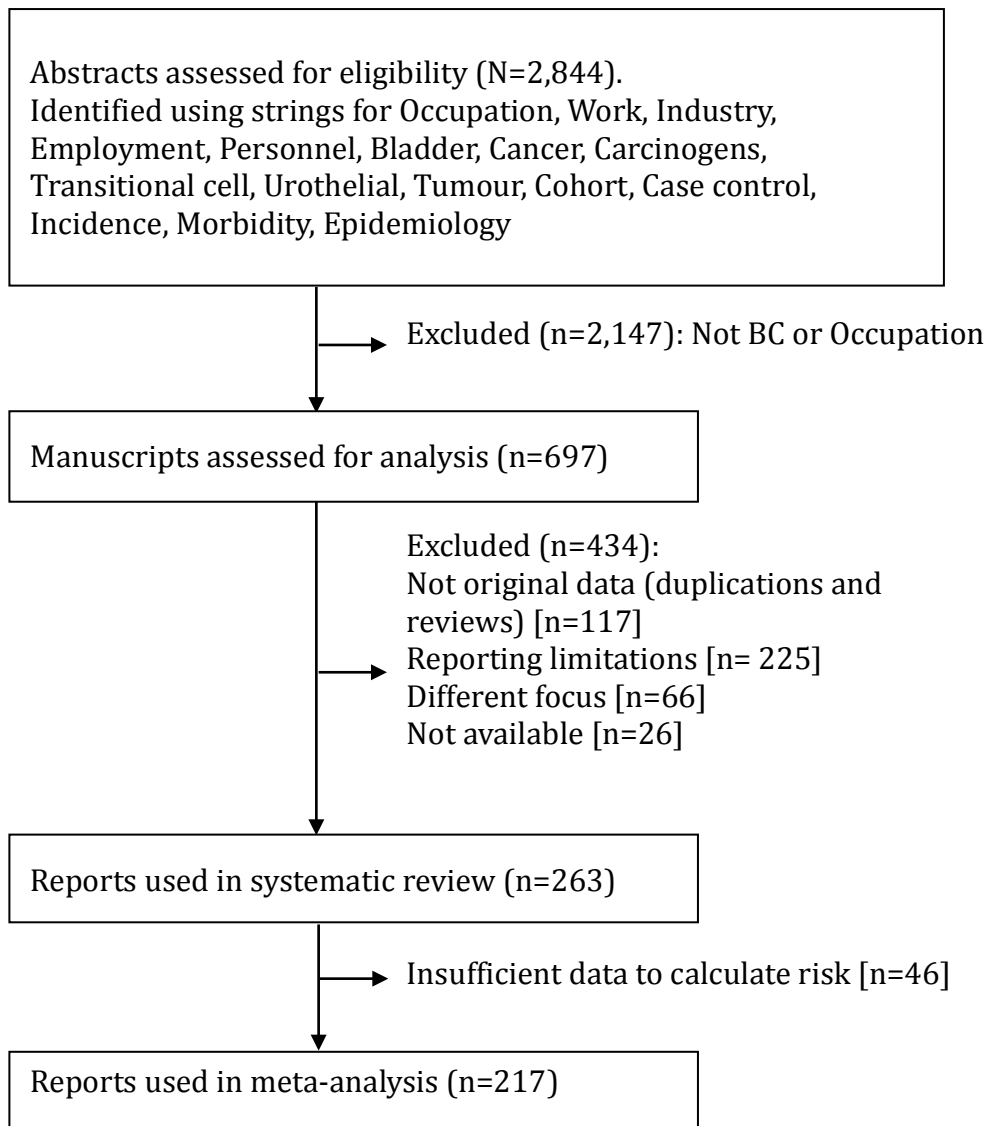


Figure 4.1. Consort diagram showing our search strategy of manuscripts for inclusion.

4.3. THE FACE OF OCCUPATIONAL BC HAS CHANGED

We identified 2,844 manuscripts, from which we read 697 full papers and selected 263 for systematic review (reporting 31.4 million persons). These manuscripts reported BC risk in 1,254 occupations, which were sub-classified into the NYK and ISCO-1958 codes for occupational class. Whilst funnel plots suggested symmetry for each comparison, statistical analyses identified potential publication bias for males and incidence data. One occupation (Racehorse Trainers/Jockeys) had a single report, whilst all other occupational classes had multiple estimations of risk (mean 27 (st. dev. 25) comparisons per occupation).

Historically, occupations exposed to aromatic amines (rubber, dye, plastic, printing and hairdressing) were at greatest risk of BC. Gradually, restrictions on the use of many implicated carcinogens have been introduced. Some of these include 2-naphthylamine in the rubber industry (sanctioned since 1949) (Zheng et al., 2002), di- and trichloroethane and MBOCA used as solvents in plastic manufacturing (Stula et al., 1978; Dost et al., 2009), and carbon black in print inks (Lynge et al., 2009).

For meta-analysis of our review data, we used data from 231,627 cases and 4.76 million controls annotated in 217 manuscripts by occupation. The highest pooled incidence risk was for tobacco workers (RR 1.72 [95%CI 1.37-2.15]) and dye workers (RR 13.4 {95%CI 1.5-48.2}) but the greatest RR in any study was for factory workers (RR 16.6 [95%CI 2.1-131.3]). Pooled DSM was greatest for metal workers (RR 10.2 [95%CI

6.89-15.09]) and gardeners (RR 5.5 [95%CI 0.84-35.89]) and the highest DSM in any report was for chemical workers (RR 27.1 [95%CI 11.7-53.4]).

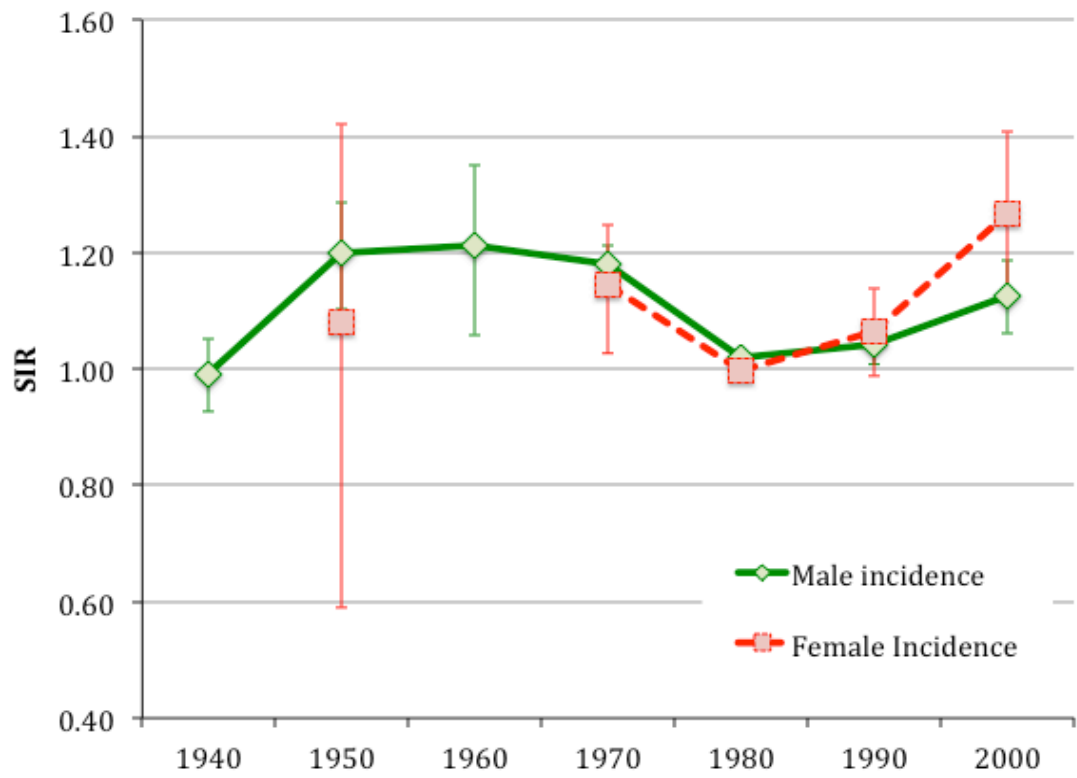


Figure 4.2. The pattern of BC incidence in males and females over the last century by decade.

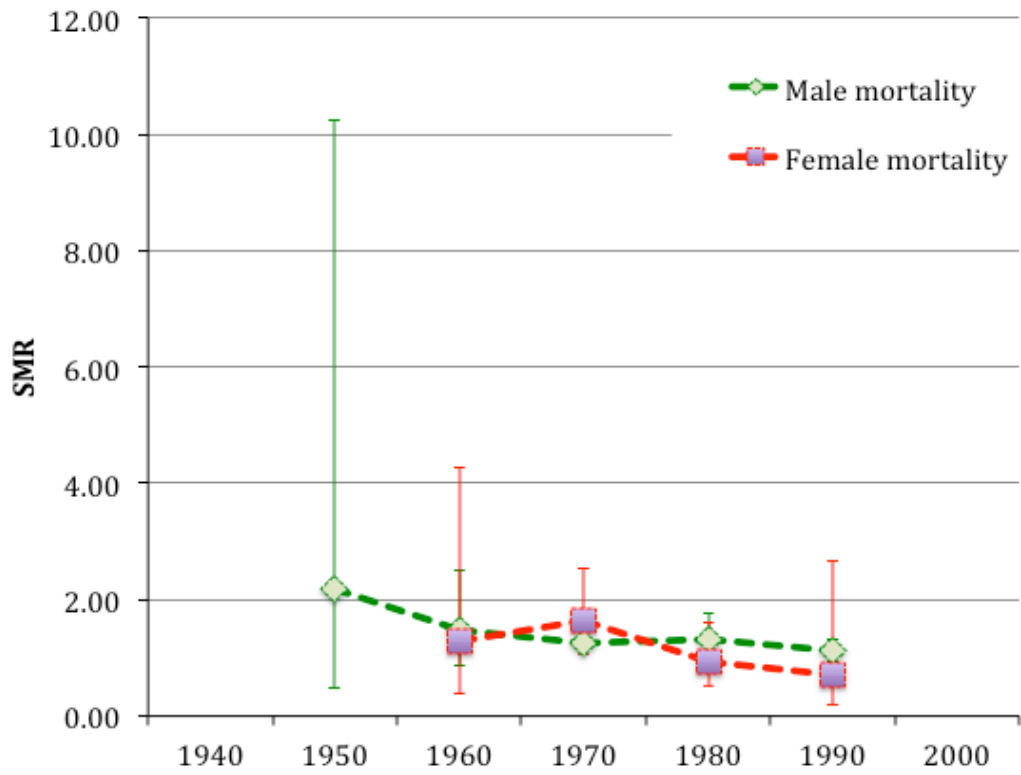


Figure 4.3. The pattern of BC mortality in males and females over the last century by decade.

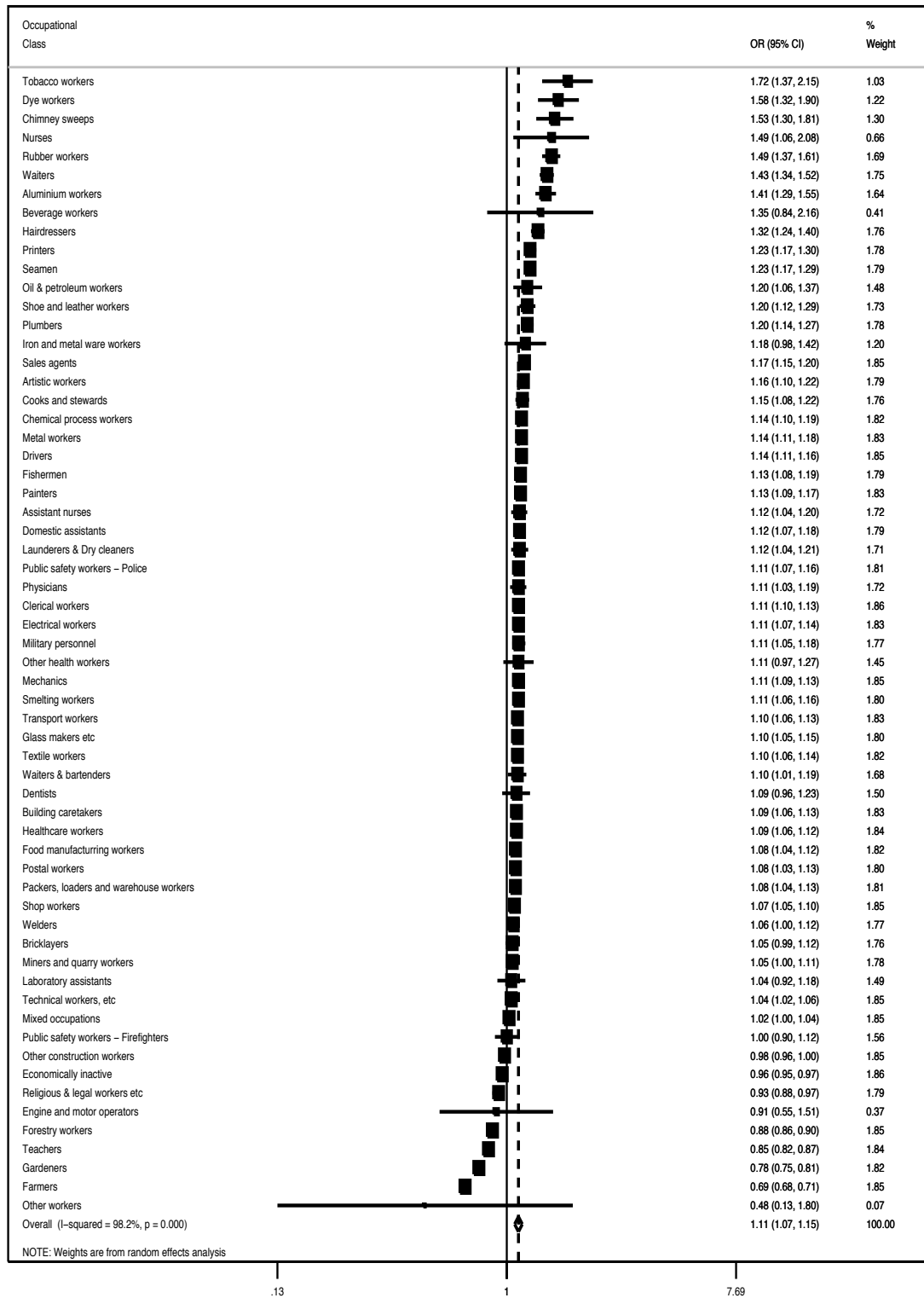


Figure 4.4. Forrest plot of BC incidence amongst all occupations

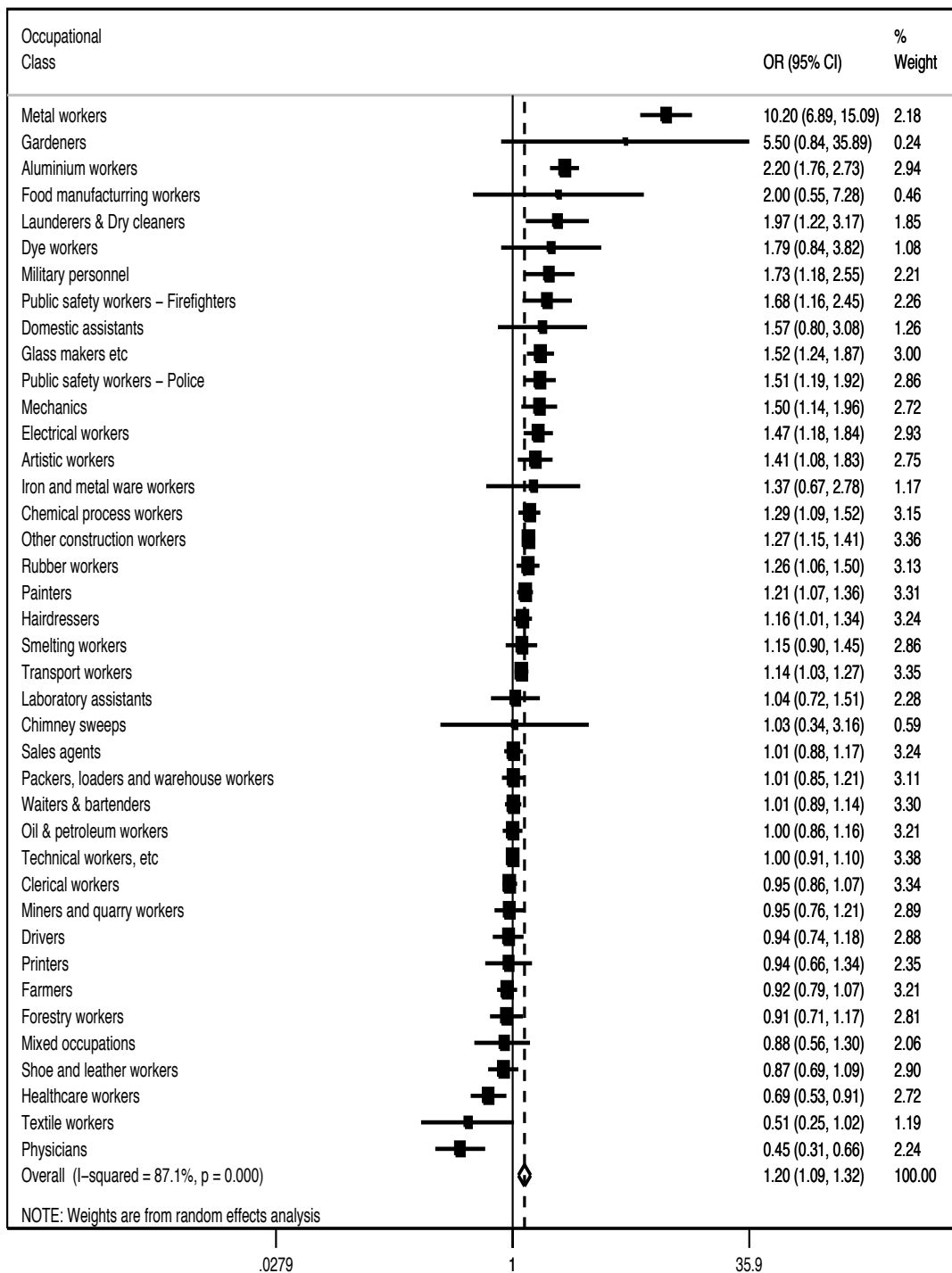


Figure 4.5. Forrest plot of BC mortality amongst all occupations

4.4 SUMMARY

Despite improvements in workplace hygiene many occupations still have an elevated BC incidence and mortality risk. This highlights the public health importance of occupational BC. When we analysed whether the risk within each occupation had declined overtime, there was no clear difference except for drivers. Overall incidence experienced an expected dip during the 1980's, however unexpectedly it appears to be on the rise again. Improved detection mechanisms or screening are possible reasons for this. This trend is most striking for women and this may reflect changes in the gender composition of the workplace and changes to social norms.

There is seemingly still an exposure risk from aromatic amines and this group have the highest incidence, whilst those exposed to polycyclic aromatic hydrocarbons and heavy metals have the greatest mortality. Other agents attracting attention are diesel fumes and combustion by-products (drivers and firefighters).

In conclusion, the profile of contemporary occupations with increased BC risk is broad and differs for incidence and mortality and it may be some time before we see whether more recent restrictions have an impact. For the meantime, these meta-analyses have informed my knowledge of current at risk groups. This information has been useful to develop a protocol for a cohort study of our local population looking more specifically at the occupational carcinogens that high-risk industry

personnel are currently handling, and during which workplace tasks. In the future, we may be look to develop cell lines from patients known to have been exposed to particular contemporary carcinogens to interrogate their gene expression profiles.

Chapter 5: LUZP4 functions as an alternative mRNA export adaptor in some cancer cells

Work in this chapter contributed towards the publication of:

Viphakone N, Cumberbatch MG, Livingstone MJ, Heath PR, Dickman MJ, Catto JW, Wilson SA. (2015) **Luzp4 defines a new mRNA export pathway in cancer cells**. *Nucleic Acids Res.* Feb 27;43(4):2353-66

Herein, we interrogate the role of the cancer testis antigen LUZP4 as a putative mRNA export adaptor.

5.1. LUZP4 AND CANCER TESTIS ANTIGENS

In the previous two chapters, I updated the literature on the aetiology of bladder cancer. Having identified that the two primary risk factors still persist in contemporary society, I accepted the challenge to investigate the basic science behind BC and cancer in general. My aim was to try and identify novel targets that might be used for diagnostics or therapeutics.

At the time of commencing this PhD there were some exciting preliminary findings in the Wilson laboratory and so I decided to focus my early efforts on a cancer testis antigen (CTA) known as LUZP4.

In order for gene expression to be successful, all steps from transcription to translation must be complete. One of the more complex tasks is to license and export mRNA from the nucleus to the cytoplasm. A key complex involved in this step is TREX. The earliest component of the TREX complex to be recruited to nascently transcribed mRNA is the RNA helicase UAP56. A canonical binding partner for UAP56 is the mRNA export adaptor ALYREF. As mentioned in the introduction, in 2011 the Wilson laboratory identified two proteins during a BLAST (basic local alignment search tool) search that contained the same peptide sequence as ALYREF at the UBM (UAP56 binding motif) domain [DMSLDDII]. Hautbergue et al (2011) published the first paper on UIF, one of these two proteins. They showed that UIF could function as an mRNA export adaptor and shared redundancy with ALYREF. UIF was able to complement the role of ALYREF when it was knocked down (Hautbergue et al., 2011) as is seen in some cancer cells.

The second protein identified in this search was LUZP4. LUZP4 was a previously uncharacterized gene. Tureci et al (2002) wrote the first paper on LUZP4. They arrived at a few interesting conclusions: LUZP4 seemed to co-localise to nuclear speckles alongside sites of transcriptional activity and splice sites; chromosomal mapping showed

that like most CTA's the gene locus for LUZP4 is housed on the X-chromosome; and it exclusively shared structural features with the N-myc proto-oncogene. Whilst, Tureci et al (2002) were successful in recording the cellular localization of LUZP4 and showed by RT-qPCR that its levels are increased at the RNA level in some cancers, they did not attempt to identify binding partners of LUZP4 and interrogate its molecular function in detail.

Investigating the role and function of LUZP4 represented the ideal project. Preliminary data suggested that LUZP4 would have a role both in mRNA export and, may be a suitable target for development as a biomarker for cancer or as a therapeutic target for vaccine therapies (Tureci et al. 2002) to treat cancer. Such promise has been seen during investigations of CTAs in other cancers such as prostate (Shiaishi et al., 2012) and pancreatic (Kubuschok et al., 2004). Finding a reliable biomarker (diagnostic or prognostic) is of particular importance to the Urologist and for the BC community. To date attempts to develop a successful one have fallen short.

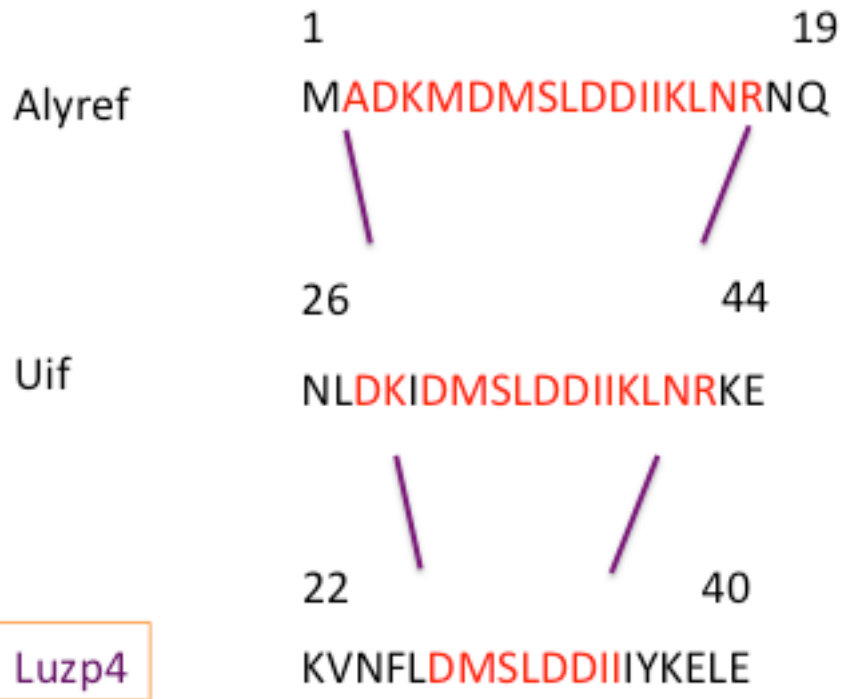


Figure 5.1. Schematic showing shared N terminal peptide sequence in ALYREF, UIF and LUZP4. The UBM previously identified in ALYREF and UIF aligns with a homologous sequence in LUZP4. Red residues show strict matching (adapted from Viphakone et al., 2015).

5.2. PRESENCE OF LUZP4 IN BLADDER CANCER

The first task was to identify how widespread is the expression of LUZP4. The experiments were run in two arms. We first confirmed that ALYREF was down-regulated in MeWo melanoma cells by blotting expression of ALYREF in 293T (control) and MeWo (experimental) cell lines. Following on from the western blotting, we then sought to see whether or not the same patterns of expression seen at the protein level were shown at the mRNA level, through qRT-PCR. This time we also probed for the expression of LUZP4. Our antibody for LUZP4 was not capable of detecting the endogenous protein and so we used qRT-PCR to detect mRNA levels of expression. We used 7 BC cell lines were tested using the standard qRT-PCR protocol from the Wilson laboratory. We performed four biological replicates and averaged the data. These showed that in the 7 BC cell lines (and MeWo positive control), when ALYREF is down-regulated in the cancer cells, LUZP4 is up regulated. The housekeeping gene U1 was used as a normalizing control. We ranked the cell lines according to their described grade (level of differentiation) and metastatic status on harvesting from the donor on review of the literature using PubMed and cell-bank databases. Having established these rankings, we noticed that as the cancer cell lines became more 'aggressive' the pattern of ALYREF down regulation with simultaneous up regulation of LUZP4 became more evident (see Figures 5.2 and 5.3). We then repeated this experiment 4 times and all results were concordant.

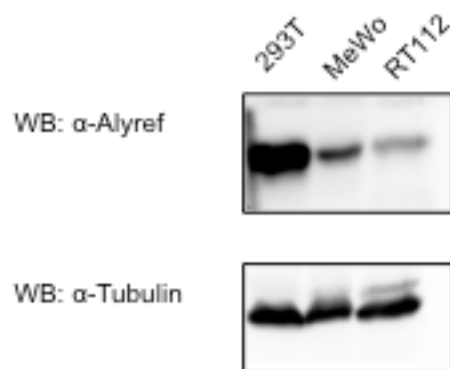
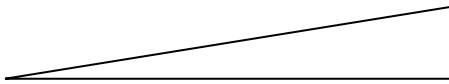


Figure 5.2. A western blotting showing that ALYREF is down-regulated in the MeWo (melanoma) and bladder cancer cell line RT112, whilst normally expressed in the 293T embryonic kidney cells. Tubulin was used as a loading control.

Controls  Bladder tumour grade

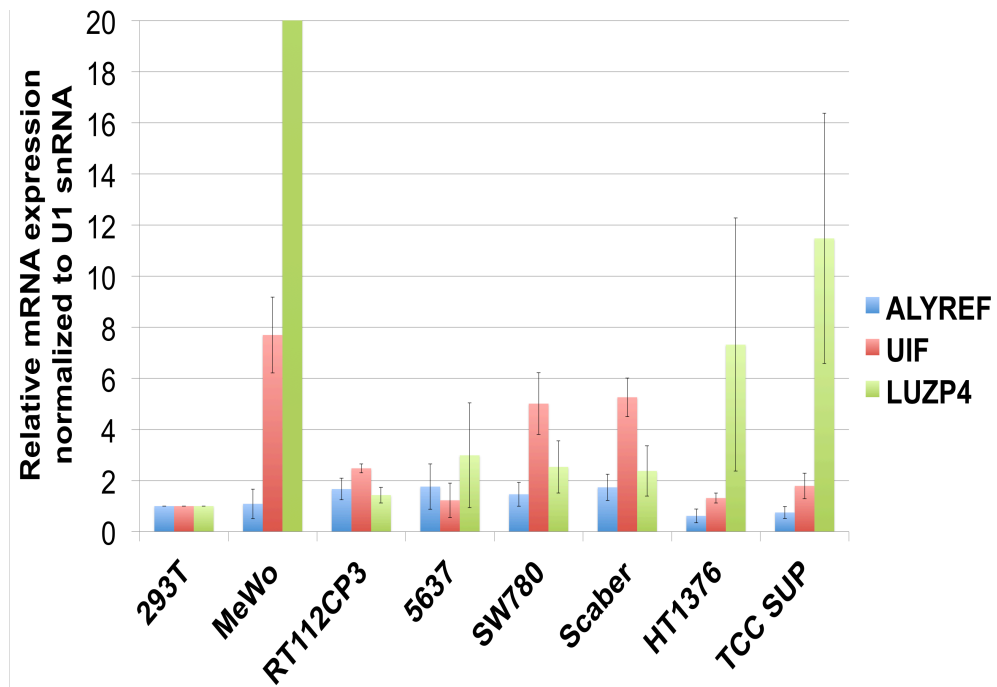


Figure 5.3. qRT-PCR results (with error bars of standard deviation) illustrating that the expression pattern of ALYREF and LUZP4 at the mRNA level.

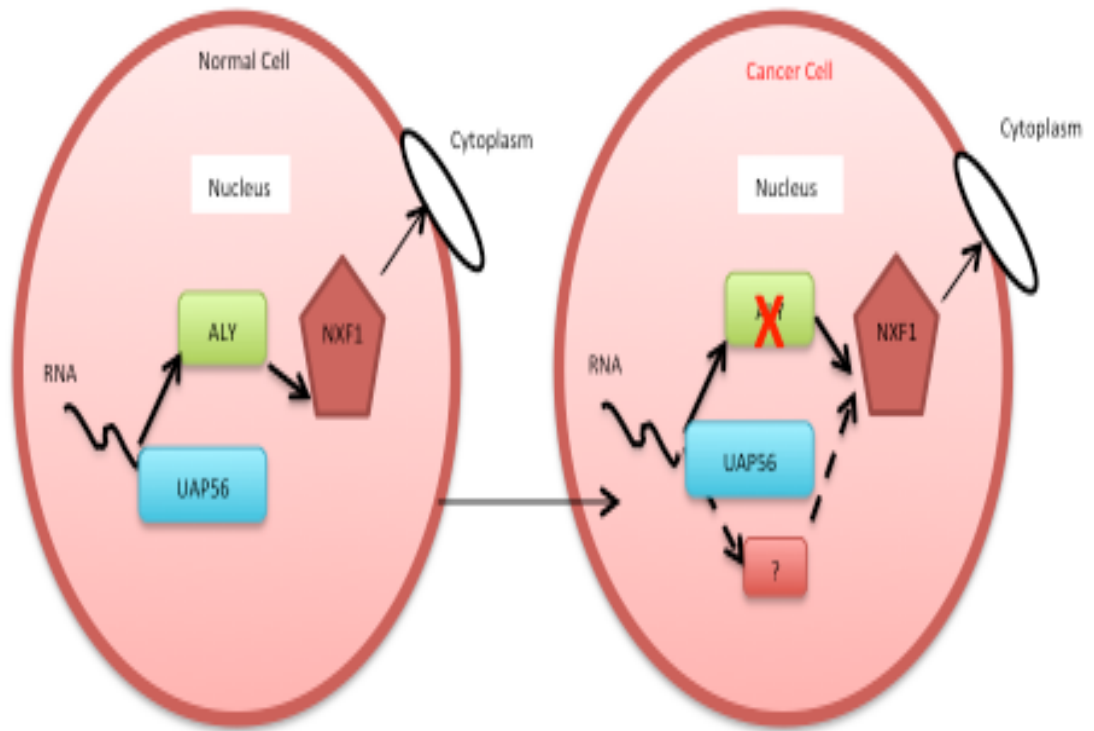


Figure 5.4. Conceptual diagram showing a simplified version of our hypothesis that cancer cells use of an alternative method of mRNA export where ALYREF levels are down-regulated.

5.3. EXPRESSION OF LUZP4 ACROSS CANCER TYPES

Following our previous line of investigation, we next wanted to illustrate whether or not the expression patterns seen in our BC qRT-PCR were also seen in cancer arising from other tissues. In order to complete this large-scale qRT-PCT experiment we purchased pre-prepared *Tissue Scan 96-well plates* from *Origene*. These are pre-made 96-well plates containing normalized cDNA for a large range of cancers. In total, 3 sets of 5 plates were used to evaluate 18 different body tissues, from adrenal gland to uterus. We adapted our qPCR protocol to be in accordance to the *Origene* protocol. Data was analyzed using the *MX-Pro* programme and Microsoft excel. The delta CT value was used to determine the relative abundance of each primer per each well condition.

One primer was used per plate. Each 96 well plate was made up of 96 different well contents but each well was exactly matched to an identical well on 2 other plates, allowing comparison. Three empty wells were provided, and these were used to evaluate a none-template control (in duplicate) for each primer. We did not probe for a housekeeping gene such as U1 because *Origene* guarantee an equal cDNA loading across all wells in all plates.

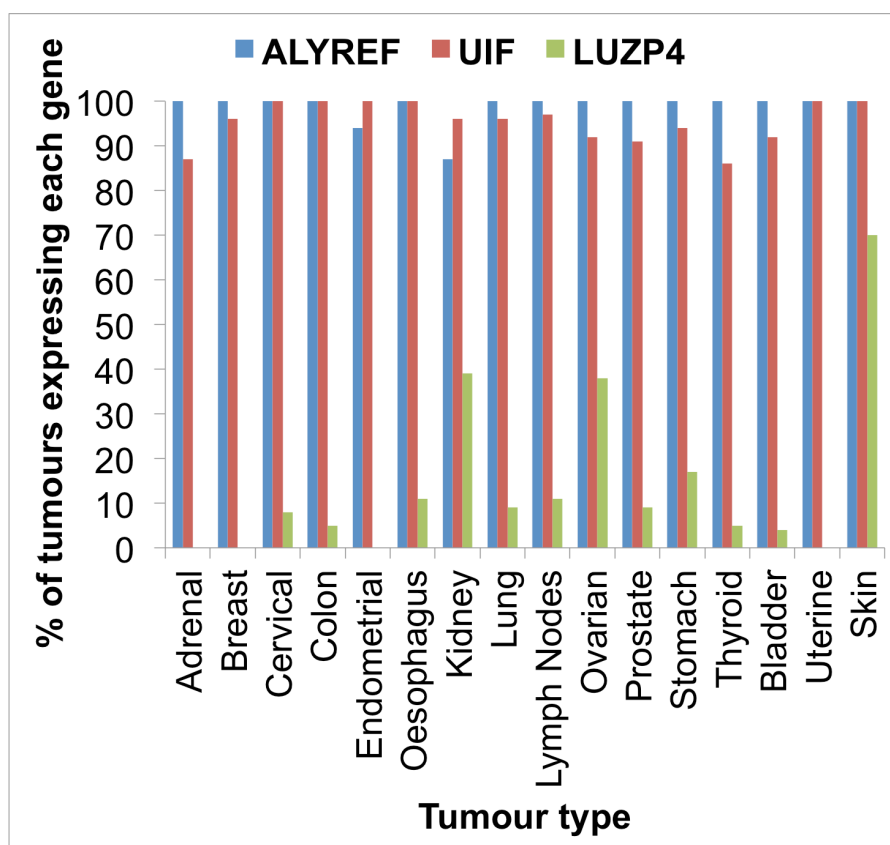


Figure 5.5. qRT-PCR of commercially purchased (Origene) cDNA arrays from cancer tissues originating from 18 different organs. Data presented show the percentage of tumour cDNAs that expressed each of the three genes. Genes were considered to be expressed when $2^{-\Delta CT}$ was >0.04 .

These data successfully show that ALYREF is down-regulated in cancer cells, whilst the LUZP4 export adaptor pathway is seemingly up-regulated (a hypothetical pathway is displayed in figure 5.4).

Overwhelmingly, it is in skin that the greatest expression level resides (figure 5.5). We believe that this may be due to an active switch from one export pathway to another in cancer cells in order to promote survival. We have seen that cells become dependent on these alternative mRNA export pathways as when ALYREF and UIF are simultaneously subjected to RNAi the cells die rapidly (Hautbergue et al., 2011). As hypothesized, there also appears to be a functional overlap between ALYREF and LUZP4 in certain cancer cells. In vivo work by Viphakone et al. (2015) showed in a cell survival assay when melanoma cells are subject to LUZP4 RNAi (shown to express low levels of ALYREF) the cells die earlier than control cells suggesting a dependence on this alternative export pathway (synthetic lethality).

In the data shown here, we have seen that the hypothesized relationship of these export adaptors within the cancer cells, appears not only restricted to one or two types of cancer, but appears to be a more widespread phenomenon.

5.4. LUZP4 AS AN ONCOGENE

Karni et al (2007) found that the splicing factor SF2 was up-regulated in some cancers. They successfully showed that by injecting immune-deficient mice with SF2 cells, malignant tumours developed above and beyond tumours seen in the control group. Taking inspiration from this we wanted to see if the presence of LUZP4 could promote de novo malignant tumour growth in immune-deficient mice. 5×10^6 cells were injected into the flanks of severe combined immune-deficient (SCID) mice of negative control (flag 3t3), positive control (SF2 3t3) and experimental (LUZP4 3t3) cells. Each condition had triplicate mice and equal distribution of gender was ensured. This experiment was conducted with full Home Office approval at Sheffield Medical School under the supervision of Professor Nicola Brown.

Every 3 days the mice were inspected for tumour growth in the flanks and standardized calipers were used to measure growth. After 18 days the mice were culled according to Home Office regulations to avoid the morbidity of a large tumour burden. SF2 and LUZP4 injected mice began to grow palpable tumours after 5 days (figure 5.6). After 12 days tumours began to grow in the negative control mice, and these eventually became larger than in the LUZP4 mice. By 18 days it was clear that no difference existed between injecting 3t3 and LUZP4 3t3 cells (figure 5.7).

The tumour sections were excised and examined in two ways: 1) Haematoxylin and Eosin staining and pathologist-led microscopy to look

for malignant properties such as apoptotic bodies, invasion and chaotic mitosis. 2) Tumours were lysed and processed for total RNA extraction and qRT-PCR was performed to look for LUZP4 expression. We found that approximately 50% of the LUZP4 tumours were sarcomatous tumours and 50% were inflammatory only. LUZP4 was negligibly detectable at the RNA level and there was no difference across experimental conditions. These results led to the conclusion that LUZP4 is not intrinsically oncogenic.

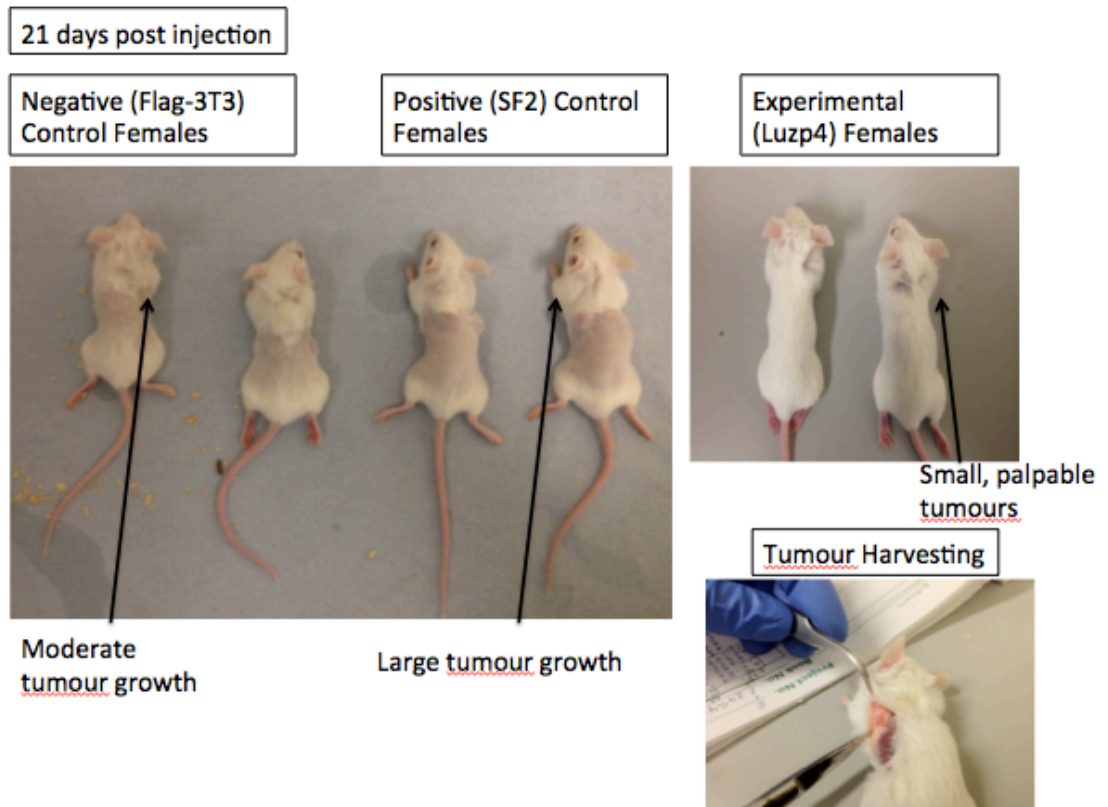


Figure 5.6. Tumour identification and excision in SCID mice following injection of 3t3 cells. The delivery of cells, tumour monitoring and culling of mice was performed by Professor Nicola Brown's laboratory. I excised the tumours and performed the subsequent analysis on them.

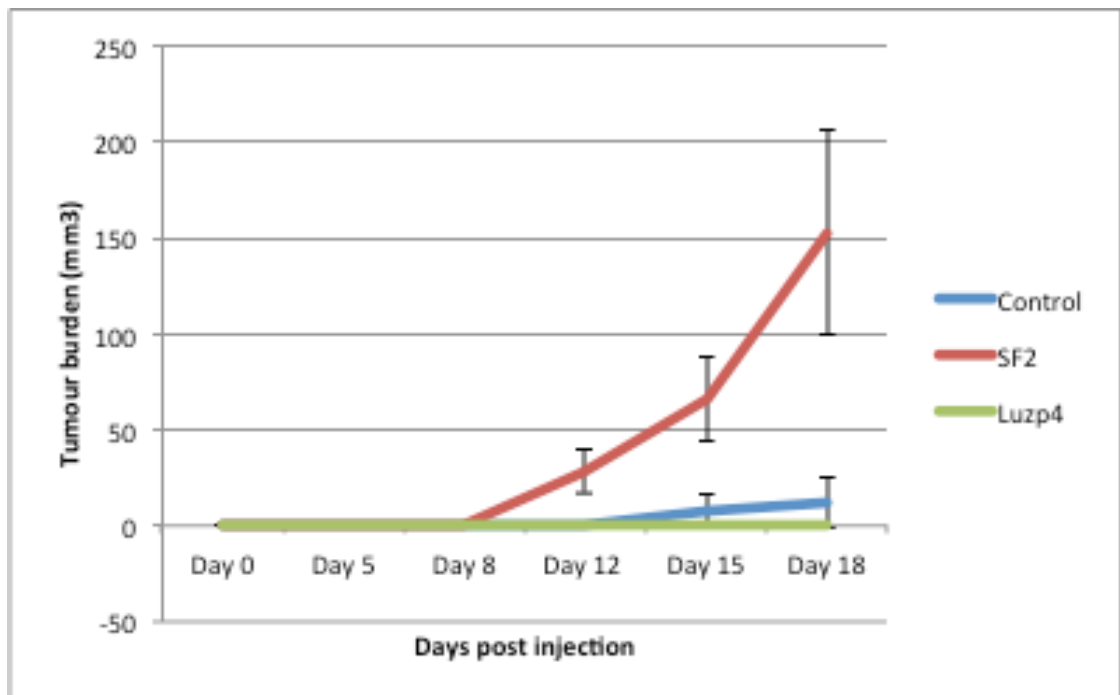


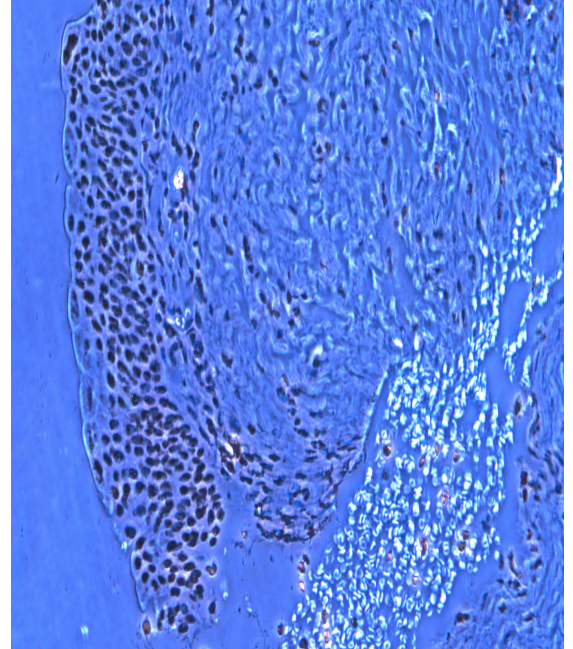
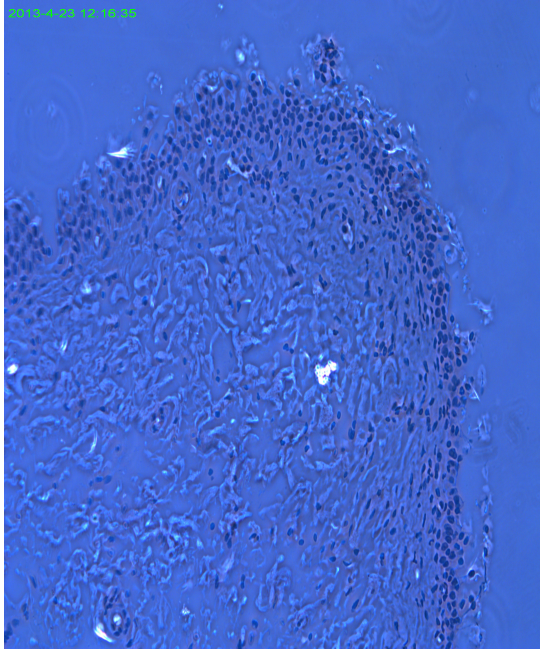
Figure 5.7. Growth curve of tumours in SCID mice injected with 5×10^6 cells of 3t3, SF2 3t3 or LUZP4 3t3. The SF2 3t3 cells were used as a positive control and 3t3 cells as a negative condition..

5.5. LUZP4 IMMUNOHISTOCHEMISTRY

Attempts were also made to extract RNA from urine of 100 BC patients matched to patients without BC. Unfortunately, the yield of RNA from the stored samples was insufficient. I therefore decided to investigate whether LUZP4 could be detected using IHC on BC tissue and whether we could delineate BC from benign tissue based upon the presence of a LUZP4 signal (figure 5.8). Such a result would potentially allow the surgeon to stain a tissue intra-operatively and assess whether surgical resection margins had been adequate much like the use of fresh frozen sections, which are sent to the pathologist intra-operatively. Patient bladder tissue samples were prepared as per our immunohistochemistry protocol. Slides were probed for localization and abundance of ALYREF, LUZP4 and UIF. There was a general localization to the urothelium but there was no difference in this between conditions despite the use of a number of different antibody dilutions, purifications and commercial antibody purchases.

No antibody control
(Goat serum only)

ALYREF



LUZP4

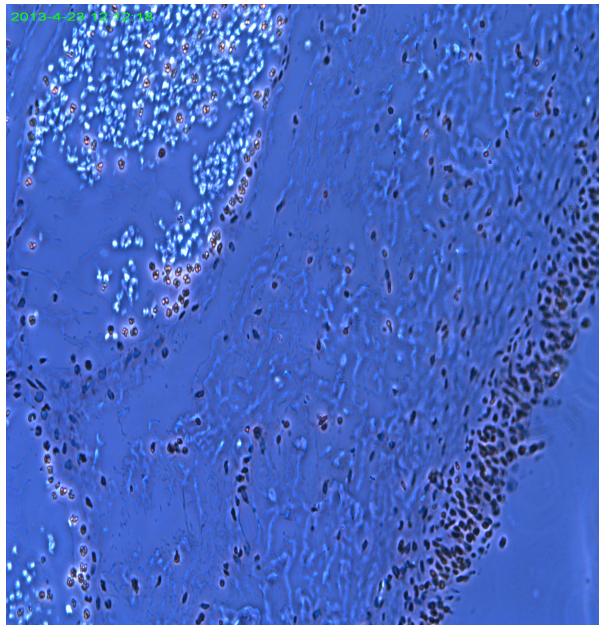


Figure 5.8. Immunohistochemistry slides of paraffin embedded bladder cancer sections incubated with ALYREF and LUZP4 antibodies. There is brown staining of DAB at the Urothelium.

5.6. EFFECTS OF DNA DAMAGE IN ALYREF RNAI CELL LINES

We performed colony survival assays on ALYREF RNAi and Control RNAi cell lines. Cells were incubated in increasing doses of Cisplatin and Mitomycin C to see whether cells devoid of ALYREF are more susceptible to DNA damaging agents. This was done to examine the hypothesis of synthetic lethality across the mRNA export adaptors. Cisplatin and Mitomycin C are both chemotherapeutic agents currently in use for the treatment of BC (figure 5.9). Mitomycin C is typically used as an intravesical instillation treatment following identification of NMIBC and Cisplatin is usually reserved for systemic treatment in patients with locally advanced or metastatic MIBC.

If preferential growth inhibition could be shown in cells with low ALYREF levels compared to cells with normal ALYREF, it might be that the inhibition being caused by the drug treatments is through action on the alternative mRNA export pathway of LUZP4-assisted mRNA export, normally redundant in control cells. This would pose an interesting therapeutic possibility.

The results showed an apparent increased sensitivity to DNA damage in ALYREF RNAi cells. However, the results were not statistically significant and error bars show a wide variation (data not shown).

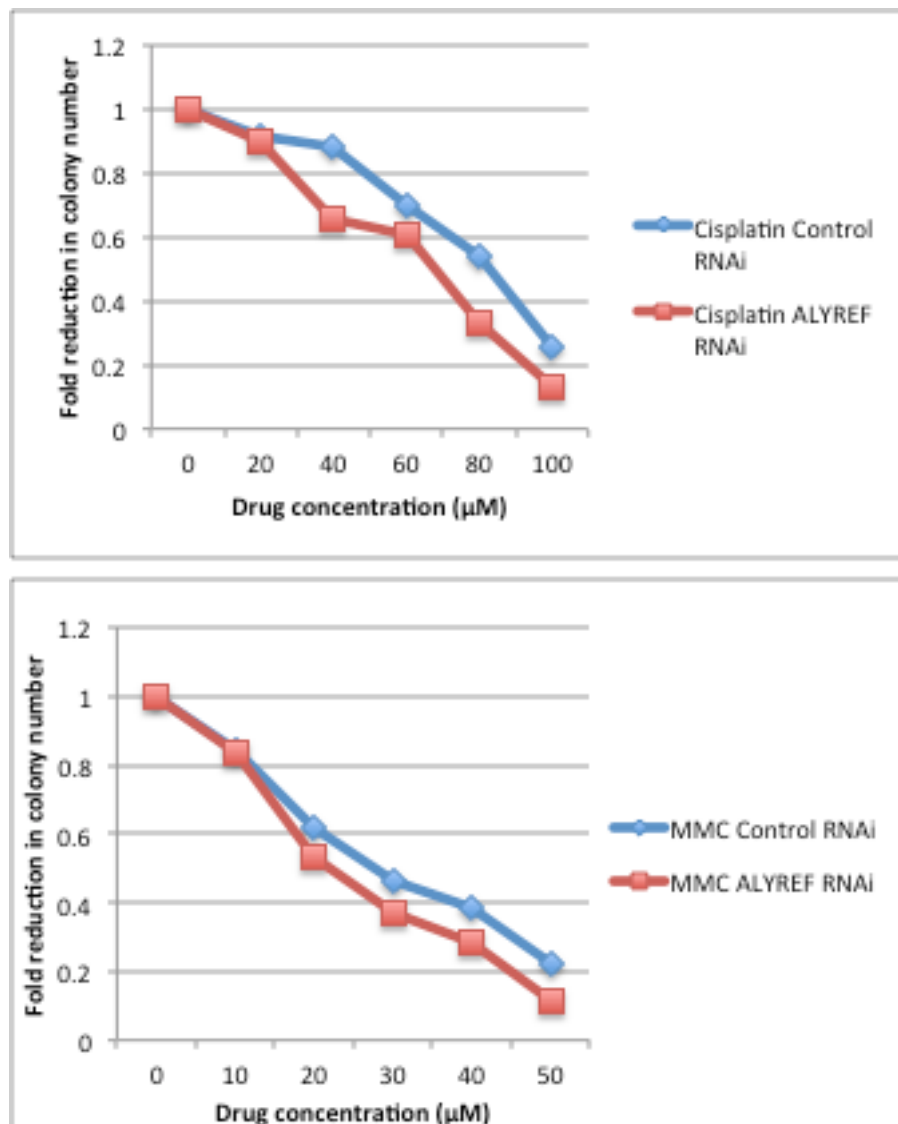


Figure 5.9. Colony forming assays using crystal violet staining performed in Control RNAi and ALYREF RNAi cell lines using the chemotherapeutic agents as labeled. These experiments we performed in triplicate and averages are shown here. The number of colonies with each drug concentration was normalized to the number of colonies at time point 0.

5.7 SUMMARY

In the publication by Viphakone et al (2015), LUZP4 is shown to function as a bona fide mRNA export adaptor. Using Co-IP and RNAi complementation assays (where a cell line co-expresses RNAi hairpins to ALYREF and an RNAi resistant LUZP4 cDNA) Viphakone et al (2015) show that LUZP4 can bind RNA, and TREX subunit UAP56, can bind the nuclear export receptor NXF1 and LUZP4 can complement the loss of ALYREF in MeWo cells rescuing cell survival. In that paper we show that LUZP4 can partially complement the survival of cells that have lost both ALYREF and UAP56 in a double knock down RNAi screen. This is a phenotype that is normally cell-lethal in 6 days. Furthermore, upon LUZP4 RNAi, malignant melanoma cells (MeWo) show a sensitivity beyond that of control RNAi cells. Given that the levels of ALYREF are low in these cells, these results suggest a functional crossover and redundancy of LUZP4 with ALYREF, which gives way to a synthetic lethality upon RNAi of LUZP4.

My contribution to this work suggested LUZP4 is an mRNA export adaptor that has raised levels, at the protein and RNA level, in a large number of cancer cell lines where ALYREF levels are down, in particular melanoma cells. This raises the suspicion that there is a 'switch' to LUZP4 governed mRNA export that occurs in certain cancer cells that have lost ALYREF. We found no evidence to support the idea that LUZP4 functions as an oncogene and we were unable to

demonstrate an increase expression of LUZP4 in BC patient urine or tissues, limiting the prospects of LUZP4 as a potential biomarker for BC.

An interesting future direction would be to screen a library of small molecule inhibitors against UIF and LUZP4 to confirm that the loss of these pathways results in selective cancer cell death.

An argument against this work would be to question the applicability and feasibility of providing a medical alternative to current therapies based on a small molecule screen. However, we have seen the possibilities with the advent of Curaxins – a group of small molecule inhibitors currently being put through the rigors of clinical trials courtesy of Cleveland Biolabs (Gasparian et al., 2011). This vastly improves the likely turn-around-time it would take to process another, similar, clinical trial involving inhibitors of the LUZP4 protein.

Chapter 6: Effect of DNA damage

and subsequent poly (ADP-ribosyl)ation on mRNA export

In this chapter I examine the relationship between DNA damage and mRNA export. Specifically, I wanted to test whether DNA damage induced poly (ADP-ribosyl)ation leads to alterations in the mRNA export pathway that culminate in an mRNA export block.

6.1. POLY (ADP-RIBOSYL)ATION

Poly (ADP-ribosyl)ation is one of many post-translational modifications. Upon such modifications, target proteins may undergo a change in their function or activity (see Introduction). Jungmichel et al. (2013) explain that poly (ADP-ribosyl)ation is a phenomena most frequently observed under conditions of genotoxic stress. This conclusion arose from the observation that PARP levels were increased when cells were subjected to treatments with DNA damaging agents such as H₂O₂ and UV radiation. The novel findings from Jungmichel et al. (2013) were that the effect is largely targeted towards proteins involved in RNA processing (Jungmichel et al., 2013).

Strikingly, we noted that a common modification site for PARylation was the UAP56-binding motif (UBM) on ALYREF that we had previously

identified was essential for multiple TREX subunit interactions with UAP56 and thus TREX assembly (figure 6.1). Therefore this led to the hypothesis that PARylation of the UBM within TREX subunits might regulate TREX assembly, thus modulating mRNA export in times of DNA damage. What we did not know was whether TREX would still function and whether mRNA would still be correctly exported. We considered that there may be an mRNA export block following genotoxic stress, since export of transcripts derived from damaged DNA would be deleterious to the cell.

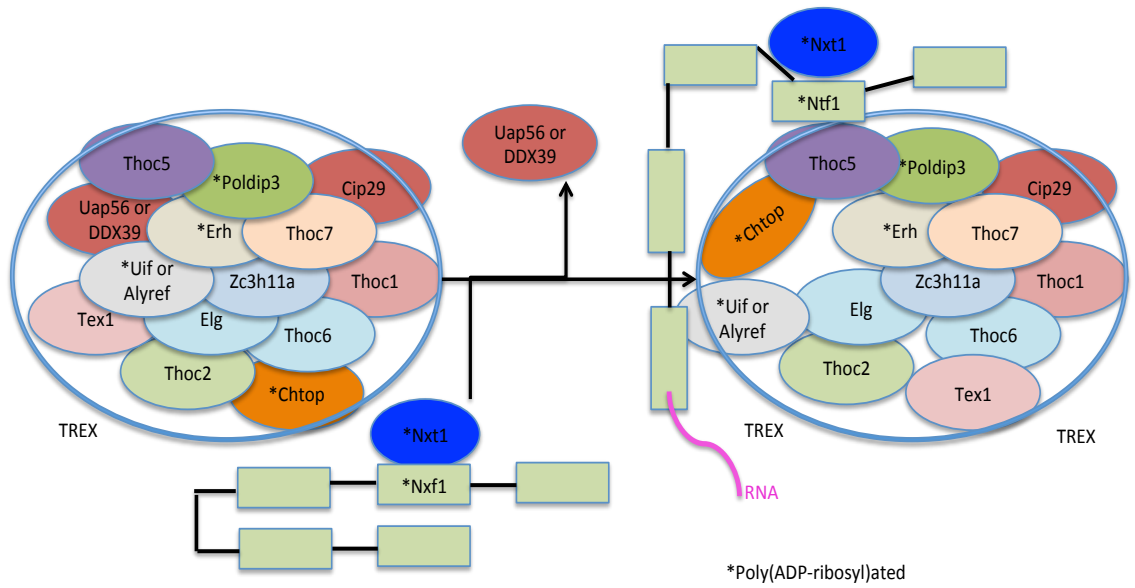


Figure 6.1. Schematic of TREX: asterisks denote subunits known to undergo poly (ADP-ribosyl)ation.

6.2. PARG RNAi

One of the first ways in which we wanted to interrogate this hypothesis was to see what happened to TREX interactions and mRNA export under conditions of DNA damage. Since PARylation is a transient, reversible modification with a short half life (Li et al., 2014; Alvarez-Gonzalez and Althaus, 1989) we generated a FLPIn 293 cell line with a stably integrated inducible miRNA which targets the major PAR glycohydrolase (PARG), allowing stable tetracycline (Tet) inducible knockdown of PARG, to reduce turnover of PAR and facilitate studies on the role of PARylation in mRNA export.

The RNAi method exploits the functions of miRNAs (microRNAs). They are short non-coding RNAs that degrade or suppress gene expression of complementary mRNA. Using the *Block-iT kit* (Invitrogen) we utilised this system to create stable inducible miRNA hairpins from a pcDNA 6.2 GW vector against our target mRNA. The engineered pre-miRNA hairpins are cloned into the Pol II miR RNAi expression vector. Once cloned in, these hairpin loop-structures are expressed by the mammalian cells and are cleaved into approximately 22 base-pairs (bp) transcripts by the enzyme Dicer. The single stranded siRNA is then incorporated into an RNA-induced silencing complex (RISC). This complex then targets the complementary mRNA and carries out specific cleavage or translational repression (depending on whether this complementarity is complete or not).

To construct the PARG RNAi cell line we followed the '*Block it' kit* protocol. We synthesized three hairpins for PARG RNAi using this

system. We then transiently transfected these hairpins (HPs) into 293T cells and performed a western blot that was probed with a 1/2000 dilution of a PARG antibody (Millipore) to look for knockdown of co-transfected PARG using tubulin as a loading control (1/10,000, Sigma). Our western blot showed that the best knockdown was with a combined transient transfection with hairpins 2 and 3 (figure 6.2). This inspired us to chain these hairpins together (as per the *Block iT* protocol) and create a stable cell line of PARG RNAi from chained HPs 2 and 3 (figure 6.3 and 6.4).

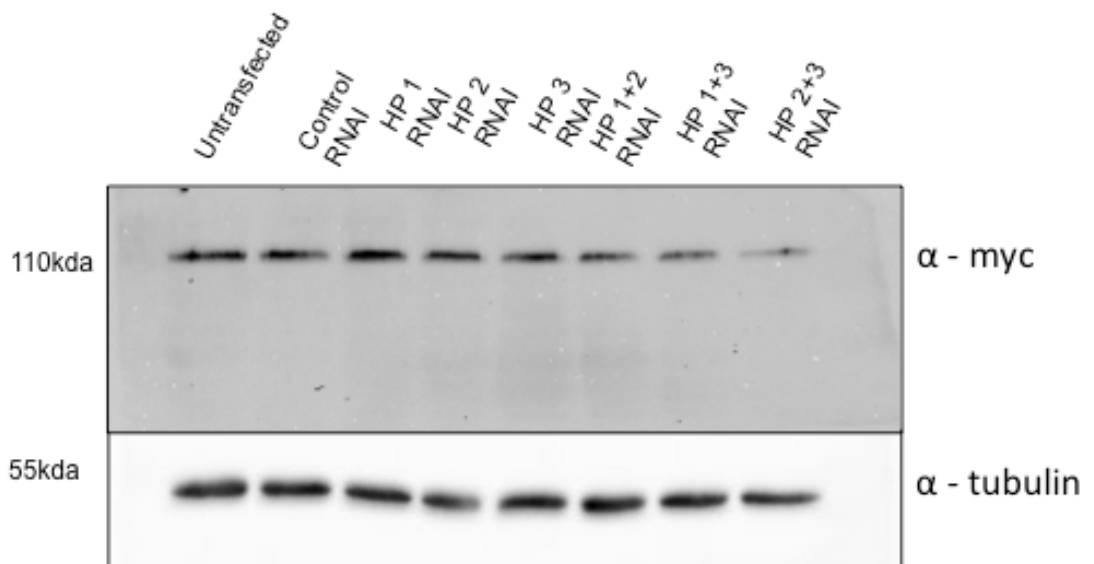


Figure 6.2. Knockdown of myc-tagged PARG in 293T cells co-transfected with myc tagged PARG and PARG RNAi hairpins (HP). Co-transfection with hairpins 2 and 3 gave the greatest knockdown. Tubulin is used as a loading control.

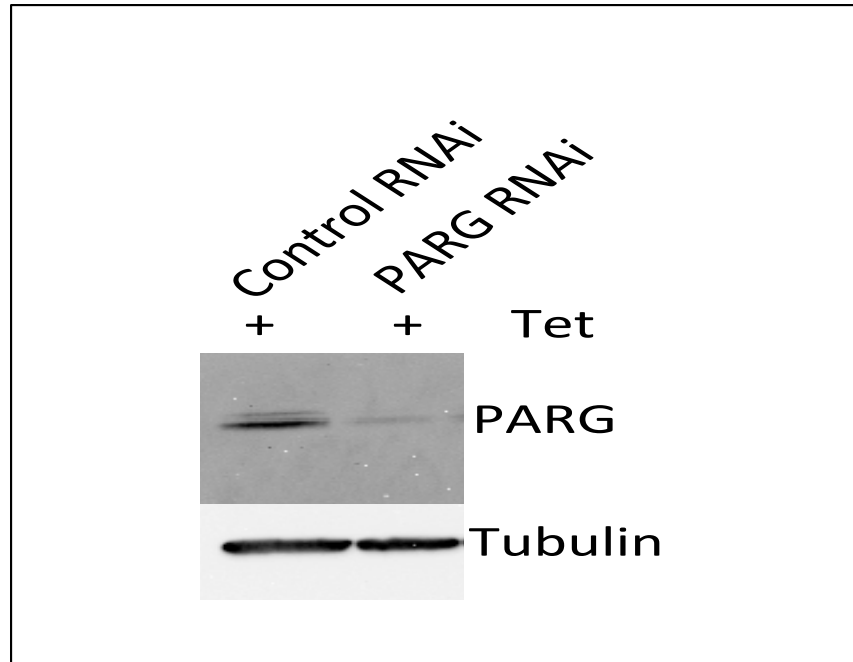


Figure 6.3. Western analysis of the FlpIn 293 cell line with a stably integrated inducible miRNA targeting PARG. Tetracycline (1 $\mu\text{g}/\mu\text{L}$) was added to induce PARG miRNA expression every 48 hours for 72 hours.

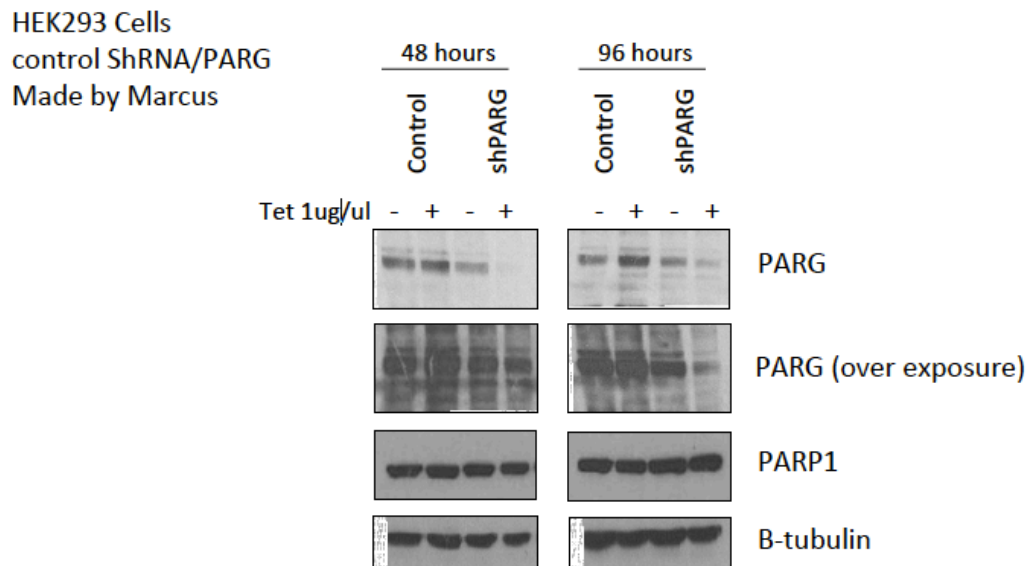


Figure 6.4. Generated by Polly Gravells of Dr Helen Bryant's laboratory. Our PARG RNAi cell line was aliquoted and shared with Dr Bryant's laboratory. This figure shows that the PARG RNAi stable cell line knocks down PARG and not PARP. Jungmichel S et al (2013) showed that it is the isoform PARP1, not PARP 2 that is responsible for the majority of poly(ADP-ribosyl)ation following DNA damage.

6.3. THERE IS A TOTAL mRNA EXPORT BLOCK UPON INDUCTION OF PARG RNAi IN CONDITIONS OF DNA DAMAGE

Jungmichel et al (2013) showed that a large proportion of PARylation protein targets are involved in RNA processing. From the supplementary data of a similar paper (Zhang et al., 2013) we found a number of the TREX subunits (20% of all targets). We hypothesized, that poly (ADP-ribosyl)ation of said targets might result in a mRNA export block. To interrogate this hypothesis we decided to first test whether there was an effect on global mRNA export when PARylation was induced using H₂O₂ oxidative stress. To conduct this experiment we used the *Click-iT* nascent mRNA capture kit (Life Technologies) (Figure 6.5).

The click-iT kit allows the labeling of nascently transcribed RNA with a fluorescent signal. In a control background, following this labeling, the RNA cytoplasmic signal diminished rapidly and was largely absent by 4 hours. This is because the mRNA is exported into the cytoplasm and turned over. The cytoplasmic RNA signal in 293 cells is very difficult to observe, even using other methods such as oligo(dT) FISH. In contrast, in PARG RNAi cells subjected to H₂O₂ treatment, the nascent RNA remained nuclear throughout the 8 hour time course and this was reversed when PARylation was blocked using a PARP inhibitor (Nu1025, Enzo) (Figure 6.6). In the absence of a DNA damaging agent, cells with PARG knocked down, also showed some accumulation of nascent RNA in the nucleus, presumably due to PARylation triggered by spontaneous DNA damage. The accumulation of nascent RNA in cells

following DNA damage was similar to that observed when TREX was disabled by the combined knockdown of THOC5 and ALYREF (figure. 6.6, right column). These experiments cannot formally exclude the possibility that the nuclear accumulation of nascent RNA arises because of a defect in RNA processing which would also trigger an mRNA export block. However, most splicing occurs co-transcriptionally and is rapidly proceeded by cleavage/polyadenylation of mRNAs. Moreover, the nascent RNA was labeled for 1 hour prior to any DNA damage; therefore many of the labeled transcripts are likely to be fully processed. Therefore the results suggest that upon H₂O₂ treatment there is an effect, caused by PARylation, which reduces mRNA export and this is in part likely to be caused by a direct effect on the export machinery.

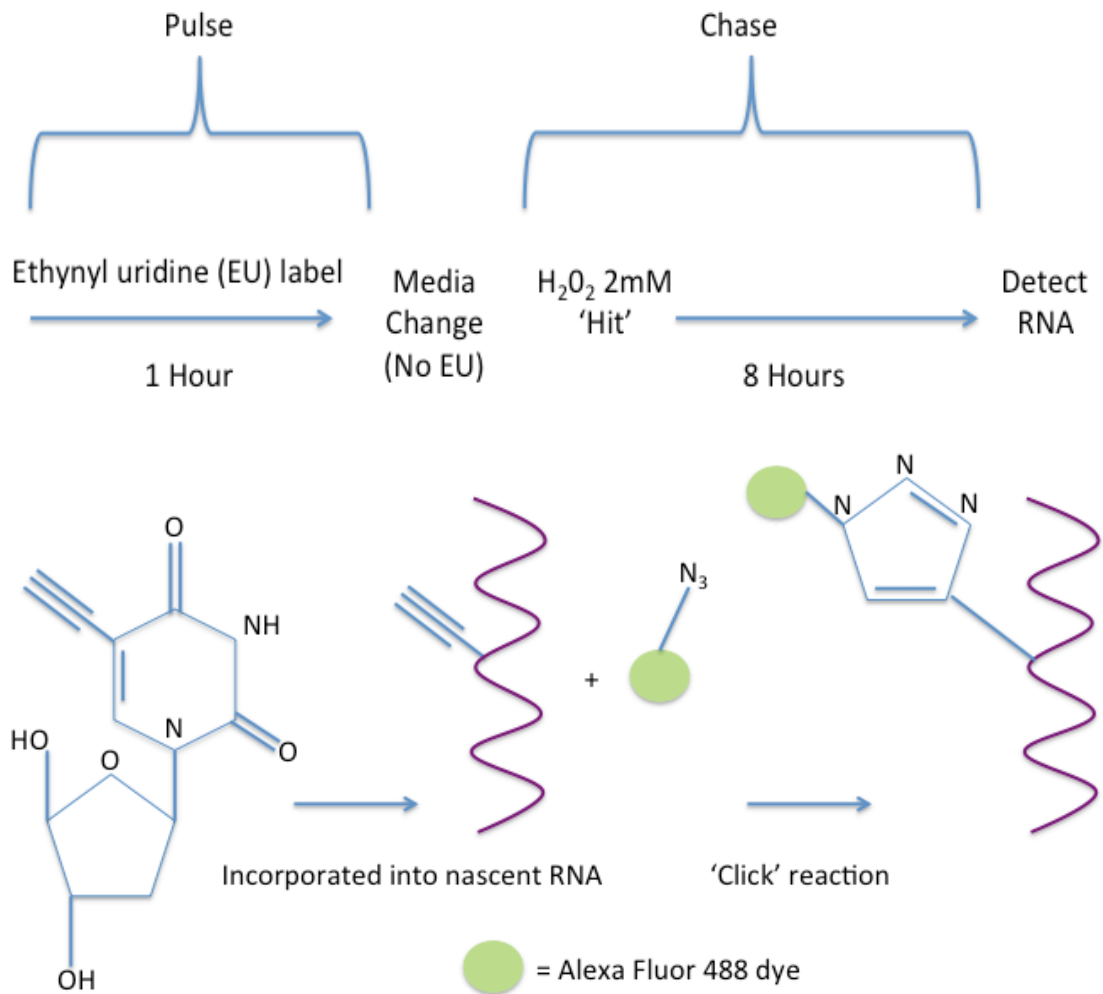


Figure 6.5. Schematic of the *Click-iT* experiment [Adapted from Buck SB et al. *BioTechniques* 2008] 1) Pulse-chase ethynyl uridine (EU) labeling 2) Click iT technology explained. There is a free alkyne group on the EU label incorporated into the RNA at uridine sites (approximately every 35th (*LifeTechnologies*)), this is then bound by an azide group on the Alexa fluorophore forming a triazole bound in a reaction catalyzed by a copper-containing reaction mixture (*LifeTechnologies*).

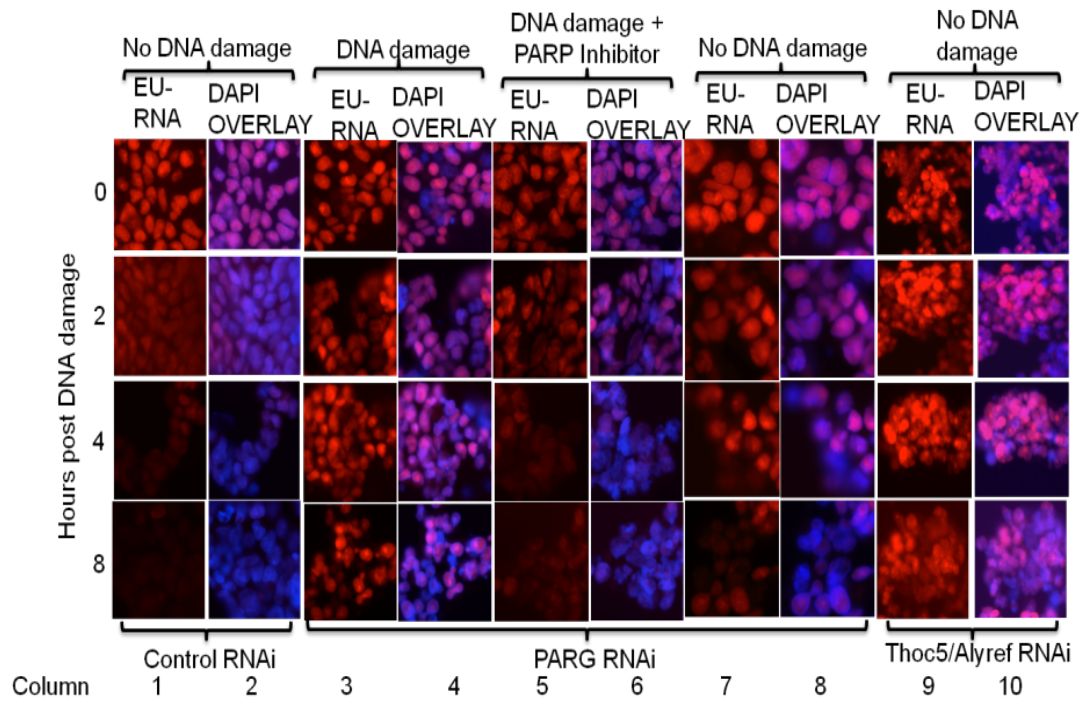


Figure 6.6. Click-iT pulse-chase EU labeling experiments. EU labeling is detected in the red channel showing nuclear accumulation of mRNA.

6.4. COIMMUNOPRECIPITATION PATTERNS OF ALYREF WITH UAP56 UNDER DNA DAMAGE STRESS

Following on from our observations during our nascent mRNA export assay, we looked back at the library of proteins shown by Jungmichel et al. (2013) and confirmed that ALYREF is a known target. Jungmichel et al. (2013) also mapped the residues of the proteins that are known to be PARylated and an overwhelming majority for ALYREF resided within the two UBM regions (see Figure 6.8). We decided to examine whether DNA damage with H₂O₂ treatment would show a PARylation effect on ALYREF binding to UAP56, as this partnership is crucial for appropriate TREX assembly (Dufu et al., 2010).

We performed our standard co-immunoprecipitation (Co-IP) experiment with initially 4 experimental conditions. We pre-incubated protein sepharose G beads with either ALYREF or Influenza Hemagglutinin (HA) as per protocol. For our DNA damage condition we exposed a 15cm dish of control or PARG RNAi cells with 200 µM H₂O₂ for 1 hour with or without a pre-incubation with 10 µM NU1025 PARP inhibitor. We then lysed the cells using a standard IP lysis buffer. For those lysates that were destined to be incubated on the ALYREF bound beads, we lysed in the presence of 1 µM of PARG inhibitor (Enzo) to further sustain the poly (ADP-ribosyl)ation modification. We saw that PARylated high molecular weight proteins were detected in the ALYREF IP, when subjected to a H₂O₂ shock (Figure 6.8, top left panel). This result

validates the mass spectrometry data and suggests that TREX subunits which will CO-IP with ALYREF are PARylated in response to DNA damage. We also noticed that there was a modest increase in the amount of UAP56 which CO-IPed with ALYREF in conditions of DNA damage when PARylation persisted due to PARG RNAi (figure 6.7, left hand side, bottom panels). To investigate this further we repeated the Co-IP experiments with ALYREF in stringent conditions using 1M NaCl in the binding and wash buffers (figure 6.7, right panels). In these conditions it was clear that DNA damage induced PARylation led to stabilisation of the UAP56:ALYREF complex particularly following PARG knockdown. Moreover, this effect was seen with two different DNA damage conditions (MMS and H₂O₂) and could be reversed by PARP inhibitor, confirming the effect was dependent upon PARylation. There is an enrichment of the Co-IP of these two TREX subunits under DNA damage conditions, which is amplified in the more stringent conditions of high salt. Appropriate levels of DNA damage are confirmed by the detected of multiple PARylated proteins by probing with the anti-PAR antibody (Enzo). Levels of ALYREF are used as a loading control across conditions.

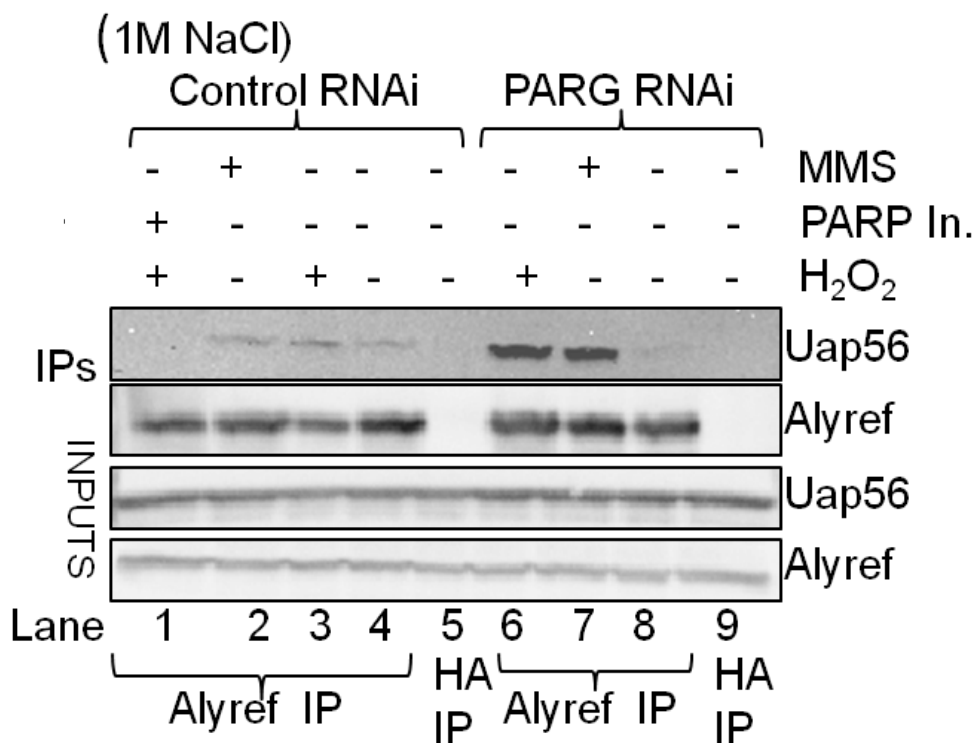
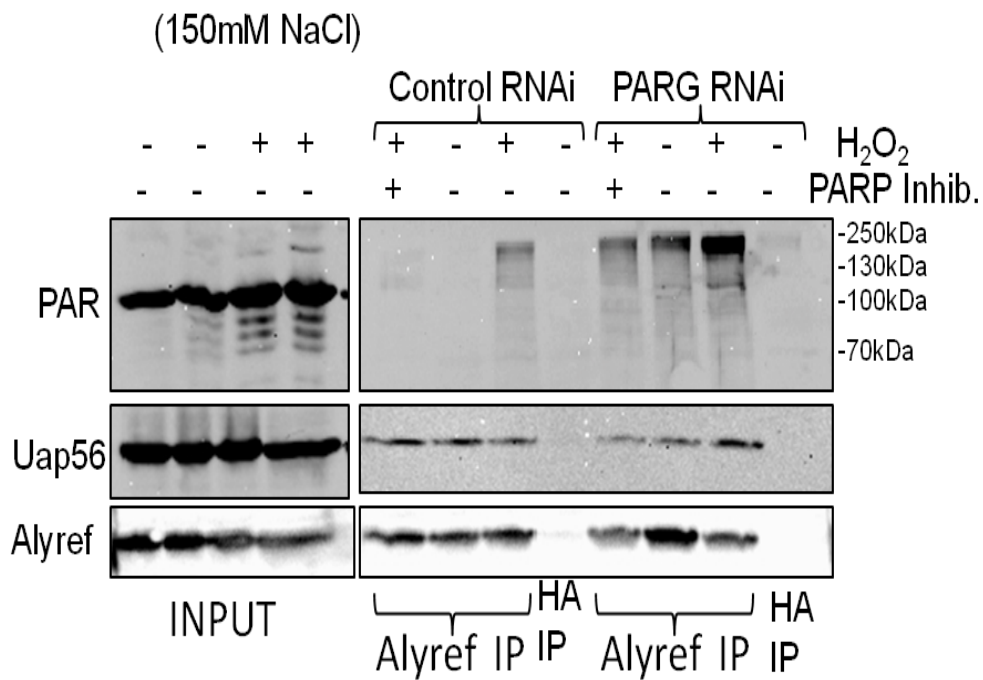


Figure 6.7: Co-Immunoprecipitation (Co-IP) of ALYREF and UAP56 under conditions of DNA damage using H₂O₂ and the alkylating agent MMS (methyl methane sulphonate).

6.5. IDENTIFYING THE PAR BINDING SITE ON UAP56

Ultimately, we wanted to design a set of experiments where we induced DNA damage and examined the interactions of TREX subunits (in particular ALYREF and UAP56) in conditions with and without PAR binding to UAP56 in order to assess the specific effects of poly (ADP-ribosyl)ation on the ability of these two proteins to bind one another and for them to carry out their normal function. For example, we wanted to determine whether the effects of PARylation would prevent UAP56 from performing its helicase and ATPase activity.

As mentioned briefly above, mass spectrometry based proteome wide studies of PARylation targets identified numerous RNA binding protein targets. Zhang Y et al (2013) showed that 20 % of the PARylated proteins mapped involved TREX subunits (Zhang et al., 2013). Within this dataset, it was striking that a common modification site for PARylation was the UBM (UAP56-binding motif) of TREX subunits ALYREF and CHTOP, previously shown to be essential for their assembly (Chang et al., 2013) (figure 6.8). Whilst it had been shown by previous authors (Jungmichel et al., 2013; Zhang et al., 2013) that ALYREF was a target of PARylation, it had not been clearly shown that UAP56 could be PARylated. Gagne et al (2008), performed an in-silico analysis of PAR-binding proteins and showed that they seem to share a consensus peptide sequence, KDFQRRIL (Gagne et al., 2008). This was hence thought to be a putative binding domain for PAR. Strikingly, this sequence resides within the C terminal half of UAP56 (figure 6.9 shows crystal structure).

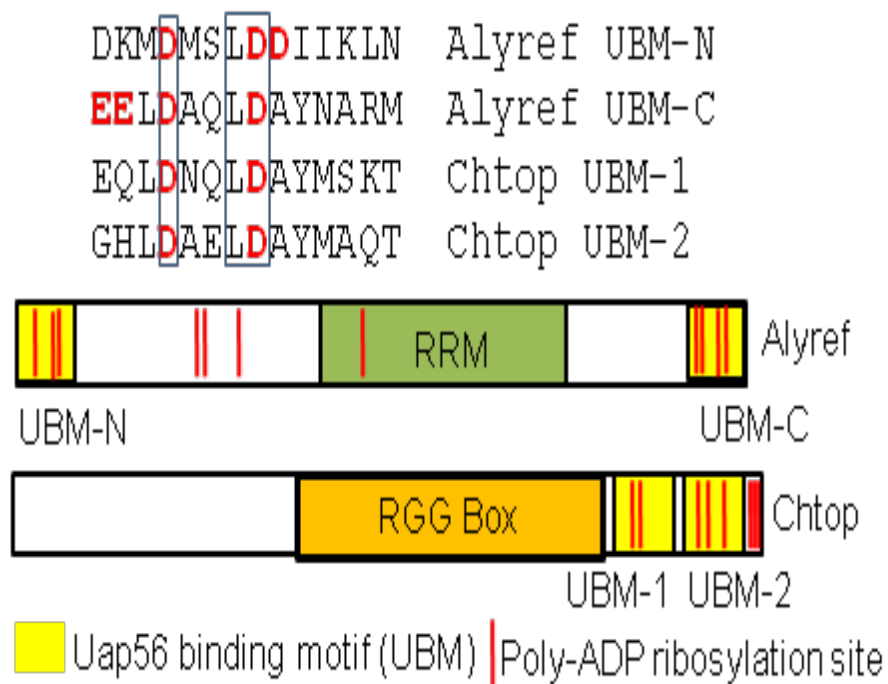


Figure 6.8. Schematic of ADP ribosylation sites on ALYREF and CHTOP. These overlap with UAP56-binding domains (UBMs).

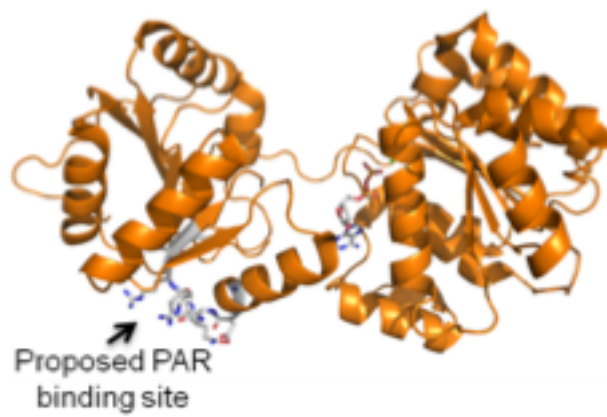


Figure 6.9. Crystal structure of Uap56 with the proposed PAR-binding site highlighted. ADP is bound at the interface between the two domains.

We designed an experiment to test whether UAP56 could bind PAR in-vitro using biotinylated PAR incubated on streptavidin beads, and tested whether His-tagged pet24b-UAP56 would pulldown with PAR in rabbit reticulocyte lysate (figure 6.10). We found that full length UAP56 bound PAR, and furthermore discovered that the N- and the C-terminal truncations of UAP56 bound PAR.

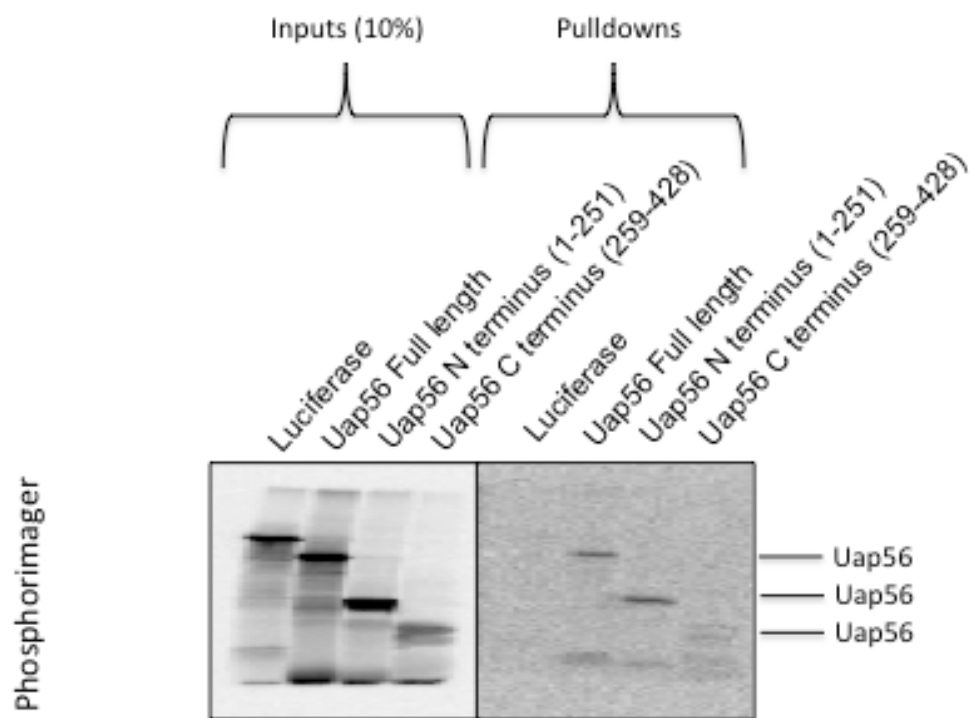


Figure 6.10. Pull-down of pet24b-UAP56 and UAP56 truncations in reticulocyte lysate by Biotin-PAR using streptavidin beads.

Having identified that UAP56 could bind PAR, we decided to test whether mutations in the putative PAR-binding site would prevent binding of UAP56 to PAR in vitro. We designed a range of mutations within the peptide sequence KDFQRRIL using our site-directed mutagenesis protocol, and our most impressive outcomes were from mutations to the juxtaposing phenylalanine and glutamate (figure 6.10, 6.11), changing them to alanines (KDAARRIL). Mutating phenylalanine and glutamate to alanines on putative PAR-binding site on UAP56 reduces binding to PAR. This experiment was conducted with and without RNase A added to the wash buffers to ensure that binding was direct and not bridged by RNA. The result was the same.

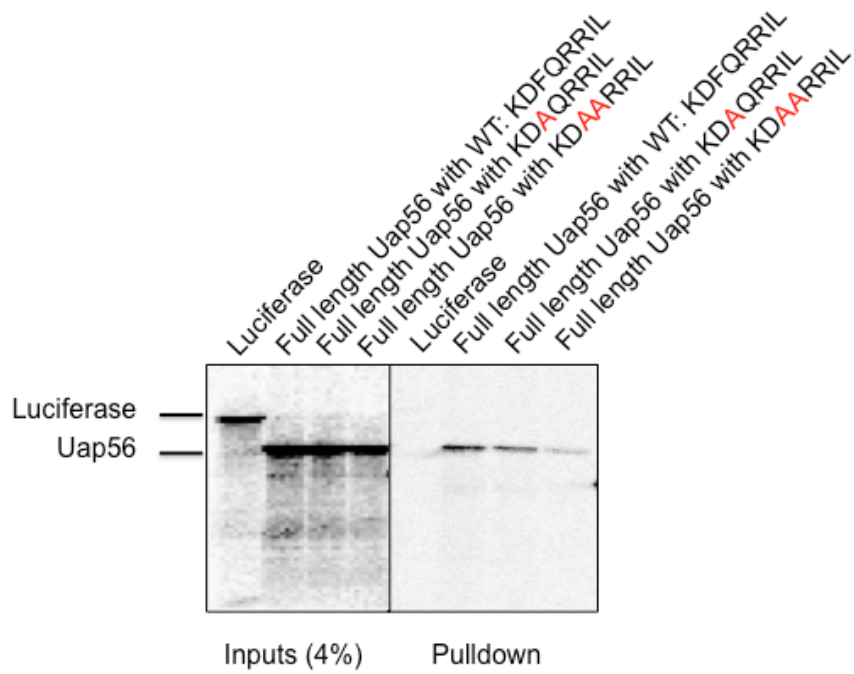


Figure 6.11. Pull-down of pet24b-UAP56 and UAP56 binding site PAR mutants in reticulocyte lysate by Biotin-PAR using streptavidin beads.

Next we wanted to assess whether the ALYREF UBM could still bind the UAP56-PAR binding site mutant. Our results show that the ALYREF UBM binds less efficiently when the putative PAR-binding site is double mutated. This experiment was conducted with and without RNase A (images with RNase A shown) added to the wash buffers to ensure that binding was direct and not bridged by RNA (figure 6.12 and 6.13). That the UBM does not pull down with the UAP56 mutant, which does not bind PAR suggests that the UBM and PAR binding sites are one and the same on UAP56. This finding suggests that the normal ALYREF UBM:UAP56 interaction is replaced with an ALYREF-PAR:UAP56 interaction ie. PAR replaces the UBM in making the interaction between ALYREF and UAP56. Contrary to this, the full length ALYREF can still bind the UAP56 mutant. This can be explained by earlier published work (Golovanov et al., 2006) because the ALYREF RRM (RNA recognition motif) outside of the UBM also makes contact with UAP56. Furthermore, the protein CIP29 can also bind the Uap56 mutants confirming that the non-binding of the UAP56-PAR binding site mutants to the ALYREF UBM is not due to the UAP56 mutants being unable to bind anything (figure 6.14).

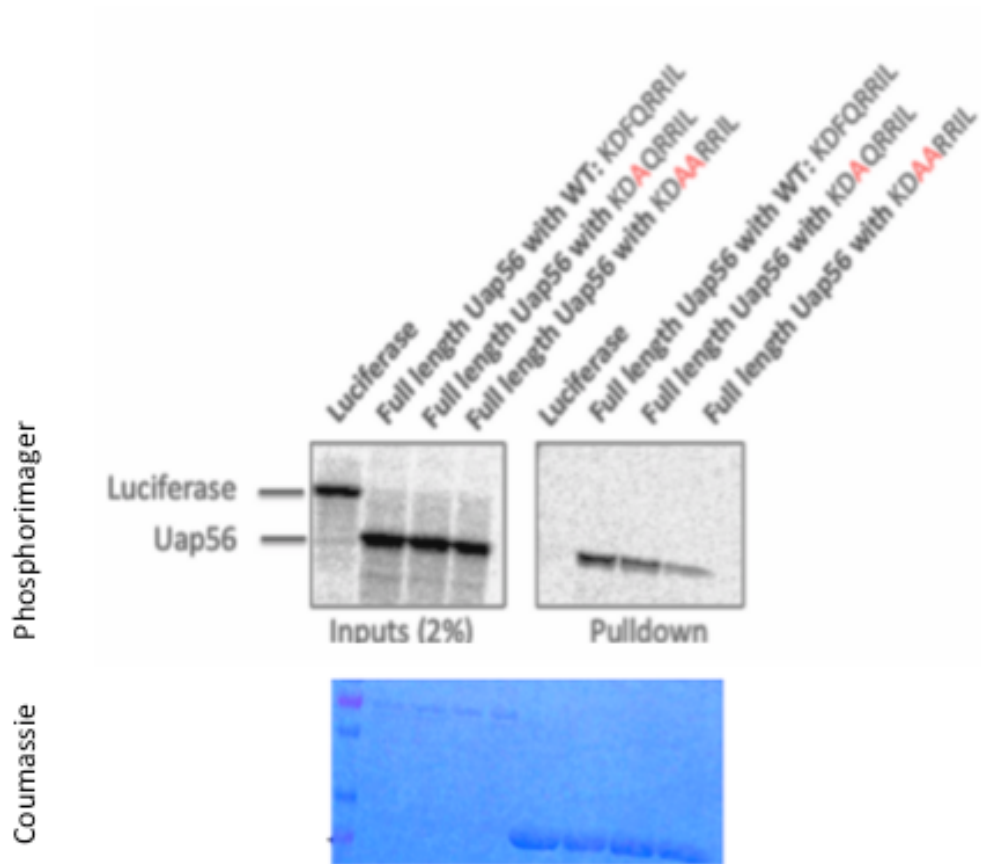


Figure 6.12. GST-ALYREF WT UBM (N terminal) pull-down with PAR-binding site mutations and full length WT UAP56-pet24b in reticulocyte lysate. The Coomassie stain is shown to illustrate equivalent GST inputs.

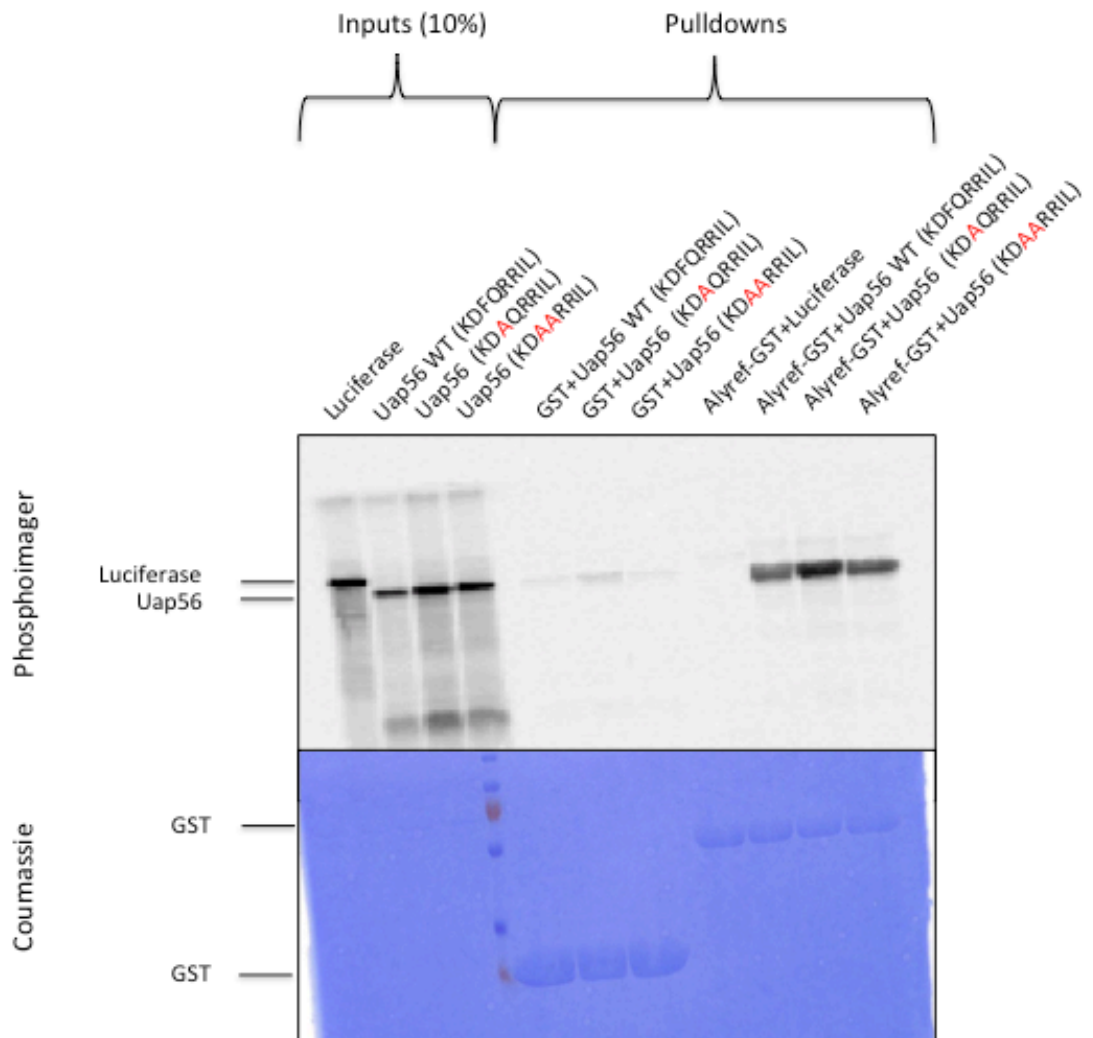


Figure 6.13. Pull-down with GST-tagged full length WT ALYREF protein and UAP56 with putative PAR-binding site mutations. GST and luciferase are used for control conditions.

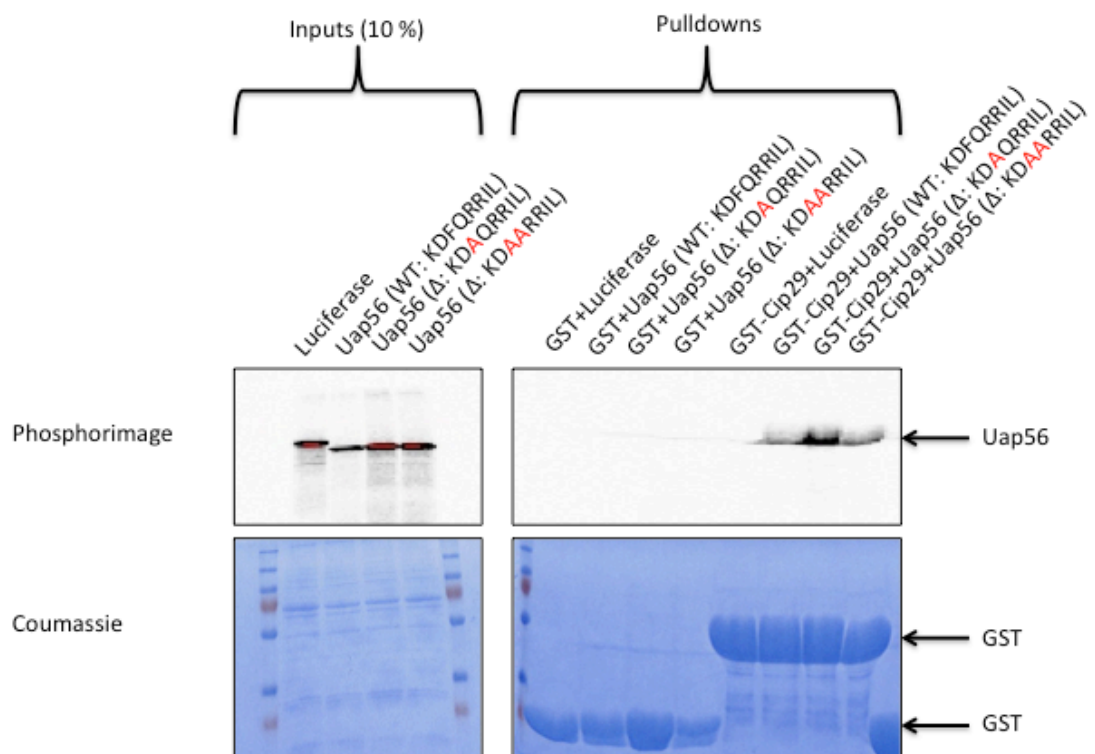


Figure 6.14. Pull-down using UAP56-pet24b in reticulocyte lysate with GST-tagged purified proteins. RNase A was added to the wash buffers to ensure that binding was direct and not bridged by RNA. Coomassie staining shows equal loading within each condition.

Having identified the PAR-binding site on UAP56 we wanted to see whether we could show, in vivo, that PARylation of UAP56 is indeed responsible for the mRNA export block that we have observed previously upon DNA damage and whether this may be because of an alteration in the activity of UAP56. By mutating the UAP56-PAR binding site, there might be an alteration in the ability of UAP56 to conduct its helicase and ATPase activities in vivo. We had the idea that we could use at least one of these biochemistry experiments along with mRNA export assays to examine this. We created a complementation cell line (Viphakone et al., 2012) whereby we inserted an RNAi resistant WT UAP56 cDNA into an FRT vector containing UAP56 and DDX39 RNAi hairpins. We also made the same cell line using our most potent mutant of the UAP56-PAR binding site. By constructing these cell lines we were hopeful that we could see whether PARylation of UAP56 and the associated mRNA export defects could be negated by the expression of a UAP56-PAR binding site mutant. The rationale being that if one has a mutant of UAP56 which no longer binds PAR well but can still bind UAP56, then we should be able to dissect the importance of ALYREF and PAR binding to UAP56 in vivo.

6.6. IS LOCALISATION OF COMMON EXPORT FACTORS ALTERED UPON DNA DAMAGE?

Subsequent to our findings above, that global mRNA export is down-regulated upon H₂O₂ induced DNA damage, we wanted to find out what cellular localization changes are occurring that might reflect/be responsible for this blockade. In addition to interrogating the interactome between core TREX components under stress conditions (above), we sought to determine whether or not TREX components have altered cellular localization upon DNA damage.

Reed and Hurt (2002) showed that subunits of TREX complex are distributed throughout the nucleoplasm, and largely reside in nuclear speckles (Reed and Hurt, 2002). This has been shown by TREX subunit co-localisation with splicing factor SC35. Viphakone et al (2015) showed that LUZP4 (see Chapter 5) had a distinctly different nuclear localization when it's UBM was deleted (truncated mutant). Given the changes to the binding of the ALYREF UBM to UAP56 when PARylated secondary to DNA damage, we wondered whether we would see a novel nuclear localization phenotype upon treatment with H₂O₂.

To investigate this, immunostaining (see materials and methods) of 293T cells was used. Cells were either probed with antibodies for endogenous proteins or were transfected with GFP-tagged TREX subunit proteins. The cells were co-stained for SC35, a protein known to localize to nuclear speckles. Cells were also stained for DAPI to highlight the nucleus (as it binds to DNA). All pictures were taken at the

same exposure level. Where indicated cells were treated with Triton-X pre-fixation and/or Actinomycin D was added for 2 hours pre-staining where indicated, to reduce the nascent RNA signal. This was performed so that any difference in localization would not be due to inadvertent perturbation of transcription (see figures 6.15 to 6.17). For ALYREF, UAP56 and CHTOP we saw no substantial changes in cellular localization upon DNA damage.

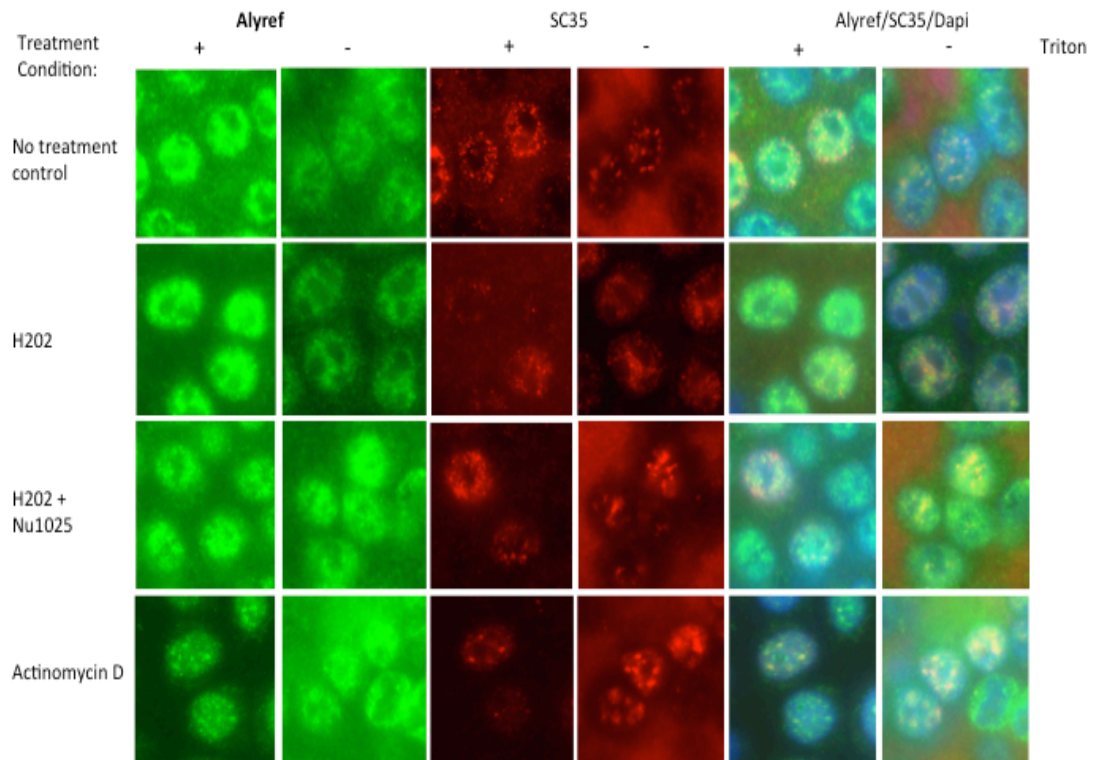


Figure 6.15. Immunofluorescence on 293T cells to assess the cellular localization of ALYREF upon under normal conditions and DNA damage with H₂O₂.

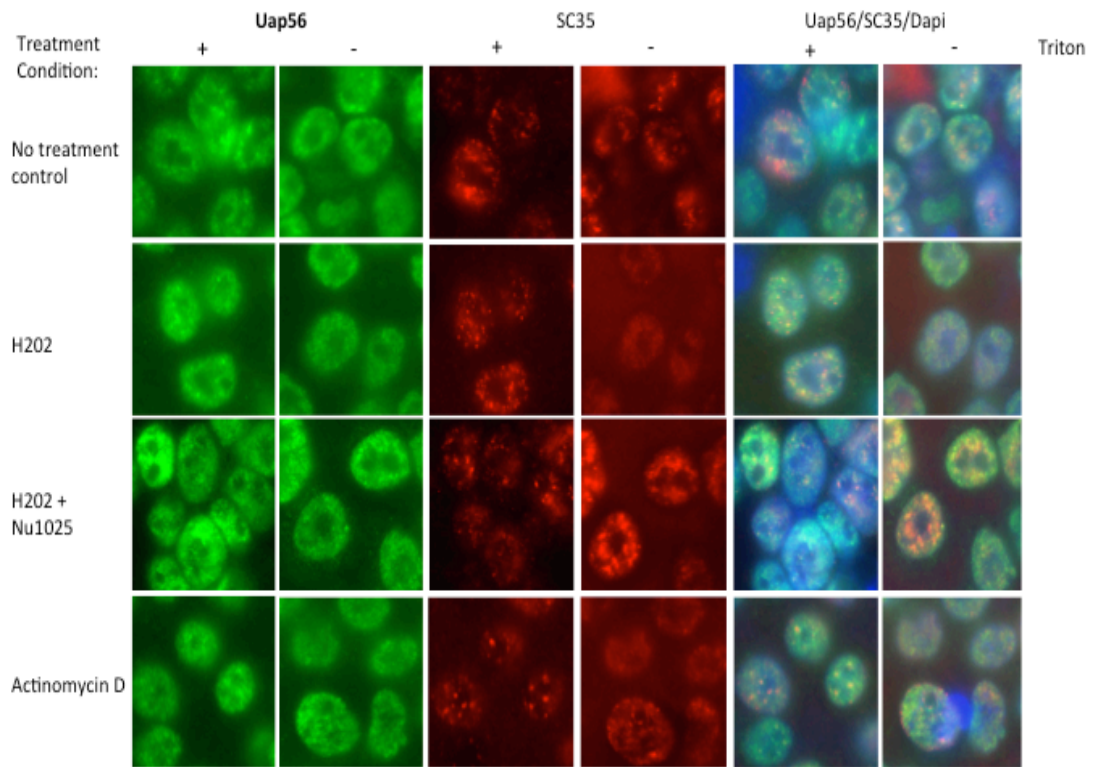


Figure 6.16. Immunofluorescence on 293T cells to assess the cellular localization of UAP56 upon under normal conditions and DNA damage with H₂O₂.

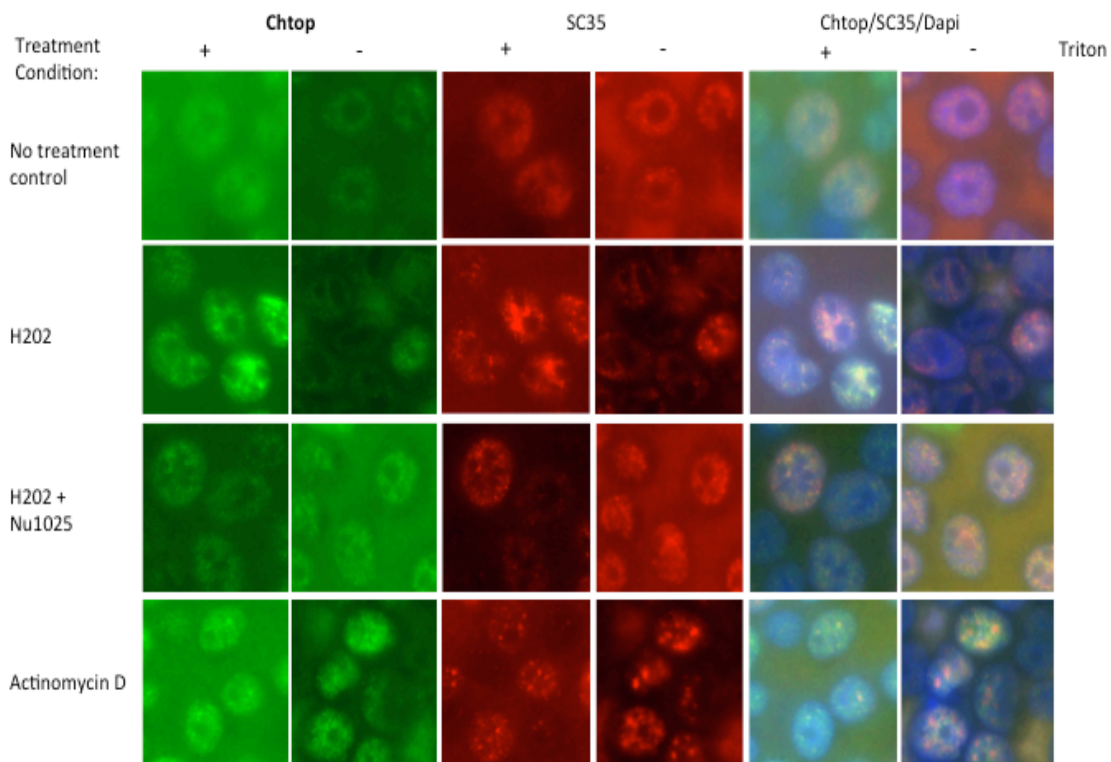


Figure 6.17. Immunofluorescence on 293T cells to assess the cellular localization of CHTOP upon under normal conditions and DNA damage with H₂O₂.

Finally, we know that the Wilson laboratory has previously shown how NXF1 associates to the nuclear envelope and that this phenotype is lost when core TREX subunits ALYREF and THOC2 are depleted by RNAi (Viphakone et al., 2012). Here we wanted to investigate whether the same defect was apparent upon treatment with H₂O₂. This was especially interesting given that NXF1 and its co-factor NXT1 are targets of poly (ADP-ribosyl)ation as reported by Jungmichel et al. (2011) (figure 6.1). There were no substantial changes in association with the nuclear envelope for either NXF1 or NXT1 upon DNA damage (figures 6.18 and 6.19). It is accepted that a limitation of immune-fluorescence is the lack of/difficulty in quantification.

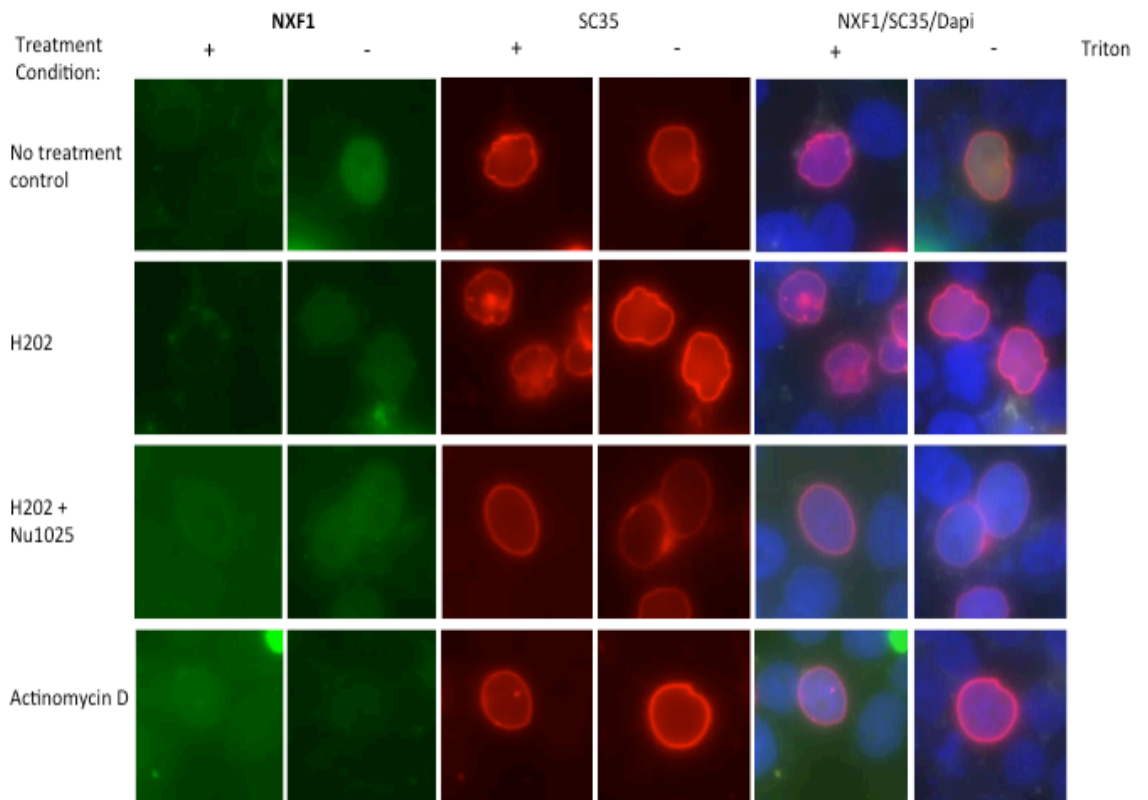


Figure 6.18. Immunofluorescence on 293T cells to assess the cellular localization of NXF1 upon under normal conditions and DNA damage with H₂O₂.

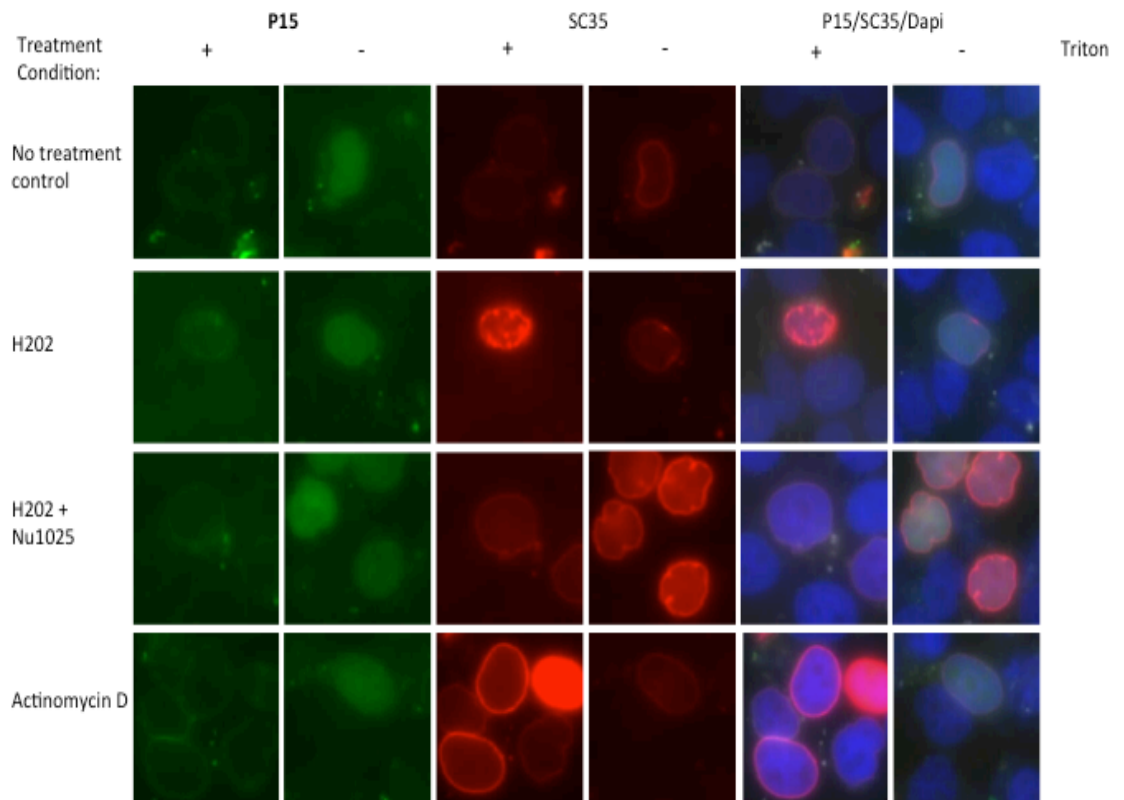


Figure 6.19. Immunofluorescence on 293T cells to assess the cellular localization of P15 (NXT1) upon under normal conditions and DNA damage with H₂O₂.

6.7. LIVE mRNA IMAGING: CLONING OF SPINACH2 AND mCHERRY INTO pCI NEO VECTOR

Following on from my *Click-iT* experiments as a mode of examining mRNA export patterns, I decided that it would be useful to build and utilize a system of *live* mRNA capture. Work by Strack and Jaffrey et al (2013) showed how a novel RNA imaging modality known as Spinach-2 could be used to perform such a task (see introduction) (Strack et al., 2013). We used a pCI Neo vector expressing the RFP mCherry as the destination for cloning in multiple copies of the Spinach2 sequence. It was not known how many repeats of the Spinach2 would be needed to adequately image the live capture of mRNA in our chosen vector. In order to maximize our chances of detection we designed oligonucleotides to permit concatemization of the Spinach2 gene sequence (below). Using the generated overhangs, we used *XhoI* and *SaI* restriction enzymes to perform repeated restriction digests of Spinach2 sequence. In total I created a 9' mer aptamer of the sequence.

**5' GAAATGGTGAAGGACGGGTCCAGTAGGCTGCTTCGGCAGCCT
ACTTGT 3'**

Following the construction of 3', 6' and 9' copy aptamers, I transfected Cos-7 cells alongside a GFP control and two aptameric constructs from the Jaffrey laboratory (CGG and 5S). Unfortunately, despite the 9-copy aptameric construct, I was unable to see a convincing green luminescence from Spinach2 despite detecting an acceptable amount of mCherry being expressed from the same construct (figure 6.20).

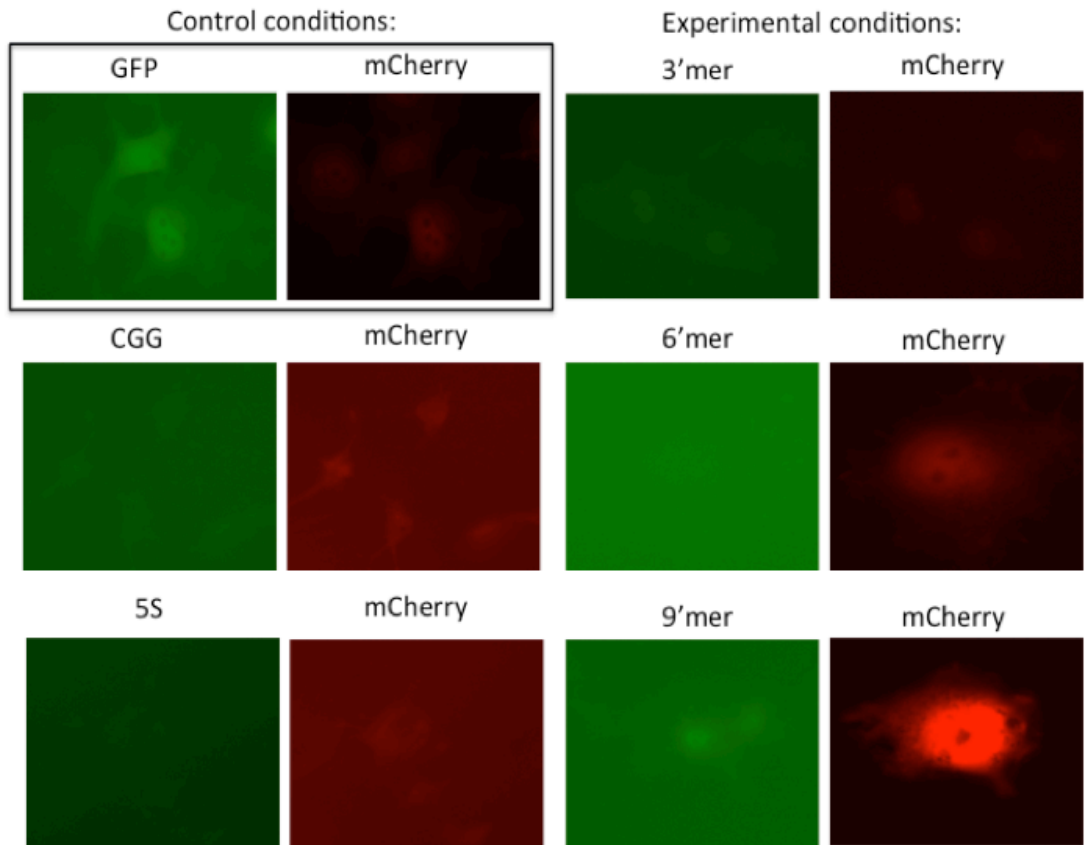


Figure 6.20. Microscope captured live-images of Spinach 2 transfected into Cos-7 cells.

6.8. SUMMARY

During this arm of my thesis, I interrogated the effects of DNA damage on TREX assembly and mRNA export. Through *Click-iT* nascent mRNA capture I have identified that a global mRNA export block ensues following treatment with H₂O₂, and that this is more pronounced following PARG RNAi suggesting a role of poly (ADP-ribosyl)ation. Following on from this I have demonstrated an effect on TREX assembly following MMS and H₂O₂ treatments. The interaction between the RNA helicase UAP56 and mRNA export adaptor ALYREF appears altered upon DNA damage, this too seems to be related to the PTM of poly(ADP-ribosyl)ation. Furthermore, I identified the PAR binding site on UAP56 and have shown that mutations in a consensus peptide sequence found in UAP56 and other PARylation targets do reduce the pulldown efficiency of UAP56 and biotinylated-PAR. Mutations in this sequence also affect the ability (in vitro) of the ALYREF N-terminal UBM to pulldown with UAP56.

An exciting future avenue would be to look at the functional significance of DNA damage induced PARylation of ALYREF and UAP56 on the ability of UAP56 to exert its ATPase or helicase roles. Work to this end is underway in the Wilson laboratory.

Lastly, in an attempt to study the effects of DNA damage on mRNA export using a live imaging technique, Spinach2, we were unable to reliably detect a fluorescence signal applicable for this aim. Since this work was completed, the Jaffrey lab have created a new construct known as Broccoli which is much improved, however, the integration of

Broccoli into this thesis was not possible within the time constraints
(Filonov et al., 2014).

CHAPTER 7: DISCUSSION

7.1. THE ROLE OF TOBACCO SMOKING AND OCCUPATIONAL CARCINOGEN EXPOSURE IN BLADDER CARCINOGENESIS: TWO META-ANALYSES

Bladder cancer is an intriguing research area with a high financial burden and high morbidity and mortality. It is among the commonest smoking-related cancers and has a clear relationship to occupational and lifestyle carcinogenic exposures. What makes the bladder susceptible to exogenous carcinogens is the way in which it acts as a reservoir for urine that may contain carcinogenic metabolites, and infrequent micturition (a risk factor for BC (Cumberbatch et al., 2015a; Cumberbatch et al., 2015b) may lead to prolonged exposure from these by the urothelial lining of the bladder. Current tobacco smoking still confers the greatest incidence and disease-specific mortality BC risk.

BC has historically been more common in men than women, but studies from the last two decades suggest that this trend has reversed. This would seem to reflect societal changes in the workplace and also lifestyle modifications.

In recent years we have started to understand the molecular basis of this cancer and these have largely arisen from a better understanding of

the aforementioned primary aetiologies (pointing to the importance of chapters 3 and 4).

Tobacco contains a rich source of polycyclic aromatic hydrocarbons, aromatic amines and N-nitroso compounds that cause DNA damage through bulky adduct formations, DNA breaks and base modifications (Stern et al., 2009). These tobacco carcinogens are detoxified by N-acetyltransferases and glutathione-S-transferases. It has been shown that individuals with slow NAT2 acetylation status clear these metabolites less efficiently and as such may be predisposed to BC. Genome-wide studies are further interrogating the link between other polymorphisms and BC (Figueroa et al., 2016).

It has been controversial whether quitting smoking actually confers a benefit to BC incidence but work in Chapter 3 suggests this is indeed the case. Another area of limited study is the role of second hand smoking (SHS), but our review suggests that there is an increased BC incidence from SHS (data not shown). It is hopeful that continuing tighter regulations on tobacco smoking will hopefully lead to reducing incidence rates in decades to come.

With regards occupational BC, despite workplace hygiene improvements and industrial sanctions, people are still at risk of occupational carcinogen exposures linked to BC. In this thesis I show that there is a disparity between occupations with high incidences and those with high mortalities. It is within the occupations with disproportionately high mortality that the greatest interventional efforts

are required as we move forward, and research in this field may be best directed towards the individual tasks that are performed by individuals in these groups to try and identify crucial processes that put people at risk and reveal occult or poorly controlled carcinogens. Interestingly, we see that it is in women that the risk is greatest at present and this must clearly reflect a change in working patterns. Efforts to identify carcinogens in workplaces more heavily populated by women must be made.

I can be confident in concluding that work within this thesis contributes towards the largest yet meta-analyses on the associations between smoking and occupational carcinogen exposure and bladder cancer.

7.2. LUZP4

Cancer testis antigens (CTAs) have been the focus of much scientific intrigue. There are currently more than 250 that have been characterized and the list is growing (Maxfield et al., 2015). As discussed earlier in this work, CTAs represent genes that are normally expressed in the testes, but may be aberrantly expressed in cancers derived from somatic cells. The testes are necessarily immune-privileged as normal spermatogenesis generates auto-antigens that can elicit immune responses. Therefore, antigens provoked from anomalously expressed CTAs can evoke cellular or humoral immune responses (Maxfield et al., 2015; Zhong et al., 2015). Therefore they offer a novel utility in being able to illicit immune responses to cancer.

Potentially, therapeutically, CTAs may be introduced as a means of immunotherapy. Indeed, early vaccinations using CTAs have been met with some success (Robbins et al., 2011; Wurz et al., 2016).

Work from this thesis has provided data for the characterization of a previously poorly understood CTA, LUZP4. Our lab has shown that LUZP4 functions as an mRNA export adaptor, adopting many of the cellular mRNA export functions of the canonical TREX subunit ALYREF. LUZP4 has been shown to bind RNA at two domains (Viphakone et al., 2015), it can Co-IP with many TREX subunits, requires a functional UBM for normal cellular localization, and is able to complement the loss of ALYREF in vivo. It seems apparent that in some cancers (melanoma is the most convincing), the normally redundant LUZP4 mRNA export pathway is active and is integral to the gene expression. Our paper on LUZP4 has shown a convincing link between mRNA export and cancer. Beyond the realm of this project but nonetheless an interesting proposition, would be the creation of a small molecule inhibitor of LUZP4 for use in a mouse model of malignant melanomas.

7.3. DNA DAMAGE

In this thesis, I interrogate the link between DNA damage and mRNA export. I have shown that the oxidative stress imposed by H₂O₂ causes a global mRNA block in 293T cells. This block has been shown to be resultant from a PARylation effect. We can be convinced of this as the RNAi of PARG emphasizes this block, and the pre-incubation of cells

with a PARP inhibitor prevents this export block. Upon the same conditions, there is an enhance Co-IP of two core TREX components ALYREF and UAP56 (this is also true when cells are exposed to the alkylating agent MMS). Having observed an mRNA export block with oxidative stress, we would have hypothesized that there might be a mal-assembly of these TREX subunits. The reason for the enhanced Co-IP is not clear. It may be hypothesized that either, under duress, TREX is stabilized as a means of promoting the processing and export of key transcripts for the cell to rescue function, or that perhaps this alteration in TREX assembly is a symptom of impending malfunction of the cell and is in fact a disabling interaction (figure 7.1).

For the first time, I have shown that UAP56 can bind PAR in vitro. As proposed by Gagne et al. (2008), this PAR-binding site seems to be represented by the peptide sequence KDFQRRIL, found in the C terminus of UAP56. Mutations in this sequence prevent normal binding of PAR to UAP56. Furthermore, mutations in this site perturb binding of UAP56 to the ALYREF N-terminal UBM but not the full-length protein. This result, along with a pulldown of UAP56 truncations, suggests that the binding of PAR is at both the N and C termini. What remains to be concluded is the functional relevance of PAR binding to UAP56. It may be that UAP56 is no longer able to perform its RNA helicase or ATPase activity. Both of these functions are necessary to recruit TREX to nascent RNA and drive its assembly. Therefore, I have set about the purification of these proteins and devised an ATPase activity protocol

(modified from Chan et al. (1986)) where we can assess the ATPase activity of UAP56 with PAR-binding site mutations alongside WT UAP56 and ALYREF. Alone, UAP56 has a weak ability to hydrolyse ATP but in the presence of ALYREF and/or RNA this is markedly increased (Chang et al., 2013). My hypothesis would be that the ATPase activity of the UAP56 mutant would be impaired following the mutation. I also plan to supplement the reactions with free-PAR (Trevigen) to see whether this stimulates or hinders the ATPase activity of UAP56.

Additionally, I have created a complementation cell line, wherein a cDNA of WT UAP56 resistant to RNAi has been incorporated into an FRT vector expressing hairpins for UAP56/DDX39 (UAP56 prologue) knockdown (figure 7.2). Concurrently, I have made the same cell line with a cDNA of the PAR-binding site double mutant also resistant to RNAi. We know from earlier work (Hautbergue et al., 2009) that UAP56/DDX39 RNAi is cell lethal in 6 days, and we know that there is an mRNA export block after 72 hours. The proposed experimental method with this cell line is to see whether the rescue of the mRNA export block expected with the WT RNAi resistant UAP56 is lost with the PAR-mutant.

These experiments are designed but due to time constraints at the end of this project, they may have to be completed at a later stage. In summary my work on DNA damage has shown that PARylation plays a role in mRNA export, which has the potential to modulate which mRNAs

are exported and thus which proteins are expressed during this cellular stress.

7.4. FUTURE DIRECTIONS

I would like study whether certain DNA damage repair transcripts are still exported under these H₂O₂ induced PARylation conditions. In order to study this, one could design single-transcript FISH probes and perform FISH under conditions of DNA damage to see whether there is preferential export of these transcripts. Identifying which transcripts to probe for would be the first step.

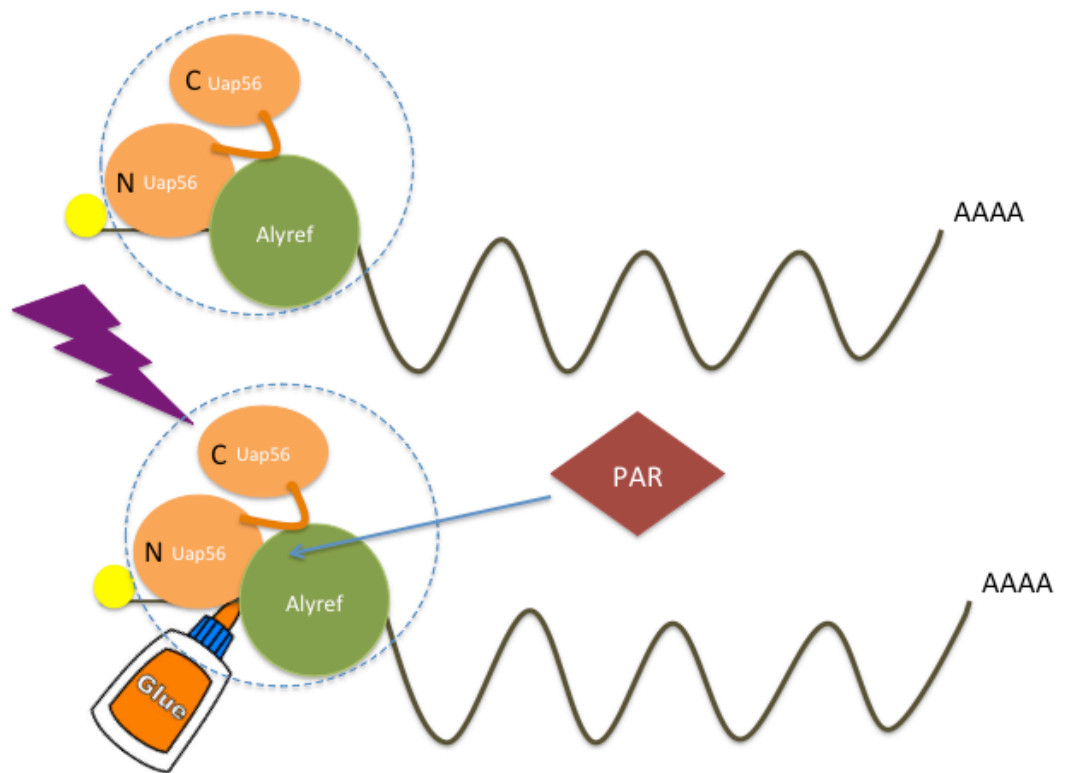


Figure 7.1. Proposed model showing that PAR can bind UAP56 and that under conditions of DNA damage, the TREX subunits ALYREF and UAP56 seem to become 'glued' together.

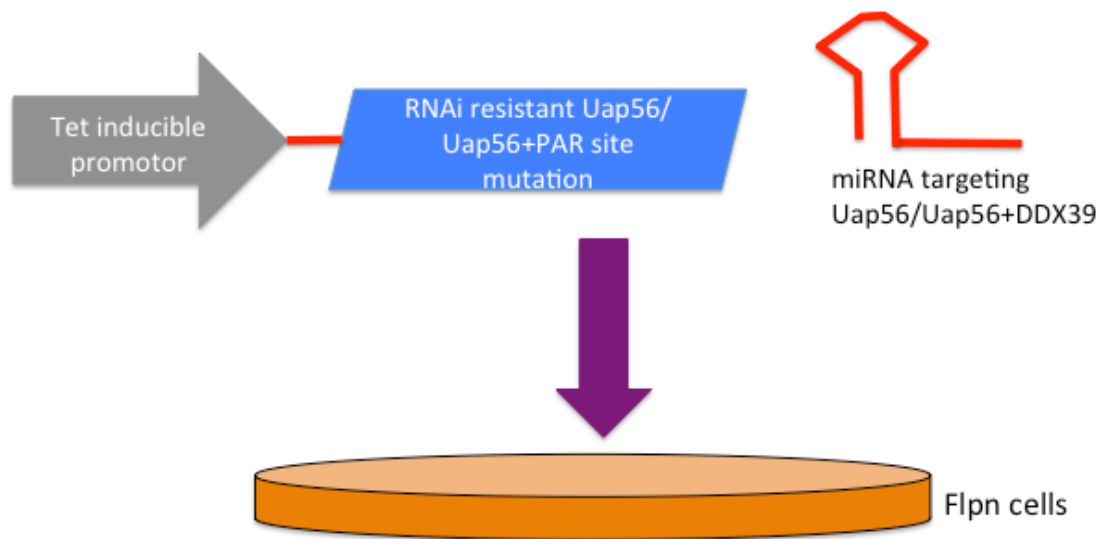


Figure 7.2. A pictorial description of the generation of a complementation cell line for UAP56 RNAi.

References

- Alvarez-Gonzalez R and Althaus FR. (1989) Poly(ADP-ribose) catabolism in mammalian cells exposed to DNA-damaging agents. *Mutation Research*. 218:67-74
- Ayubi TA and Van De Ven WJ. (1996) Regulation of gene expression by alternative promoters. *FASEB J*. Mar;10(4):453-60
- Baan R, Grosse Y, Straif K, et al. (2009) A review of human carcinogens--Part F: chemical agents and related occupations. *Lancet Oncol*. (10): 1143-1144
- Babjuk M, Bohle M, Burger M et al. (2015) Guidelines on non-muscle-invasive bladder cancer (Ta, T1 and CIS). European Association of Urology. Available from URL: <http://uroweb.org/wp-content/uploads/EAU-Guidelines-Non-muscle-invasive-Bladder-Cancer-2015-v1.pdf>
- Baker M. (2012) RNA imaging in situ. *Nature Methods*. (9): 987-790
- Bartkova J, Resaei N, Linton M et al. (2006) Oncogene-induced senescence is part of the tumorigenesis barrier imposed by DNA damage checkpoints. *Nature*. Nov 30;444(7119):633-7

Begg CB, Mazumdar M. (1994) Operating characteristics of a rank correlation test for publication bias. *Biometrics*. (50): 1088-1101

Bladder cancer statistics and outlook. Cancer research UK (cited Dec 2015). Available from URL: <http://www.cancerresearchuk.org/about-cancer/type/bladder-cancer/treatment/bladder-cancer-statistics-and-outlook>

Blower MD. (2013) Molecular insights into intracellular RNA localization. *Int Rev Cell Mol Biol*; 302: 1–39

Borzym-Kluczyk M, Radziejewska I, Zaniewska A et al. (2009) Effect of smoking on activity of N-acetyl-beta-hexosaminidase in serum and urine of renal cancer patients. *Clin Biochem*;42:1565-7

Breast cancer screening. NHS choices (cited Jan 2016). Available from URL: <http://www.nhs.uk/conditions/breast-cancer-screening/Pages/Introduction.aspx>

Britton JP, Dowell AC, Whelan P. (1989) Dipstick haematuria and bladder cancer in men over 60: results of a community study. *BMJ*. Oct 21;299(6706):1010-2.

Britton JP, Dowell AC, Whelan P, Harris CM. (1992) A community study of bladder cancer screening by the detection of occult urinary bleeding. J Urol. Sep;148(3):788-90.

Broude NE. (2011) Analysis of RNA localisation and metabolism in single live bacterial cells: achievements and challenges. Molecular microbiology. 80(5), 1137-1147

Bryant HE, Schultz N, Thomas HD et al. (2005) Specific killing of BRCA2-deficient tumours with inhibitors of poly(ADP-ribose) polymerase. Nature. Apr 14;434(7035):913-7.

Bryant HE, Petermann E, Schultz N, Jemth AN et al. (2009) PARP is activated at stalled forks to mediate Mre11-dependent replication restart and recombination. EMBO J. Sep 2; 28(17): 2601–2615.

BTA Stat® test. A Rapid Test For the Qualitative Detection of Bladder Tumor Associated Antigen in Human Urine. BTASat.com. Available from URL: http://www.btastat.com/package_insertp1.html

Buck SB, Bradford J, Gee KR, Agnew BJ, Clarke ST, Salic A. (2008) Detection of S-phase cell cycle progression using 5-ethynyl-2'-deoxyuridine incorporation with click chemistry, an alternative to using 5-bromo-2'-deoxyuridine antibodies. Biotechniques. June;44:927-929

Burger M, Catto JW, Dalbagni et al. (2013) Epidemiology and risk factors of urothelial bladder cancer. Eur Urol. Feb;63(2):234-41

Catto JW, Hartmann A, Stoehr R et al. (2006) Multifocal urothelial cancers with the mutator phenotype are of monoclonal origin and require panurothelial treatment for tumor clearance. J Urol. Jun;175(6):2323-30

Cervical screening: programme (cited Jan 2016). Available from URL: <https://www.gov.uk/guidance/cervical-screening-programme-overview>

Chan KM, Delfert D, Junger KD. (1986) A direct colorimetric assay for Ca²⁺-stimulated ATPase activity. Analytical biochemistry 157,375-380

Chang CT, Haurtbergue GM, Walsh MJ et al. (2013) CHTOP is a component of the dynamic TREX mRNA export complex. EMBO J. Feb 6;32(3):473-86

Chavan S, Bray F, Lortet-Tieulent J, Goodman M, Jemal A. (2014) International variations in bladder cancer incidence and mortality. Eur Urol. 66:59-73

Cheng L, Davidson DD, Maclennan GT et al. (2010) The origins of urothelial carcinoma. Expert Rev Anticancer Ther. Jun;10(6):865-80.

Chudakov DM, Matz MV, Lukyanov S, Lukyanov KA. (2010) Fluorescent proteins and their applications in imaging living cells and tissues.

Physiol Rev. Jul;90(3):1103-63.

Cohen SM, Shirai T, Steineck G. (2000) Epidemiology and etiology of premalignant and malignant urothelial changes. Scand J Urol Nephrol

Suppl. (205):105-15.

Cronshaw JM, Krutchinsky AN, Zhang W, Chait BT, Matunis MJ. (2002)

Proteomic analysis of the mammalian nuclear pore complex. J Cell Biol.

Sep 2;158(5):915-27.

Cumberbatch MG, Rota M, Catto JW, La Vecchia C. (2015a) The Role of Tobacco Smoke in Bladder and Kidney Carcinogenesis: A

Comparison of Exposures and Meta-analysis of Incidence and Mortality Risks. Eur Urol. Jul 3. pii: S0302-2838(15)00548-5.

Cumberbatch MG, Cox A, Teare D, Catto JW. (2015b) Changing trends in occupational bladder cancer: A systematic review and meta-analysis.

JAMA Oncology. Dec 1;1(9):1282-90

De Stefani E, Correa P, Fierro L, Fontham E, Chen V, Zavala D. (1991)

Black tobacco, mate and bladder cancer. A case-control study from

Uruguay. Cancer 67:536-40

Dey P. (2004) Urinary markers of bladder carcinoma. Clin Chim Acta. Feb;340(1-2):57-65

Doll R, Peto R. (1981) The causes of cancer: quantitative estimates of avoidable risks of cancer in the United States today. J Natl Cancer Inst. (66): 1191-1308.

Dominquez-Sanchez MS, Saez C, Japon MA, Aguilera A, Luna R. (2011) BMC Cancer. 11:17.

Dost A, Staughan JK, Sorohan T. (2009) Cancer incidence and exposure to 4,4'-methylene-bis-ortho-chloroaniline (MbOCA). Occup Med (Lond). 59(6):402-405.

Dufu K, Livingstone MJ, Seebacher J, Gygi SP, Wilson SA and Reed R. (2010) ATP is required for interactions between UAP56 and two conserved mRNA export proteins, Aly and CIP29, to assemble the TREX complex. Genes Dev. Sep 15;24(18):2043-53.

Egger M, Davey Smith G, Schneider M, Minder C. (1997) Bias in meta-analysis detected by a simple, graphical test. BMJ. (315): 629-634.

Emerging safety science: workshop summary. (2008) National Academies Press (US)

Fahrer J, Kranaster R, Altmeyer M, Marx A, Burkle A. (2007) Quantitative analysis of the binding affinity of poly(ADP-ribose) to specific binding proteins as a function of chain length. *Nucleic Acids Res.* Dec; 35(21): e143.

Fathers C, Drayton RM, Solovieva S, Bryant HE. (2012) Inhibition of poly (ADP-ribose) glycohydrolase (PARG) specifically kills BRCA-2 deficient tumour cells. *Cell Cycle*, Mar 1;11(5):990-7.

Figuroa JD, Middlebrooks CD, Banday AR et al. (2016) Identification of a novel susceptibility locus at 13q34 and refinement of the 20p12.2 region as a multi-signal locus associated with bladder cancer risk in individuals of European ancestry, *Hum Mol Genet.* Jan 4.

Filonov GS, Moon JD, Svensen N, Jaffrey SR. (2014) Broccoli: rapid selection of an RNA mimic of green fluorescent protein by fluorescence-based selection and directed evolution. *J Am Chem Soc.* Nov 19;136(46):16299-308.

Fratta E, Coral S, Covre A et al. (2011) The biology of cancer testis antigens: putative function, regulation and therapeutic potential. *Mol Oncol.* Apr;5(2):164-82

Freedman ND, Silverman DT, Hollenbeck AR, Schatzkin A, Abnet CC. (2011) Association between smoking and risk of bladder cancer among men and women. *JAMA*. Aug 17;306(7):737-45.

Friedrich MG, Toma MI, Hellstern KP et al. (2003) Comparison of multitarget fluorescence in situ hybridization in urine with other noninvasive tests for detecting bladder cancer. *BJU Int*. Dec;92(9):911-4

Gabriel U, Li L, Bolenz C et al. (2012) New insights into the influence of cigarette smoking on urothelial carcinogenesis: smoking-induced gene expression in tumour-free urothelium might discriminate muscle-invasive from non-muscle-invasive urothelial bladder cancer. *Mol Carcinog*. Nov;51(11):907-15

Gagne JP, Pic E, Isabelle M et al. (2012) Quantitative proteomics profiling of the poly(ADP-ribose)-related response to genotoxic stress. *Nucleic Acids Res*. Sep;40(16):7788-805.

Gasparian AV, Burkhart CA, Purmal AA et al. (2011) Curaxins: anticancer compounds that simultaneously suppress NF- κ B and activate p53 by targeting FACT. *Sci Transl Med*. Aug 10;3(95):95ra74

Gebhardt A, Habjan M, Benda C et al. (2015) mRNA export through an additional cap-binding complex consisting of NCBP1 and NCBP3. *Nat Comms*.

Golovanov AP, Hautbergue GM, Tinaru AM, Lian LY, Wilson SA. (2006) The solution structure of REF2-I reveals interdomain interactions and regions involved in binding mRNA factors and RNA. *RNA*. Nov;12(11):1933-48.

Greene KL, Berry A, Konety BR. (2006) Diagnostic Utility of the ImmunoCyt/uCyt+ Test in Bladder Cancer *Rev Urol*. Fall; 8(4): 190–197

Greenland S. (1987) Quantitative methods in the review of epidemiologic literature. *Epidemiologic Rev* 9:1-30.

Grossman HB, Soloway M, Messing E et al (2006) Surveillance for recurrent bladder cancer using a point-of-care proteomic assay. *JAMA*. 2006 Jan 18;295(3):299-305.

Hanahan D, Weinberg RA. (2000) The hallmarks of cancer. *Cell*. Jan 7;100(1):57-70

Hanahan D, Weinberg RA. (2011) Hallmarks of cancer: the next generation. *Cell*. Mar 4;144(5):646-74

Hautbergue GM, Hung ML, Walsh MJ et al. (2009) UIF, a New mRNA export adaptor that works together with REF/ALY, requires FACT for recruitment to mRNA *Curr Biol.* Dec 1;19(22):1918-24

Hung ML, Hautbergue GM, Snijders APL, Dickman MJ, Wilson SA. (2010) Arginine methylation of REF/ALY promotes efficient handover of mRNA to TAP/NXF1. *Nucleic Acids Research.* Vol. 38, No. 10 3351-3361

International Human Genome Sequencing Consortium. (2004) Finishing the euchromatic sequence of the human genome. *Nature.* Oct 21;431(7011):931-45.

Islami F, Stoklosa M, Drope J, Jemal A. (2015) Global and regional patterns of tobacco smoking and tobacco control policies. *Eur Urol Focus.* 1:3-16.

Jungmichel S, Rosenthal F, Altmeyer M et al. (2013) Proteome-wide identification of poly(ADP-ribosyl)ation targets in different genotoxic stress responses. *Mol Cell.* Oct 24;52(2):272-85.

Karni R, de Stanchina E, Lowe SW, Sinha R, Mu D, Krainer AR. (2007) The gene encoding the splicing factor SF2/ASF is a proto-oncogene. *Nat Struct Mol Biol.* Mar;14(3):185-93.

Katahira J, Inoue H, Hurt E, Yoneda Y. (2009) Adaptor Aly and co-adaptor THOC5 function in the Tap-p15-mediated nuclear export of HSP70 mRNA. *EMBO J.* Mar 4;28(5):556-67

Kinders R, Jones T, Root R et al. (1998) Complement factor H or a related protein is a marker for transitional cell cancer of the bladder. *Clin Cancer Res.* Oct;4(10):2511-20.

Kohler A, Hurt E. (2007) Exporting RNA from the nucleus to the cytoplasm. *Nat Rev Mol Cell Biol.* Oct;8(10):761-73.

Kubuschok B, Xie X, Jesnowski R et al. (2004) Expression of cancer testis antigens in pancreatic carcinoma cell lines, pancreatic adenocarcinoma and chronic pancreatitis. *Int J Cancer.* Apr 20;109(4):568-75.

Le Hir H, Gatfield D, Izaurralde E, Moore MJ. (2001) The exon-exon junction complex provides a binding platform for factors involved in mRNA export and nonsense-mediated mRNA decay. *EMBO J.* Sep 3;20(17):4987-97.

Li N, Chen J. (2014) ADP-ribosylation: activation, recognition, and removal. *Mol Cells.* Jan;37(1):9-16.

Lord CJ, Ashworth A. (2012) The DNA damage response and cancer therapy. *Nature*. Jan 18;481(7381):287-94

Lotan Y, Svatek RS, Krabbe LM, Xylinas E, Klatte T, Shariat SF. (2014) Prospective external validation of a bladder cancer detection model. *J Urol*. Nov;192(5):1343-8

Lynge E, Rix BA, Villadsen E et al. (1996) Cancer in printing workers in Denmark. *Occup Environ Med*. 52(11):738-744.

Hirose Y, Tacke R, Manley JL. (1999) Phosphorylated RNA polymerase II stimulates pre-mRNA splicing. *Genes Dev*. May 15;13(10):1234-9.

Houtgraaf JH, Vermissen J, van der Giessen WJ. (2006) A concise review of DNA damage checkpoints and repair in mammalian cells. *Cardiovasc. Revasc. Med*. Jul-Sep;7(3):165-72.

Human Nuclear matrix protein 22 (NMP-22) ELISA Kit (cited Aug 2015)

Mybiosource.com. Available from URL:

http://www.mybiosource.com/prods/ELISA-Kit/Human/Nuclear-matrix-protein-22-NMP-22/NMP-22/datasheet.php?products_id=264227.

Iglesias N, Stutz F. (2008) Regulation of mRNP dynamics along the export pathway. *FEBS Lett*. Jun 18;582(14):1987-96.

Izaurre E, Lewis J, Gamberi C, Jarmolowski A, McGuigan C, Mattaj IW. (1995) A cap-binding protein complex mediating U snRNA export. Nature. Aug 24;376(6542):709-12

Izaurre E, Lewis J, McGuigan C, Jankowska M, Darzynkiewicz E, Mattaj IW. (1994) A nuclear cap binding protein complex involved in pre-mRNA splicing. Cell. Aug 26;78(4):657-68.

Maxfield KE, Taus PJ, Corcoran K et al. (2015) Comprehensive functional characterization of cancer-testis antigens defines obligate participation in multiple hallmarks of cancer. Nat Commun. Nov 16;6:8840

Messing EM, Madeb R, Young T et al. (2006). [Long-term outcome of hematuria home screening for bladder cancer in men.](#) Cancer. Nov 1;107(9):2173-9.

Mitchell P and Tollervey D. (2003) An NMD pathway in yeast involving accelerated deadenylation and exosome-mediated 3'→5' degradation. Mol Cell. May;11(5):1405-13.

Moher D, Liberati A, Tetzlaff J, Altman DG; PRISMA Group. (2009) Preferred reporting items for systematic reviews and meta-analyses: the PRISMA statement. PLoS Med. Jul 21;6(7):e1000097

Momas I, Daures JP, Festy B, Bontoux J, Gremy F. (1994) Bladder cancer and black tobacco cigarette smoking. Some results from a French case-control study. *Eur J Epidemiol.* 10:599-604

Mortusewicz O, Fourquerel E, Ame, JC, Leonhardt H, Schreiber V. (2011) PARG is recruited to DNA damage sites through poly(ADP-ribose)- and PCNA dependent mechanisms. *Nucleic Acids Res.* Jul; 39(12): 5045-5056.

Moore MJ, Proudfoot NJ. (2009) Pre-mRNA processing reaches back to transcription and ahead to translation. *Cell.* Feb 20;136(4):688-700.

Mueller-Dieckmann C1, Kernstock S, Lisurek M et al. (2006) The structure of human ADP-ribosylhydrolase 3 (ARH3) provides insights into the reversibility of protein ADP-ribosylation. *Proc Natl Acad Sci U S A.* Oct 10;103(41):15026-31

Murphy WM, Rivera-Ramirez I, Medine CA, Wright NJ, Wajsman Z. *J Urol.* 1997 Dec;158(6):2102-6.

Noon AP, Pickvance SV, Catto JW. Occupational exposure to dye penetrants used for metal crack detection and the potential for bladder cancer. *Occup Environ Med.* 2012;(69): 768-774.

Office of National Statistics. Bladder cancer incidence. Available from

URL:

<http://www.ons.gov.uk/ons/taxonomy/index.html?nscl=Businesses+by+Industry+Sector>. Cited Aug 2015.

O’Gorman S, Fox DT, Wahl GM. Recombinase-mediated gene activation and site-specific integration in mammalian cells. *Science*. 1991 Mar 15;251(4999):1351-5.

Overview of Post Translational Modifications. ThermoScientific (Cited Sept 2015). Available from URL:

<https://www.thermofisher.com/uk/en/home/life-science/protein-biology/protein-biology-learning-center/protein-biology-resource-library/pierce-protein-methods/overview-post-translational-modification.html>.

Pearl LH, Schierz AC, Ward SE, Al-Lazikani B, Pearl FMG. (2015) Therapeutic opportunities within the DNA damage response. *Nature Reviews Cancer*. 15, 166–180.

Pesch B, Gawrych K, Rabstein S. (2013) et al. N-acetyltransferase 2 phenotype, occupation, and bladder cancer risk: results from the EPIC cohort. *Cancer Epidemiol Biomarkers Prev*. (22): 2055-2065.

Porru S, Pavanello S, Carta A, et al. (2014) Complex relationships between occupation, environment, DNA adducts, genetic polymorphisms and bladder cancer in a case-control study using a structural equation modeling. PLoS One. (9): e94566.

Powles T, Eder JP, Fine GD et al. (2014) [MPDL3280A \(anti-PD-L1\) treatment leads to clinical activity in metastatic bladder cancer](#). Nature. Nov 27;515(7528):558-62

Proudfoot NJ, Brownlee GG. (1976) 3' non-coding region sequences in eukaryotic messenger RNA. Nature. Sep 16;263(5574):211-4.

Pukkala E, Martinsen JI, Lynge E, et al. (2009) Occupation and cancer - follow-up of 15 million people in five Nordic countries. Acta oncologica. (48): 646-790.

Rabut G, Lenart P, Ellenberg J. (2004) Dynamics of nuclear pore complex organization through the cell cycle. Curr Opin Cell Biol. Jun;16(3):314-21.

Reed R, Hurt E. A conserved mRNA export machinery couple to pre-mRNA splicing. Cell. 2002 Feb 22;108(4):523-31

Reinhert T. (2012) Methylation Markers for Urine-Based Detection of Bladder Cancer: The Next Generation of Urinary Markers for Diagnosis and Surveillance of Bladder Cancer. *Adv Urol*. Jun 18

Reulen RC, Kellen E, Buntinx F, Brinkman M, Zeegers MP. (2008) A meta-analysis on the association between bladder cancer and occupation. *Scand J Urol Nephrol Suppl*. Sep;(218):64-78.

Robbins PF, Morgan RA, Feldman SA et al. (2011) Tumor regression in patients with metastatic synovial cell sarcoma and melanoma using genetically engineered lymphocytes reactive with NY-ESO-1. *J Clin Oncol*. Mar 1;29(7):917-24.

Rouissi K, OuERHani S, Hamrita B et al. (2011) Smoking and polymorphisms in xenobiotic metabolism and DNA repair genes are additive risk factors affecting bladder cancer in Northern Tunisia. *Pathol Oncol Res*. 17:879-86

Rout MP, Aitchison JD. (2000) Pore relations: nuclear pore complexes and nucleocytoplasmic exchange. *Essays Biochem*. 36:75-88.

Rushton L, Bagga S, Bevan R, et al. (2010) Occupation and cancer in Britain. *Br J Cancer*. (102): 1428-1437.

Samanic C, Kogevinas M, Dosemeci M et al. (2006) Smoking and bladder cancer in Spain: effects of tobacco type, timing, environmental tobacco smoke, and gender. *Cancer Epidemiol Biomarkers Prev.* Jul;15(7):1348-54.

Satoh MS and Lindahl T. (2014) Role of poly(ADP-ribose) formation in DNA repair. *Nature.* 1992 Mar 26;356(6367):356-8.

Savage KI, Gorki JJ, Barros EM et al. Identification of a BRCA1-mRNA splicing complex required for efficient DNA repair and maintenance of genomic stability. *Mol Cell.* May 8;54(3):445-59.

Schonemann L, Kuhn U, Martin G, Schafer P et al. (2014) Reconstitution of CPSF active in polyadenylation: recognition of the polyadenylation signal by WDR33. *Genes Dev.* Nov 1; 28(21): 2381–2393.

Shatkin AJ and Manley JL. (2000) The ends of the affair: capping and polyadenylation. *Nat Struct Biol.* Oct;7(10):838-42.

Shiaishi T, Gutenberg RH, Kulkarni P. (2012) Cancer/testis antigens: novel tools for discerning aggressive and non-aggressive prostate cancer. *Asian J of Androl.* May;14(3):400-4.

Siddiqui N, Borden KL. (2012) mRNA export and cancer. *Wiley Interdiscip Rev RNA.* Jan-Feb;3(1):13-25.

Simpson A.J, Caballero OL, Jungbluth A, Chen YT, Old LJ. (2005) Cancer/testis antigens, gametogenesis and cancer. *Nat Rev Cancer*. Aug;5(8):615-25.

Soloway MS, Briggman V, Carpinito GA et al. (1996) Use of a new tumor marker, urinary NMP22, in the detection of occult or rapidly recurring transitional cell carcinoma of the urinary tract following surgical treatment. *J Urol*. Aug;156(2 Pt 1):363-7.

Stampfer DS, Carpinito GA, Rodriguez-Villanueva J et al. (1998) Evaluation of NMP22 in the detection of transitional cell carcinoma of the bladder. *J Urol*. Feb;159(2):394-8.

Sternberg CN, Skonecna I, Kerst Jm et al. (2015) Immediate versus deferred chemotherapy after radical cystectomy in patients with pT3–pT4 or N+ M0 urothelial carcinoma of the bladder (EORTC 30994): an intergroup, open-label, randomised phase 3 trial. *Lancet Oncol*. Jan;16(1):76-86.

Strack RL, Disney MD, Jaffrey SR. (2013) A superfolding Spinach2 reveals the dynamic nature of trinucleotide repeat-containing RNA. *Nat Methods*. Dec;10(12):1219-24.

Stula EF, Barnes JR, Sherman H, Reinhardt CF, Zapp JA Jr. (1978)

Urinary bladder tumours in dogs from 4,4'-methylene-bis(2-chloroaniline) (MOCA). *J Environ Pathol Toxicol.* 1(1):31-50.

Svatek RS, Hollenbeck BK, Halmang S et al. (2014) The economics of bladder cancer: costs and considerations of caring for this disease. *Eur Urol* Aug;66(2):253-62.

Tsuji FI. (2010) Early history, discovery, and expression of Aequorea green fluorescent protein, with a note on an unfinished experiment. *Microsc Res Tech.* Aug;73(8):785-96.

Tureci O, Sahin U, Koslowski M et al. (2002) A novel tumour associated leucine zipper protein targeting to sites of gene transcription and splicing. *Oncogene.* May 30;21(24):3879-88

Urovysion. Abbott Molecular. (cited Oct 2015) Available from URL: <https://www.abbottmolecular.com/us/products/urovysion.html>.

Van Rhijn BWG, Burger M, Lotan Y et al. Recurrence and Progression of Disease in Non–Muscle-Invasive Bladder Cancer: From Epidemiology to Treatment Strategy. *Eur Urol.* 2009 Sep;56(3):430-42.

Viphakone N, Hautbergue GM, Walsh M et al. (2012) TREX exposes the RNA-binding domain of NXF1 to enable mRNA export. *Nat Commun.* 3:1006

Viphakone N, Cumberbatch MG, Livingstone MJ, Heath PR, Dickman MJ, Catto JW, Wilson SA. (2015) LUZP4 defines a new mRNA export pathway in cancer cells. *Nucleic Acids Res.* Feb 27;43(4):2353-66.

Walsh MJ, Hautbergue GM, Wilson SA. (2010) Structure and function of mRNA export adaptors. *Biochem Soc Trans.* Feb;38(Pt 1):232-6.

Whelan P, Britton JP, Dowell AC. (1993) Three-year follow-up of bladder tumours found on screening. *Br J Urol.* Dec;72(6):893-6.

Witjes JA, Comperat A, Cowan NC et al. (cited Dec 2015). Guidelines on muscle-invasive and metastatic bladder cancer. European Association of Urology Available from URL: <http://uroweb.org/wp-content/uploads/EAU-Guidelines-Muscle-invasive-and-Metastatic-Bladder-Cancer-2015-v1.pdf>

Wu X and Brewer G. (2012) The regulation of mRNA stability in mammalian cells: 2.0. *Gene.* May 25;500(1):10-21.

Wurz GT, Kao CJ, DeGregorio MW. (2016) Novel cancer antigens for personalized immunotherapies: latest evidence and clinical potential. *Ther Adv Med Oncol.* Jan;8(1):4-31

Yang E, van Nimwegen E, Zavolan M et al. (2003) Decay rates of human mRNAs: correlation with functional characteristics and sequence attributes. *Genome Res.* Aug;13(8):1863-72.

Zhang Y, Wang J, Ding M, Yu Y. (2013) Site-specific characterization of the Asp- and Glu-ADP-ribosylated proteome. *Nat Methods.* Oct;10(10):981-4.

Zheng T, Cantor KP, Zhang Y, Lynch CF. (2002) Occupation and bladder cancer: a population-based, case-control study in Iowa. *J Occup Environ Med.* 44(7):685-691

Zhong J, Chen Y, Liao X et al. (2015) Testis expressed 19 is a novel cancer-testis antigen expressed in bladder cancer. *Tumour Biol.* Dec 22.

**COPIES OF PUBLICATIONS ARISING FROM
THESIS**